Role of Dielectric Strength of Gases on the Degree of Solids Electrostatic Charging and Fouling in Fluidization and Pneumatic Conveying Systems

Nikhil Sridhar

Thesis submitted to the University of Ottawa
in partial Fulfillment of the requirements for the
Master's Degree in Applied Science

Department of Chemical and Biological Engineering
Faculty of Engineering
University of Ottawa

Abstract

Electrostatic charging is a widely known natural phenomenon that has been observed since ancient times. This phenomenon is also reported in solids handling and processing industries with varying extent of its interference in established processes and operations. Particle collisions lead to electrostatic charge generation through triboelectrification. Sustained charging leads to particle agglomeration and adhesion, or even explosions. Hence, the presence of charged particles are seen as a hindrance and a risk in certain processes. The focus of this thesis is directed at gas-solid fluidization and pneumatic conveying where this holds true.

Polyethylene is commonly manufactured in catalytic gas-solid fluidized bed reactors. The insulative nature of the polymer particles, the catalyst particles and the surrounding gas set up a conducive environment for electrostatic charge generation. Charged particles adhere on to nearby surfaces forming fused masses of polymer sheets. Presence of sheets in the reactor hinders the reactor productivity, thus warranting reactor shutdown and maintenance. On the other hand, catalyst introduction into the polyethylene reactor is performed through pneumatic conveying systems. In general, solids pneumatic conveying is known to cause the largest degree of triboelectrification among many gas-solid systems. Therefore, the charging of catalyst particles may also contribute to operational challenges faced by this industry.

Numerous studies have attributed particle characteristics, system variables, and operating parameters as probable sources contributing to electrostatic charging in both fluidization process and pneumatic conveying systems. However, a comprehensive consensus explaining particle charging in real-world scenarios and suitable methods to mitigate or prevent charging still require further investigation. Thus, desirable control of charging in affected industrial sectors is still not present.

Beyond the scope of fluidization and pneumatic conveying, certain studies have investigated the influence of dielectric strength of gases on the charging behaviour of solids. The works claim that gases with low dielectric strength perform better in minimizing electrostatic charge of solids in controlled environments due to gas discharge and subsequent charge dissipation. Thus, applicability of such gases in dynamic processes like fluidization and pneumatic conveying must be investigated in hopes of reproducing similar observations. The principal aim of this thesis was to uncover a functional method to limit charging and particle adhesion in fluidization and other solids handling systems. As a means of accomplishing this, the objective of this thesis was directed to study the efficacy of argon, which has a low dielectric

strength, against nitrogen in reducing triboelectrification of polyethylene particles in fluidization and pneumatic conveying operations.

A stainless-steel fluidization apparatus was used to study the charging behaviour of a commercially produced polyethylene resin at atmospheric pressure. Results were drawn for pure argon and compared against pure nitrogen. Aiming to minimize the quantity of argon while simultaneously retaining as much efficacy as possible, binary mixtures of nitrogen and argon were also tested along with successive fluidization trials. Pure argon resulted in 90% reduction in fouling compared to pure nitrogen. Even binary mixture of 10 vol % argon showed a reduction of 50% in fouling values. Successive fluidization resulted in fouling values comparable to pure argon trials. Multiple pulse pneumatic conveying was carried out in a stainless-steel tube with dehydrated amorphous silica that is a commonly used catalyst base in polyethylene process. The net specific charge of the particles and the fouling inside the tube were smaller under argon in the first injections. Subsequent injections were not as significant. Results from the above operations were validated through bench-scale shake tests performed under controlled gaseous environment. Single large polyethylene particle charging was first tested in nitrogen and argon atmosphere followed by multiple smaller particles. Bench-scale shake tests showed argon influenced the saturation charges, reducing it and reaching it earlier compared to nitrogen. However, the degree of charge and fouling reduction was not as significant as observed in fluidization trials.

The thesis concludes that argon is indeed influential in reducing particle charge and particle adhesion in applicable systems. Influence of argon was observed in all operations with fluidization exhibiting the greatest degree of reduction in charging and fouling values. Furthermore, even small quantities of argon can make a non-linear impact on said parameters. The results also suggest that the majority of gas discharge and subsequent charge dissipation occurs in areas of considerable electric fields. These are observed to entertain large number of particles contact and separation, providing plenty of opportunities for gas molecules to ionize.

Résumé

La charge électrostatique est un phénomène naturel grandement connu qui a été observé depuis l'Antiquité. Ce phénomène est également signalé dans les industries de manipulation et de traitement des solides avec une ampleur variable de son interférence dans les procédés et opérations établis. Les collisions de particules mènent à la génération de charges électrostatiques par triboélectrification. Une charge soutenue entraîne une agglomération et une adhérence des particules, ou même des explosions. Par conséquent, la présence de particules chargées est considérée comme une entrave et un risque dans certains procédés. L'objet de cette thèse se concentre sur la fluidisation gaz-solide et le transport pneumatique où cela est vrai.

Le polyéthylène est couramment fabriqué dans un réacteur catalytique à lit fluidisé gaz-solide. La nature isolante des particules de polymère, des particules de catalyseur et du gaz environnant crée un environnement propice à la génération de charges électrostatiques. Les particules chargées adhèrent aux surfaces voisines formant des masses fusionnées de feuilles de polymère. La présence de feuilles dans le réacteur entrave la productivité du réacteur, justifiant ainsi l'arrêt et la maintenance du réacteur. D'autre part, l'introduction du catalyseur dans le réacteur en polyéthylène est réalisée par des systèmes de transport pneumatique. En général, le transport pneumatique de solides est connu pour provoquer le plus grand degré de triboélectrification parmi de nombreux systèmes gaz-solide. Par conséquent, le chargement de particules de catalyseur peut également contribuer aux défis opérationnels auxquels est confrontée cette industrie.

De nombreuses études ont attribué plusieurs particules, systèmes et paramètres de fonctionnement comme sources probables contribuant à la charge électrostatique dans les procédés de fluidisation et les systèmes de transport pneumatique. Cependant, un grand consensus expliquant la charge des particules dans des scénarios réels et des méthodes appropriées pour atténuer ou prévenir la charge nécessitent encore des recherches plus approfondies. Ainsi, le contrôle souhaitable de la charge dans les secteurs industriels concernés n'est toujours pas présent.

Au-delà du domaine de la fluidisation et du transport pneumatique, certaines études ont examiné l'influence de la rigidité diélectrique des gaz sur le comportement de charge des solides. Les travaux affirment que les gaz à faible rigidité diélectrique réussissent mieux à minimiser la charge électrostatique des solides dans des environnements contrôlés en raison de la décharge de gaz et de la dissipation de charge qui s'ensuit. Ainsi, l'applicabilité de ces gaz

dans des procédés dynamiques tels que la fluidisation et le transport pneumatique doit être étudiée dans l'espoir de reproduire des observations similaires. L'objectif principal de cette thèse était de découvrir une méthode fonctionnelle pour limiter la charge et l'adhérence des particules dans la fluidisation et autres systèmes de manutention des solides. Pour y parvenir, l'objectif de cette thèse visait à étudier l'efficacité de l'argon, qui a une faible rigidité diélectrique, contre l'azote pour réduire la triboélectrification des particules de polyéthylène dans les opérations de fluidisation et de transport pneumatique.

Un appareil de fluidisation en acier inoxydable a été utilisé pour étudier le comportement de charge d'une résine de polyéthylène produite commercialement à la pression atmosphérique. Les résultats ont été obtenus pour l'argon pur et comparés à l'azote pur. Afin de minimiser la quantité d'argon tout en conservant le maximum d'efficacité, des mélanges binaires d'azote et d'argon ont également été testés ainsi que des essais de fluidisation successifs. L'argon pur a entraîné une réduction de 90 % de l'encrassement par rapport à l'azote pur. Même un mélange binaire de 10% en volume d'argon a montré une réduction de 50% des valeurs d'encrassement. Des fluidisations successives ont donné des valeurs d'encrassement comparables aux essais d'argon pur. Un transport pneumatique à impulsions multiples a été effectué dans un tube en acier inoxydable avec de la silice amorphe déshydratée qui est une base de catalyseur couramment utilisée dans le processus de polyéthylène. La charge spécifique nette des particules et l'encrassement à l'intérieur du tube étaient plus faibles sous argon lors des premières injections. Les injections suivantes n'étaient pas aussi significatives. Les résultats des opérations ci-dessus ont été validés par des tests d'agitation à l'échelle du laboratoires réalisés dans un environnement gazeux contrôlé. Le chargement d'une seule grande particule de polyéthylène a d'abord été testé dans une atmosphère d'azote et d'argon, suivi de plusieurs particules plus petites. Des tests d'agitation à l'échelle du laboratoire ont montré que l'argon influençait les charges de saturation, les réduisant et les atteignant plus tôt que l'azote. Cependant, le degré de réduction de la charge et de l'encrassement n'était pas aussi important que celui observé lors des essais de fluidisation.

La thèse conclut que l'argon a effectivement une influence sur la réduction de la charge et de l'adhérence des particules dans les systèmes applicables. L'influence de l'argon a été observée dans toutes les opérations avec la fluidisation présentant le plus grand degré de réduction des valeurs de charge et d'encrassement. De plus, même de petites quantités d'argon peuvent avoir un impact non linéaire sur ces paramètres. Les résultats suggèrent également que la majorité des décharges de gaz et la dissipation de charge subséquente se produisent dans des zones de

champs électriques considérables. On observe que ceux-ci permettent le contact et la séparation d'un grand nombre de particules, offrant de nombreuses opportunités aux molécules de gaz de s'ioniser.

Statement of Contribution of Collaborators

I hereby declare that I am the sole author of this thesis. I authored all the chapters collated under this thesis with editorial comments and critique offered by my supervisor Professor Poupak Mehrani. All experiments were performed by me with some assistance provided by PhD student Mohsen I. Nimvari for work carried out in pneumatic conveying. The research team at Univation Technologies, LLC (USA) provided valuable insight in ensuring applicability of the results in industrial polyethylene reactors.

Chapters 1, 3, 4, and 5 were written by me with feedback furnished by Professor Poupak Mehrani.

Chapter 2 is compiled as a manuscript to be submitted for publication. The experimentation and data compilation were performed by me. The team at Univation Technologies, LLC, provided worthwhile comments regarding some of the design of experiment.

Acknowledgement

I would like to offer my earnest gratitude to Dr. Poupak Mehrani for all her contributions in making my time as her student an enriching experience. I appreciate the time and effort she bestowed on me and her supervision in the entirety of my thesis program. The time I spent under her mentorship has been extremely fruitful. I would also like to thank Dr. Andrew Sowinski for his guidance and support in completing this study.

The inputs provided by the team at Univation Technologies, LLC, Mr. John Szul, Dr. Kishori Deshpande, and Mr. David Pearson, is greatly appreciated. I would also like to thank them for the experimental material used in this study.

I would also like to recognize the support and well-wishes graciously extended by the PhD students Mohsen Isaac Nimvari and Otome Obukohwo.

I would also like to extend my gratitude to the staff of the Department of Chemical and Biological Engineering and the University as a whole. This work would not have been successful without the help of Franco Ziroldo, Patrick Pageau, Francine Petrin, Chantal Dube, Lise Rousseau, and Frantz Célestin.

The financial support offered by the National Sciences and Engineering Research Council (NSERC) is greatly appreciated.

Lastly, I would like to convey my sincere gratitude to my family and friends who encouraged me to pursue my Master's.

Table of content

List of figures

List of tables

Nomenclature

General

A	Gas constant
B	Gas constant
C	Capacitance, F
d	Distance between electrodes, m
d_c	Distance between charged objects particles, m
dl	Electron path length, m
d_p	Particle diameter, m
e	Charge of an electron, -1.602×10^{-19} C
E	Electric field generated by a charged object, V/m
F	Electrostatic force, N
I(A)	Current, A
kc	Charging efficiency
L	Length of the line, m
n	Energy level
P	Gas pressure, Pa
$P_{Reactor}$	Reactor pressure, atm
Q(C)	Charge, C
q, q'	Charge on a particle, C
Q/m	Specific charge expressed as net charge over mass, nC/g

q_{max}	Maximum charge, nC
R	Radius, m
RH	Relative humidity, %
r_o	Equilibrium distance, m
S	Surface area enclosing all charges, m^2
$T_{Reactor}$	Reactor temperature, °C
U	Superficial gas velocity, m/s
u_{mf}	Minimum fluidization velocity, m/s
V	Voltage, V
V_B	Breakdown voltage, V
V_c	Contact potential, V
x	Displacement of charge, m
z_0	Capacitor gap distance, m
Δq	Charge difference, C

Greek letters

α	Primary ionization coefficient
γ	Secondary ionization coefficient
ε_0	Permittivity of free space, C V^{-1} m^{-1}
$\in_r$	Relative permittivity of the material
η	Attachment coefficient
ϕ	Work function, eV

Chapter 1 Introduction

Industries that employ solids and particulates in their processes at times report electrostatic charge generation while processing and handling them. These charges are generated when solid particles collide with each other and nearby surfaces. The charged particles are susceptible to electrostatic forces that hinder the process and introduce risks which mandate additional controls to maintain efficiency. Examples of processes where electrostatic charge generation can be detrimental include pneumatic conveying, size reduction (e.g., grinding), gas-phase fluidization, etc.

Gas-solid fluidization, one of the processes mentioned above, could face significant degree of solids charging during operation. For instance, polyethylene that is a commercially significant product, is manufactured through the polymerization of ethylene monomers in gas-phase catalytic fluidized bed reactors. Due to continuous solid-solid and solid-column wall collisions, , fluidization process provides a favorable environment for solids to become electrostatically charged. Depending on the degree of fluidizing particle charge, challenges such as particle agglomeration as well as particle fouling on the column wall could arise. Noticeably, gas-phase fluidization is susceptible to electrostatic charge generation due to the poor charge conducting properties of the fluidizing gas. For example, although gas-phase polyethylene process is an established process, it could face severe operational challenges with respect to reactor fouling (known as “sheeting”) which leads to issues in reactor operability and in turn process productivity. If left unchecked, the sheets break off from the reactor wall and fall onto the gas distributor [1]. This mandates reactor shutdown and cleaning ranging from couple of days to over thirty days or longer depending on the severity of the problem. The current consensus points to electrostatic charge generation within the fluidized bed reactor as the leading cause for particle adhesion and subsequent formation of sheets. Due to significant economic losses caused by reactor shutdown, understanding and mitigating the detrimental effects of electrostatics is of utmost importance for this sector.

Pneumatic conveying, which is employed by solids-handling industries to transport solid components, could also face solids electrostatic charging. Solid particles transport through pneumatic conveying is often considered to generate some of the highest charges in solids handling operations [2]. A similar mechanism is understood to cause electrostatic charging of solids in pneumatic conveying. The gas velocities are much higher in comparison to fluidization, which also implies a higher particle velocity and larger charge generation. In

general, the impact of electrostatic charge generation could disrupt process productivity through particle agglomeration and adhesion on surfaces in contact, and even pose a serious risk of electrostatic discharge and subsequent explosions [2–5]. Particle agglomeration might even change the particle characteristics which impacts the conveying efficiency, increasing the power demand, as well as reducing the reactivity in certain reactive systems when conveyed solids are catalyst. Particle fouling might also plug the conveying tube, causing material loss and a drop in productivity. Thus, as with gas-phase fluidization, understanding and mitigating electrostatic charging is of significant interest.

The mechanism of charge generation and transfer has been the topic of interest for a number of studies in the past, especially in relation to the polyethylene gas-phase fluidized bed reactors. Several studies have looked at the mechanism of charge generation and the parameters that contribute to its generation including fluidizing gas velocity, moisture content, operating temperature, and pressure, etc. [6]. However, limited studies have investigated the effect of the fluidizing gas type on charge generation and dissipation within fluidized beds. Similarly, a number of studies have investigated the degree of charging in dilute conveying systems by varying many parameters including gas velocity, conveying line length and pathway, solids mass loading. However, no work has studied the influence of the conveying gas type. Hence, the objective of this thesis is to investigate the degree of charging of particles in gas-solid fluidization and pulse pneumatic conveying using different gases. This thesis was carried out based on polyethylene processing, therefore, solids employed were similar to that used in commercial operations.

1.1 Electrostatic Fundamentals

This thesis focuses on charging of solid particles through contact with other neutral and/or charged solid objects. Generation and accumulation of electrostatic charge on a solid particle tends to create an electrostatic force, which if not controlled, could lead to particle agglomeration, adhesion to surrounding surfaces, as well as explosions in dire cases.

1.1.1 Charge and electron energies in materials

In the 1700s the characteristics of electricity and charge was vaguely understood as no real means of measurement was discovered. This changed when a simple torsion balance allowed Coulomb to measure the forces exerted by objects that are charged. As the understanding of electricity grew, new fundamental terms to quantify the effects of electricity were defined. The Coulomb's law (equation 1-1) gives the force F, exerted by an object having charge q, on

another object having charge q'. ε_0 is the permittivity of free space and d_c is the distance between the charged objects. The electric field E that is generated by an object having a charge q' is defined in equation 1-2, and the electric potential V, which denotes the work done in moving a unit charge against a uniform electric field E by a distance x, is defined in equation 1-3.

$$F = \frac{Cqq'}{{d_c}^2} = \frac{qq'}{4\pi\varepsilon_0 {d_c}^2} \qquad \text{Equation 1-1}$$

$$E = \frac{q'}{4\pi\varepsilon_0 {d_c}^2} \qquad \text{Equation 1-2}$$

$$V = Ex \qquad \text{Equation 1-3}$$

In addition to quantifying electrical forces of objects, it is realized that objects hold electronic energy in a microscopic scale. The simple band model is often used to quantify the electronic energies of materials. The model introduces a number of energy levels and bands to explain the energies observed in materials. According to the model, an isolated atom holds a fixed number of electrons in various energy levels or orbits around the nucleus. Each energy level can hold a set number of electrons and has a fixed energy, which is a function of the distance of the orbit from the nucleus. Depending on the material, these levels can be occupied or unoccupied. When atoms are brought together, the energy levels merge into an imprecise band, known as an energy band (Fig. 1-1).

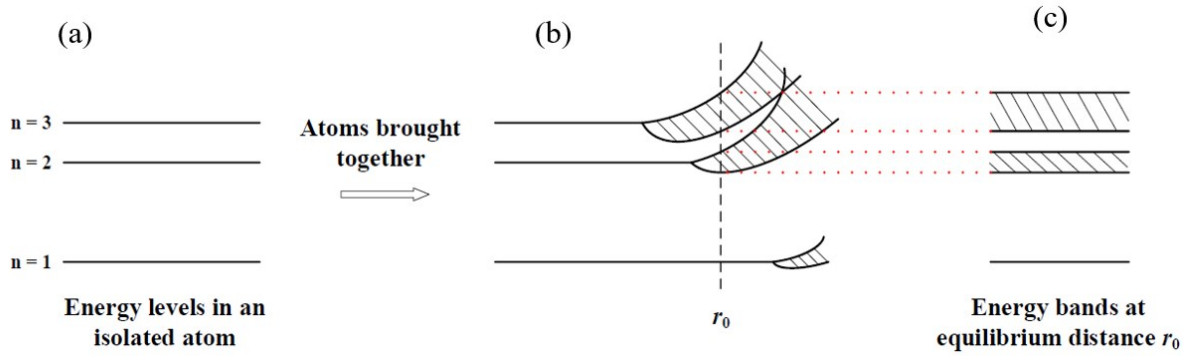

Fig. 1-1. Energy levels in an isolated atom (a); variation in energies (b); energy band at an equilibrium distance (c) (copied from [7]).

The outer electrons hold higher influence over their neighbours and have a wider energy band, termed as a valence band. The inner electrons have a lower influence and have a narrower energy band, termed as a core band. The bands corresponding to the orbits quantify the range of energies the electrons can possess. In Fig. 1-1, r_0 is the equilibrium distance between the atoms and the energy bands corresponding to this distance is shown as well. Energy bands associated with excited electrons are termed as conduction bands, generally displaying a higher energy density relative to the valence band. The gap between the valence and the conduction band is termed as the forbidden gap.

Metals display a partially filled valence band or an overlap between the conduction and the valence band. This makes it easier for electrons to gain energy and jump to the conduction band, thus conduct electricity. Insulators, however, have filled valence bands and the gap between the conduction band and the valence band is sufficiently high. Thus, electrons require significantly higher energies to jump to the conduction band. Fig. 1-2 shows the band structures of insulators, semi-conductors, and conductors.

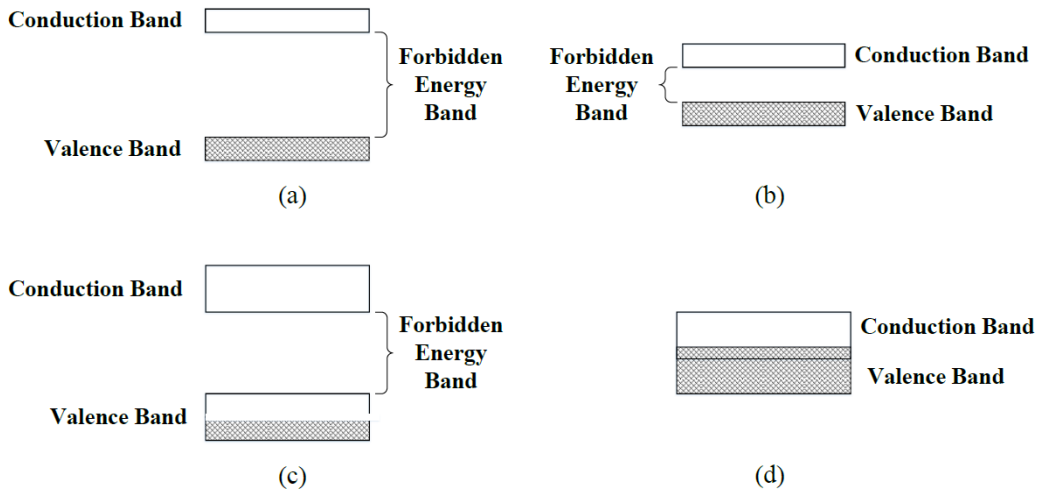

Fig. 1-2. Band structures of insulators (a); semi-conductors (b); partially filled conductors (c); overlapping conductors (d).

1.1.2 Charging mechanisms

Mechanism of charge generation in solids is broadly classified into contact charging, frictional charging, and induction charging.

Electrostatic charge generation through *contact charging mechanism* is believed to take place when solids make brief contact with each other and develop equal but opposite charges on their

surface (Fig. 1-3a). The charge gained by the solids is attributed to the difference in surface energies of the solids [8].

When solids make prolonged contact with each other through a sliding or rubbing action and then separate, charges are believed to be generated due to *frictional charging* (Fig. 1-3b). Since it is difficult to distinguish the duration and the type of contact between solids, contact charging and frictional charging mechanism are referred to as tribocharging or triboelectrification [8].

Induction charging mechanism is observed when a charged solid object enters the vicinity of a neutral conductive surface. Unlike tribocharging, induction charging generates charges on solids without contact. As the charged object is in close proximity to the conductor, the charge carriers in the conductor rearrange themselves as shown in Fig. 1-3c. Charge carriers of the opposite polarity accumulate at the surface closest to the charged object. If the conductive solid where then to be grounded, charge carriers of the same polarity will be dispersed, and the conductor retains a net charge of the same magnitude as the charged object but the opposite polarity.

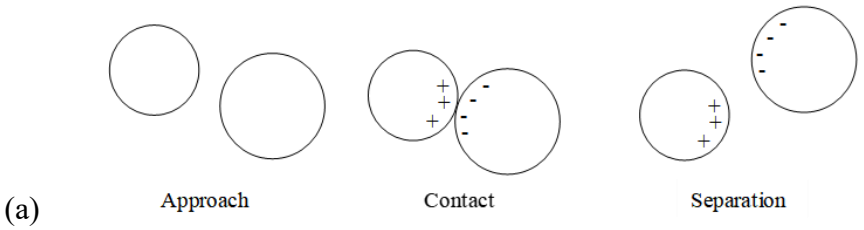

(a)

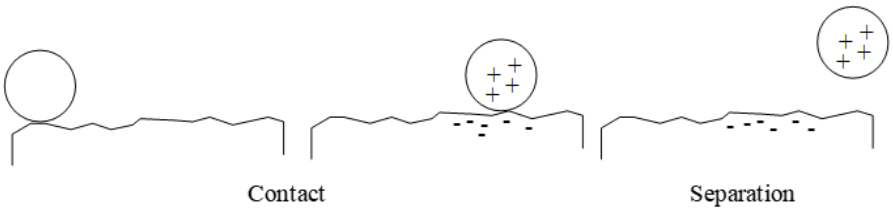

(b)

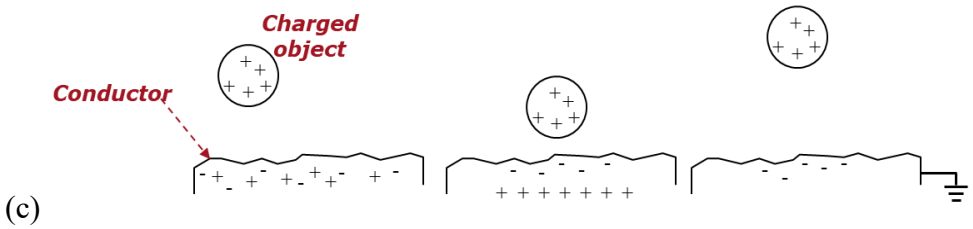

(c)

Fig. 1-3. Electrostatic charging mechanisms. (a) Contact charging; (b) Frictional charging; and (c) Induction charging.

1.1.3 Charge transfer mechanism

Charging behaviour observed in solids and the mechanism of charge transfer (ion, electron, or material transfer) between them depends on the characteristics of the solids themselves, being a conductor versus an insulator.

According to Lowell and Rose-Innes [9], as the surfaces of two conductors come into contact, electrons flow across the interface until a thermodynamic equilibrium is reached. The amount of charge transferred is then dependent on the work functions of the two surfaces in contact. The concept of work function was introduced in the early 1950s to explain the contact charging behaviour observed when two metal objects made contact [8]. Work function, which is an inherent property of the material, is defined as the energy needed to remove an electron from an object and transfer it to a point in infinity [7]. The contact potential (V_c) is expressed to be proportional to the difference of the work functions of the metals making contact.

$$V_c = -\frac{(\phi_{M1} - \phi_{M2})}{e} \qquad \text{Equation 1-4}$$

In equation 1-4, ϕ_{M1} and ϕ_{M2} are the work functions of the two metals making contact and e is the elementary charge (-1.602 × 10^{-19} C). A schematic representation of the work function and contact potential concept is shown in Fig. 1-4. As shown in this figure, Metal 1 with the lower work function has electrons at higher energy levels and thus some of its valence electrons transfer to Metal 2 in turn resulting in a positive charge on Metal 1 and a negative charge on Metal 2.

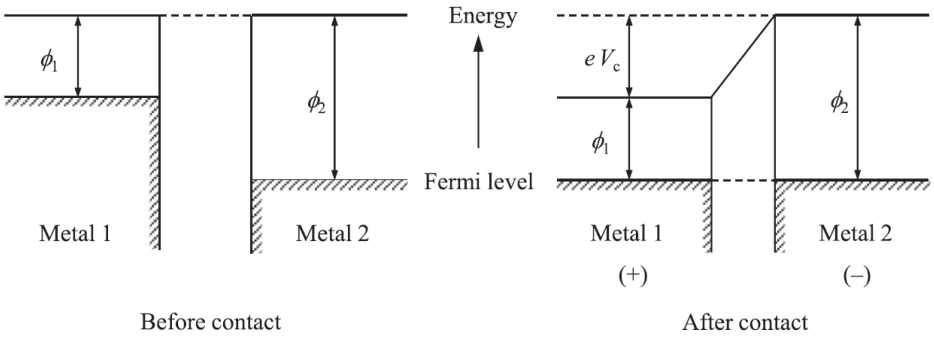

Fig. 1-4. Metal-metal contact potential difference (copied from [8]).

Looking closely at equation 1-4, we can notice that it is only valid for metal-metal contacts as the charge transfer occurs through electrons. For insulator-metal contacts, an effective work function is assigned to the insulator [8].

$$V_c = -\frac{(\phi_E - \phi_M)}{e} \qquad \text{Equation 1-5}$$

The contact potential difference V_c is then expressed in terms of the effective work function of the insulator, ϕ_E, and the work function of the metal, ϕ_M. Even with the effective work function model, charge transfer between insulators and other objects cannot be explained due to the lack of free electrons in insulators. To explain charge transfer between insulators and insulator-metal contacts, surface state models were put forth. The model assumes movement of electrons only on the surface of the insulators and not the bulk or body of the insulator [8]. One model suggests available energy levels for electron transfer are only on the surface, named as surface states. Accordingly, when two insulators make contact, electrons are transferred from the filled surface states of one insulator to the empty surface state of another [10].

In addition to *electron transfer*, researchers also put forth *ion transfer* and *material transfer* mechanisms to explain charging behaviour of insulators. Ruckdeschel and Hunter [11] first theorized ion transfer mechanism as a non-equilibrium process dependent on the dielectric constants of the insulators and the separation distance between them. In recent years, ionic charge control agents have been observed to impact degree of charging. Cationic additives seem to charge positively, and anionic additives charge negatively [12].

A simpler method to predict polarity of charging of insulators is through a triboelectric series. The series comprises of materials placed in order of their polarity. A typical triboelectric series is shown in Fig. 1-5. For instance, if an object made of cotton is rubbed against an object made

of fur, the series dictates the fur object to charge positively and the cotton object to charge negatively. As a general tool to predict charging polarity, the triboelectric series works well. However, the degree of charge generation is not predictable.

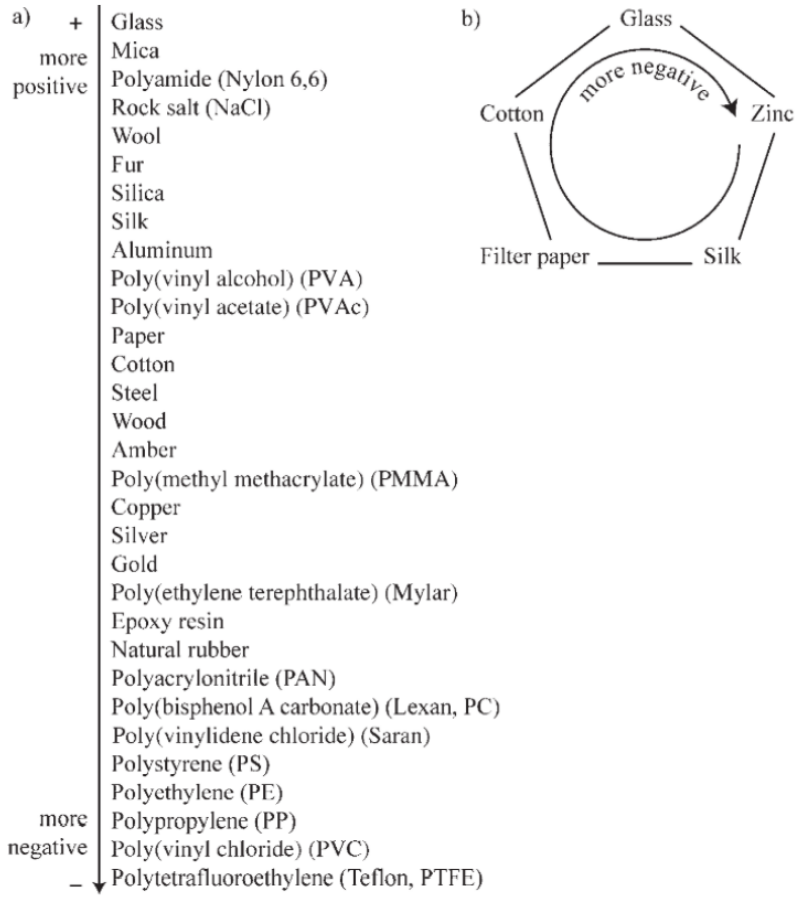

Fig. 1-5. A linear triboelectric series showing various commonly used polymers and a cyclic series (copied from [13]).

1.1.4 Charge measurement techniques

There are two main charge measurement techniques that are commonly used, which work on the same basic principle of induction charging: (a) Faraday cage; and (b) electrostatic probe**.**

(a) Faraday cage

A Faraday cage consists of two concentric cylinders made of a highly conducting material like copper. The inner cylinder is electrically isolated from the outer cylinder using an insulating pad and the outer cylinder is grounded as shown in Fig. 1-6. The outer cylinder shields the inner cylinder from external electric fields that might distort the charge measurement. When solids are introduced into the inner cylinder, charges of the opposite polarity accumulate on the inner surface of the inner cylinder due to induction charging. Due to the conductive nature of

the cylinder, charges of the same polarity accumulate on the outer surface of the inner cylinder that is then measured by an electrometer connected to the outer surface of the inner cylinder.

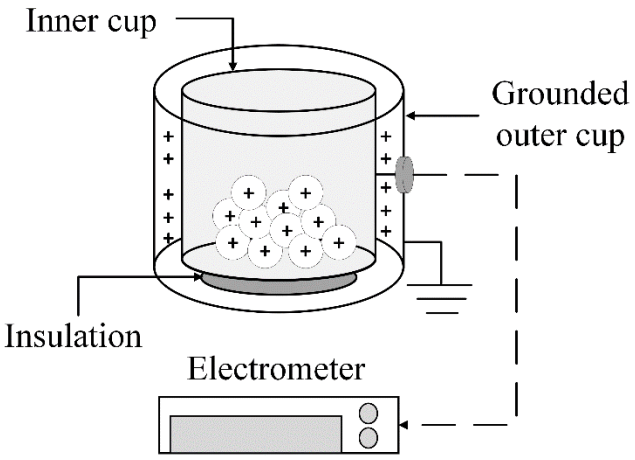

Fig. 1-6. Schematic of a Faraday cage

(b) Electrostatic probe

An electrostatic probe consists of an inner metal rod separated from an outer grounded shield through an insulating sheath as shown in Fig. 1-7. When a charged object passes through the vicinity of the probe, an image charge is generated on the inner rod of the probe. This is then measured by an electrometer that is connected to the other end of the inner rod of the probe. Commercial polyethylene gas-phase fluidized bed reactors use electrostatic probes to monitor changes in the level of charge generation within the system. The probes are inserted into the reactor and extend past the inner surface of the reactor wall. On-field applications, electrostatic probes face difficulties due to particle adhesion on to the probes themselves. Additionally, particles may accumulate a higher charge due to impact charging when they collide against the probe.

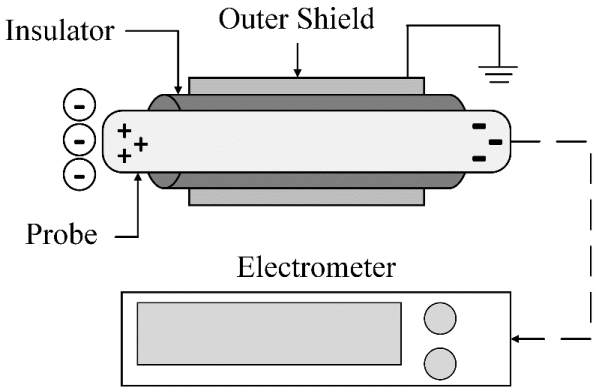

Fig. 1-7. Schematic of an electrostatic probe.

1.1.5 Charge dissipation- Gas ionization and discharge

The maximum charge gained by a particle is a function of the particle characteristics that include the surface area, diameter, surface composition, particle charging mechanism, and charge dissipation mechanism that is influenced by the gaseous environment around it. Under normal conditions gases are electrically insulative and do not conduct electrons. However, under sufficiently high electric fields, gases may undergo ionization. Potential difference that generates strong electric fields can be formed by electrodes within a system or even by highly charged surfaces that develop a temporary potential between each other after a collision. The resulting free electrons get accelerated by the electric field leading to the generation of large number of charge carriers. This results in a conducive path being formed by the charge carries, increasing the conductivity of the gas and bridging the two electrodes or potential differences. This phenomenon is termed as *gas discharge*.

The ions formed during gas discharge may recombine with each other, or neutralize charges present on surfaces within their vicinity. Jiang et al. (1994) referred to Cross's work [7] in applying Gauss' law on a spherical polymer particle in air to arrive at the theoretical maximum electrostatic charge [14].

$$q_{max} = E\varepsilon_0 S = 2.64 \times 10^{-5}(\pi d_p)p \qquad \text{Equation 1-6}$$

Where E is the electric field strength generated by the charges, ε_0 is the permittivity of free space, S is the surface area that encloses all the charges and $p = 3\epsilon_r/(\epsilon_r + 2)$, where ϵ_r is the dielectric constant of the polymer and d_p is the particle diameter.

Evident from equation 1-6, as the maximum charge increases, the resulting electric field increases too. The rising electric field reaches the dielectric strength of the surrounding medium, which then serves to limit the maximum charge on the surface. The term *dielectric strength* or *breakdown voltage* refers to the electric field required to breakdown gas molecules, forming ion pairs. These ion pairs dissipate nearby charges, thus limiting the maximum surface charge. Generally, gas dielectric strength is measured by applying a set potential difference across two metal electrodes in a closed chamber. The electrode composition (e.g., Tungsten, copper, aluminium etc.) and work function, gap distance between the electrodes, the pressure, temperature and composition of the gas influence the breakdown value [15]. The dielectric strengths of some select gases are mentioned in Table 1-1.

Table 1-1. Dielectric strength of different gases at 0.1 MPa pressure and 20°C [16].

Gas Type	**Dielectric strength (kV/mm)**
Neon (Ne)	0.05
Argon (Ar)	0.6
Hydrogen (H_2)	1.6
Air (Calculated)	3.25
Nitrogen (N_2)	3.4
Sulfur hexafluoride (SF_6)	8.86

It is observed that noble gases have a relatively lower dielectric strength. This essentially means that it is easier to ionize noble gases and generate charge carriers. Pashcen curves derive the relation between the minimum breakdown voltage, V_B, and the product of gas pressure and separation gap between the electrodes used in an experiment [15].

$$V_B = \frac{BPd}{\ln(Pd) + \ln\left(A/\alpha d\right)} \qquad \text{Equation 1-7}$$

The constants A and B are dependent on the gas type and α is the primary ionization coefficient. P is the pressure of the gas, d is the distance between the two electrodes across which the potential V_B is measured. A typical Paschen curve is shown in Sparking or breakdown voltage of argon and n-pentane mixtures at 0°C [17]. The breakdown voltage (also known as sparking voltage) strength of pure argon, n-pentane, and mixtures of the two are presented at pressures close to 700 torr (93.3 kPa).

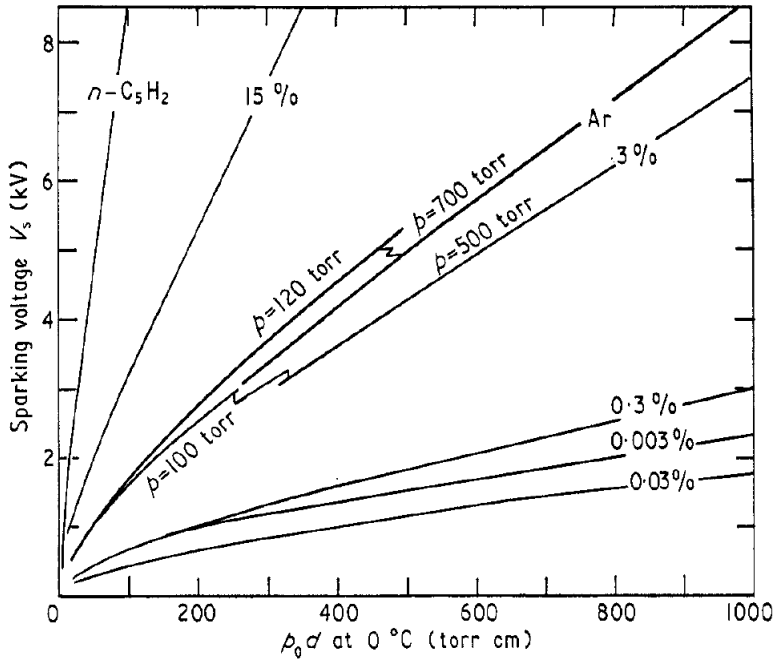

Fig. 1-8. Sparking or breakdown voltage of argon and n-pentane mixtures at 0°C [17]

The Townsend criterion is frequently applied to explain gas discharge in uniform electrical fields. The criterion considers the drift velocity of an electron under an electric field and its ability to generate secondary electrons to self sustain the discharge process [7].

$$\gamma[\exp(\alpha - \eta)\, dl - 1] = 1 \qquad \text{Equation 1-8}$$

Here, γ is the secondary ionization coefficient, α is the primary ionization coefficient or the Townsend coefficient, η is attachment coefficient of the gas, and *dl* is the path length of the electron. The coefficients are functions of the local electric field, which is non uniform.

Gases may not undergo complete gas discharge if the potential difference is localized and short-lived. Partial discharge phenomena may occur at these localized points, which are termed as *corona discharge*. In a study performed by Hiziroglu et al. [18], as shown in Fig. 1-9 pure gases and mixtures of argon and SF_6 showed a difference between the corona insipient voltage and the complete breakdown voltage. For all the mixtures, corona insipient voltage was much lower than the complete breakdown voltage, hinting at localized discharge phenomena occurring before complete breakdown takes place. Furthermore, they concluded that positive polarity systems showed a lower corona insipient voltage but a higher breakdown voltage relative to a negative polarity system.

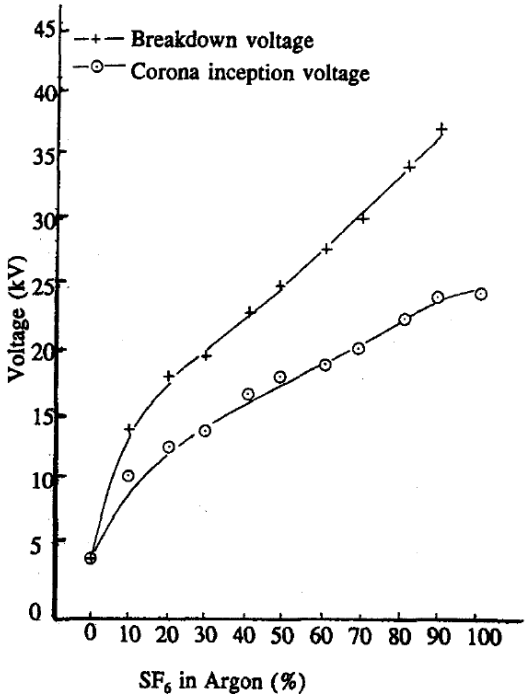

Fig. 1-9. Corona inception voltage and breakdown voltage for varying mixtures of SF_6 and Argon at 50 kPa under positive applied voltage (copied from [18]).

Miura [19] measured the electrostatic charge on a metal pin (conductor) sliding on a quartz disc (insulator) in a closed chamber under vacuum and various gaseous environments (Fig. 1-10). As seen in Fig. 1-10, in vacuum, the charge rose without any dissipation. Under gaseous environments however, charge dissipation was observed. Argon exhibited a constant charge magnitude wherein the dissipation of charge was uniform and was approximately the same as the magnitude of charge gained by the pin through contact electrification. Dry air, nitrogen, and ambient air displayed charge dissipation as well, but the average charge on the pin was on an upward trend indicating the magnitude of charge dissipation was lower than the acquired charge. Miura attributed this dissipation to the breakdown of the gas molecules around the pin in turn neutralizing the surface charge.

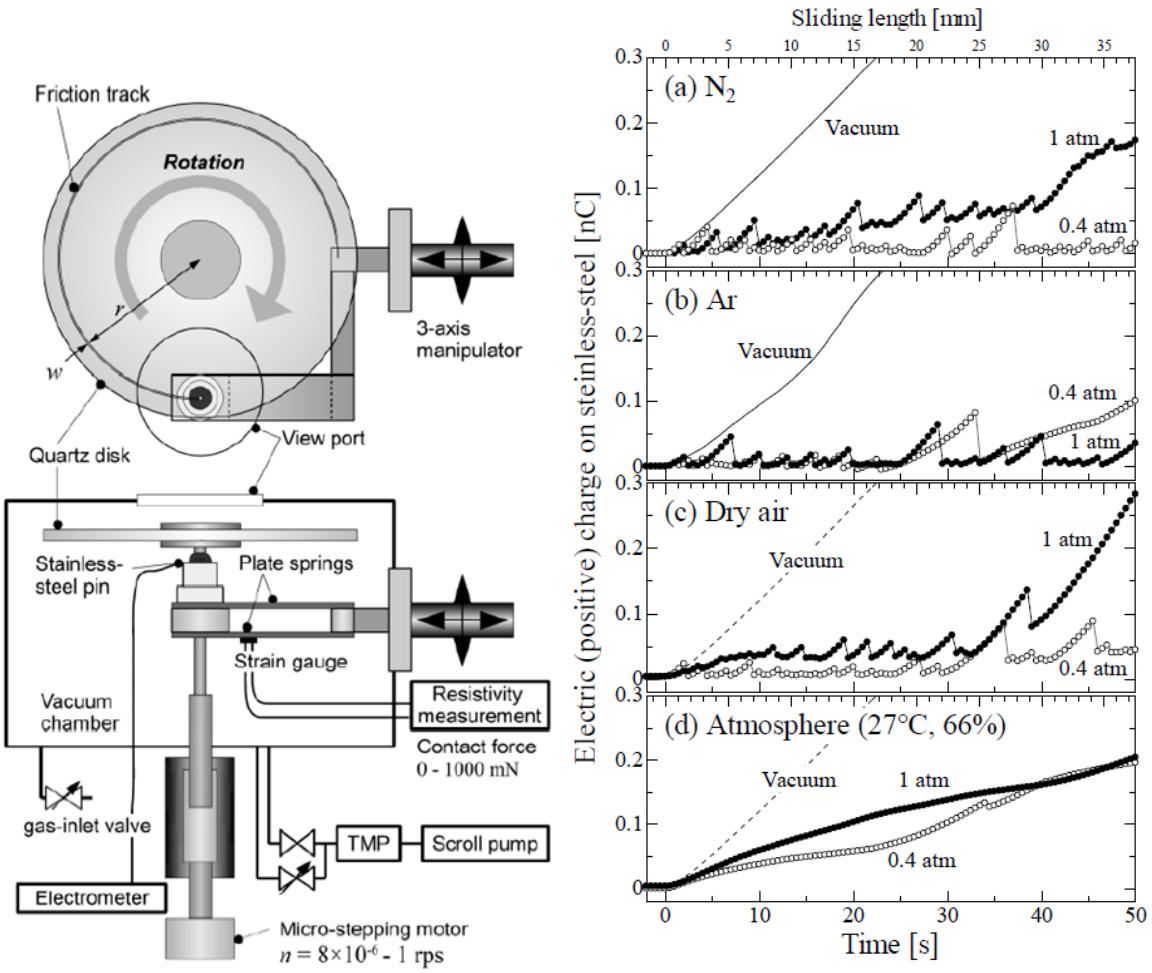

(a) (b)

Fig. 1-10. Experimental apparatus (a); charging results observed for various gases and vacuum (b) (copied from [19]).

In a second study, Miura and Arakawa [20] made use of an insulator pin sliding on a quartz, and a diamond disc (insulator) under nitrogen, neon and krypton atmospheres. In addition to observing the same results, they were also able to photograph the micro-gap discharge during the experiment. In another work, Matsuyama and Yamamoto [21,22] contacted single particles of various polymers against a metal plate in a closed chamber filled with air or argon. The study measured the charge on the particle before and after collision to understand the degree of charge generation due to contact. Their results, presented in Fig. 1-11, showed a smaller charge generation in argon compared to air. The study concluded that the lower breakdown voltage of argon contributed to the lower charge generation.

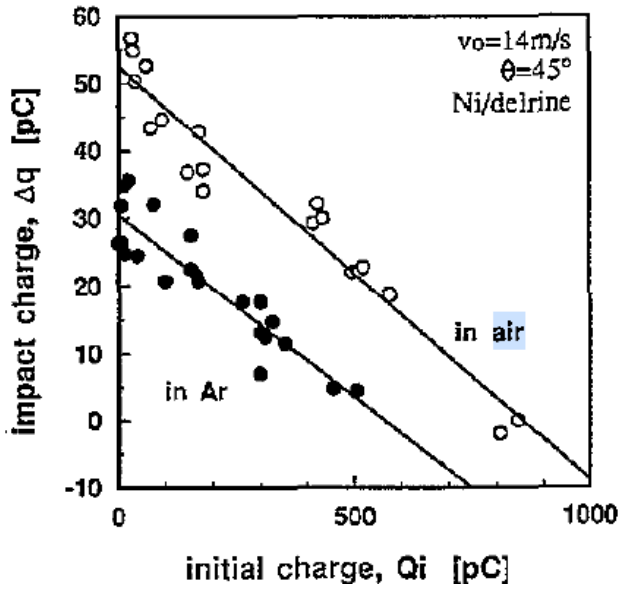

Fig. 1-11. Charge gained by Delrin particles after impact with Nickel plate in air and argon environments (copied from [21]).

1.2 Gas-phase fluidization

Gas-phase fluidization is a key process often employed to dry, coat, combust, and perform reactions with solid components. Fluidization is widely applied in many industries including oil and gas, petrochemical, pharmaceutical, agriculture and food. Gas-solid fluidization employs a gas as the fluidizing agent to convert a static bed of solid particles into a fluid like state. This is achieved by passing the fluidizing gas through the bed of solids until the drag force generated by the upward flowing gas balances the apparent weight of the solid particles. The minimum gas velocity required to fluidize a bed of solids is known as minimum fluidization velocity, U_{mf}. The pressure drop across the bed provides an indication of the initiation of fluidization when it becomes constant while the gas velocity is increased. As the gas velocity is increased beyond minimum fluidization velocity, the bed experiences various flow regimes as shown in Fig. 1-12. In the polymer sector, fluidized bed reactors are used to carry out polymerization reaction. Generally, commercial gas-solid fluidized beds are operated in the bubbling or the turbulent flow regime.

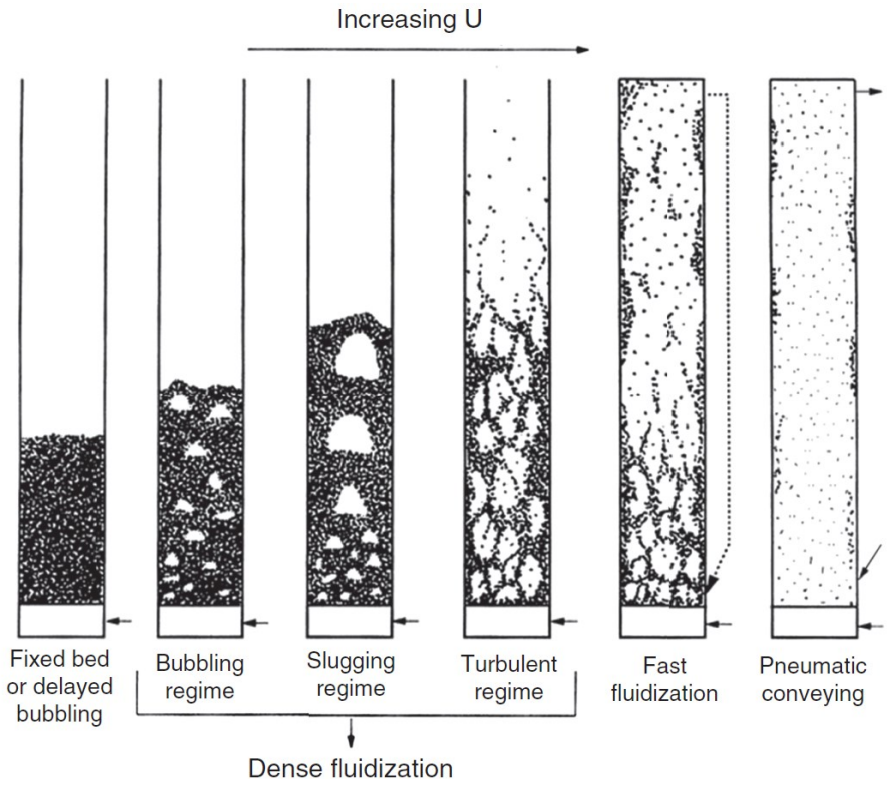

Fig. 1-12. Flow regimes encountered in fluidization operations (copied from [23]).

Regardless of the regime employed, frequent collisions between particles and particles and the fluidization column wall will result in some degree of electrostatic charge generation on all surfaces involved. Solids with poor electrical conductivity tend to hold on to the charges they accumulate. Uncontrolled generation of charge within gas-solid fluidized bed may lead to economic losses in terms of deviations in product quality, material loss, increased load on equipment like compressors, frequent maintenance and may even pose an explosion risk.

1.2.1 Polyethylene process

Polyethylene (PE) is a versatile polymer used in several applications catering to a wide consumer base, ranging from food packaging to plastic consumables. Polyethylene products are usually fabricated through blow moulding, extrusion moulding, and injection moulding methods. Extrusion moulding markets manufacture bottles, polymer tanks, drums, etc., while injection moulding markets produce cups and containers, crates, and enclosures, etc. The blow moulding market produces coatings and films, in addition to sheets, pipes, insulations, reusable bags and sacks [24].

Polyethylene is manufactured through a polymerization reaction of ethylene monomer in the presence of suitable catalysts. The ethylene monomers form a chain which acts as the backbone

of the product with other olefin blocks embedded in between, that act as comonomers. The key feature that imparts the versatility we observe, is the semi-crystalline morphology, which can be manipulated through process controls or suitable additives. Related physical properties like toughness, hardness, conductivity, etc., can be manipulated by controlling the average molecular weight and the concentration of copolymers. Thus, the process conditions dictate the end-use of polyethylene. The American Society for Testing Materials (ASTM) broadly groups polyethylene based on the density as group I with a density of 0.910 to 0.925 g/cm^3, group II with a density range of 0.926 to 0.940 g/cm^3, group III with a density range of 0.941 to 0.959 g/cm^3, and group IV with a density of 0.960 g/cm^3 and higher. Groups I and II are classified in literature as low-density polyethylene and groups III and IV are classified as high-density polyethylene (HDPE). Low-density polyethylene (LDPE) is further sub divided into linear low-density polyethylene (LLDPE) and low-density polyethylene (LDPE) based on the morphology [25].

Commercially, polyethylene is manufactured either through a high-pressure (600 to 3000 atm) process or a low-pressure (30-35 atm) process as shown in Table 1-2 The high-pressure process was initially developed by Imperial Chemical Industries in support of the war effort in the 1930s which produced a branched polyethylene product (LDPE). The discovery of the low pressure, using a transition metallic catalyst, paved the way for production of HDPE products in the 1950s [26]. Due to the rising costs associated with the high-pressure process, interest grew in finding a cheaper alternative for producing LDPE products. Globally, around 70 million metric tonnes of polyethylene were produced in 2010 with a vast majority being manufactured through the low-pressure process. It is estimated that 45% of the total production was under the HDPE market, 30% under the LLDPE market and 25% under the LDPE market [27].

Table 1-2. Process parameters of select polyethylene manufacturing processes [25]

Parameter	Conventional high-pressure process	High-pressure bulk process	Solution polymerization	Slurry polymerization	Gas-phase polymerization
Reactor type	Tubular or autoclave	Autoclave	CSTR	Loop or CSTR	Fluidized or stirred bed
$P_{Reactor}$ (atm)	1200-3000	600-800	~ 100	30-35	30-35
$T_{Reactor}$ (°C)	130-350	200-300	140-200	85-110	80-100
PE Density (g/cm^3)	0.91-0.93	0.91-0.955	0.91-0.97	0.93-0.97	0.91-0.97

Commonly used commercial catalysts in low-pressure gas-phase and slurry processes can broadly be classified as Titanium based (Zeigler), Chromium based (Phillips), and single active-site catalysts (metallocene) [26]. Polyethylene is polymerized using copolymers in addition to the ethylene monomer to regulate the density and molecular weight of the product. Common copolymers include 1-butene, 1-hexene and 1-octene [28]. In addition to comonomers, hydrogen is also used to control the molecular weight of the product [29].

Among the processes mentioned above in Table 1-2, this thesis focuses on the gas-phase polymerization process. Gas-phase processing of polyethylene was discovered in the late 1950s and the first fluidized bed reactors were used in the 1960s. Gas-phase processes completely remove the usage of solvents and diluents and run at a lower pressure [30]. The UNIPOL™ process developed by Univation utilizes a fluidized bed reactor capable of producing a wide range of polyethylene resin. A schematic of the process is shown in Fig. 1-13.

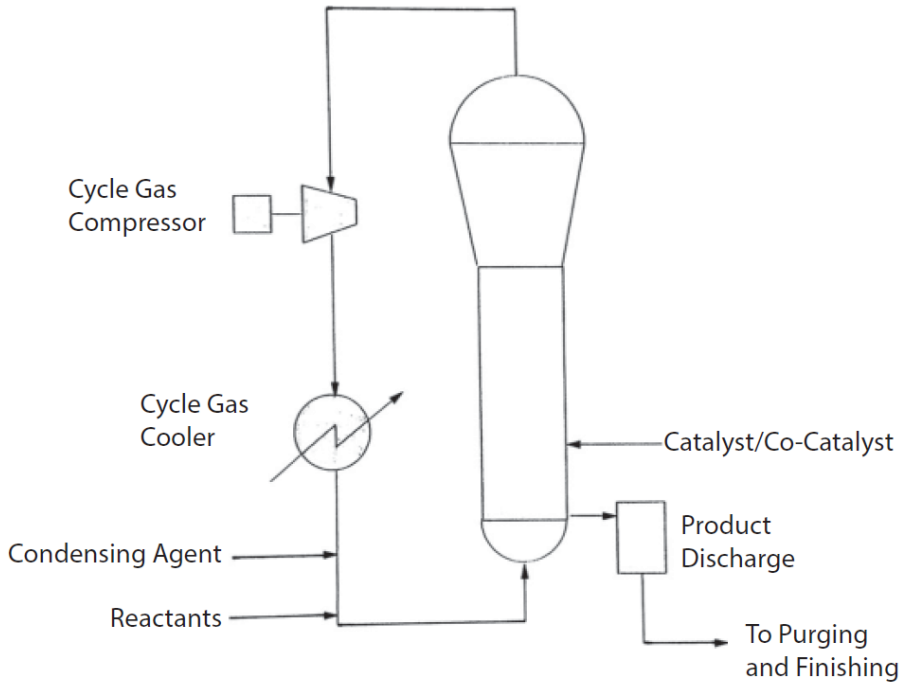

Fig. 1-13. A simple schematic of UNIPOL^{TM} process (copied from [26]).

Ethylene is fed from the bottom of the reactor and the catalyst and co catalyst are introduced above the distributor plate in the reaction zone. Catalyst is fed into the reactor either via solid feeding by pneumatic conveying using inert gases like nitrogen, or via slurry feeding using a liquid [31]. The monomers polymerize on the catalyst and heat of reaction is removed by continuously cooling and recycling the ethylene gas. Fragmentation of the catalyst particles by the polyethylene chain, entrap the active sites, which promotes polymerization. The polyethylene product is continuously removed from the bottom of the reactor and transferred into a separate chamber to be degassed and processed further. The feed rate of ethylene is dictated by several factors which include the comonomer feed rate and the ethylene-hydrogen molar ratio used to regulate the molecular weight of the product. Typically, the UNIPOL^{TM} process is carried out at a temperature range of 60-110°C and a total pressure of 690 to 2500 kPa. A gas analyser located at the expanded section of the reactor monitors the vapour content to adjust the flow of reactants and catalysts [26]. The average residence time of the product is approximately 1 to 2 hours.

1.2.2 Electrostatic charging in PE gas-solid fluidized beds

The solid components used in polyethylene manufacturing are insulative in nature. Thus, as mentioned in earlier sections, tribocharging of polymer particles inside the gas-phase fluidized bed reactor is unavoidable due to continuous collisions among the fluidizing particles as well

as the particles and fluidization column wall. In relation to gas-phase polyethylene process, the persistent and short-lived particle-particle (PE-PE), particle-catalyst (PE-catalyst) and particle-wall contacts during the polymerization reaction, gives rise to electrostatic charge generation within the fluidized bed reactor. The generated charges add to the interparticle forces which leads to agglomeration and adhesion of the particles onto the reactor inner surfaces [32]. Particles that adhere to the reactor wall continue to polymerize, but due to their immobility and the exothermic nature of the reaction, they heat up and fuse together. Since the heat of reaction is not adequately removed by the fluidizing gas, the temperature increases and the polymer particles melt and further fuse together, forming "sheets". This is a common occurrence in the polymer industry, termed as "sheeting" [1]. Fig. 1-14 shows locations where sheeting of polymer particles has been observed in commercial fluidized bed reactors.

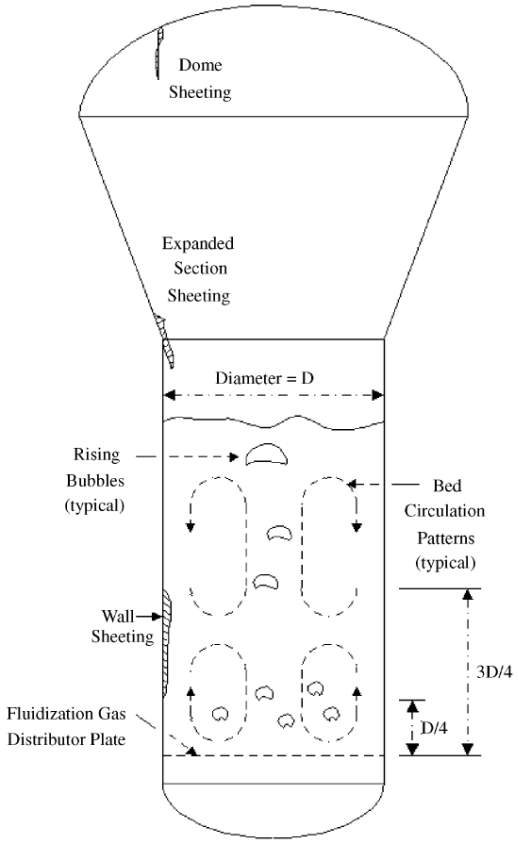

Fig. 1-14. Locations of sheeting occurrence in a fluidized bed reactors (copied from [1]).

Generally, sheeting is classified as warm and cold sheets, depending on the particle characteristics and the temperature observed on the reactor walls [1]. Warm sheets are formed by the adherence of catalyst rich fine polymer particles. The temperature of the reactor wall increases and then gradually decreases as the reaction front moves away from the wall. The core of warm sheets is composed of fine fused polymer while the outer surface is composed of

granular polymer particles. Cold sheets are formed by adhesion of granular polymer particles and subsequent polymerization while stationary. The adhered particles form a sintered sheet as they heat up and reach the sintering temperature. As the sheet thickens, the reactor wall is insulated and the measured skin temperature decreases. The sheets thus formed, peel off from the reactor wall and fall onto the gas distributor plate. In addition to this, uncontrolled sheeting leads to a stunted productivity and mandates reactor shutdown and cleaning. From commercial perspective, this would imply significant economic losses. Typically, a reactor shutdown due to sheeting can span from 2 to 30 days. An approximate marginal estimation of a loss in productivity for a sizeable commercial unit yields economic losses close to USD 2.0M/day.

Regardless of the mechanisms involved, mitigation and control of electrostatic charging within the gas-solid fluidized beds and in particular commercial PE reactors is of utmost importance to industries. In commercial PE reactors, typically, charge generation is attempted to be controlled through reactor wall surface treatment, usage of antistatic agents, charge inducing agents, optimising operating parameters [1].

1.2.3 Parameters that affect charging in fluidized beds

Much work has been carried out previously, including those by this research group, to understand the factors that contribute to triboelectric charging of polyethylene during fluidization. In this regard, the effects of particle size distribution [33], gas velocity [34] and flow regime [35], gas pressure [36], humidity [37], temperature [38], and the addition of antistatic agents (also known as continuity additives) [39] have been studied. These studies conclude that the degree of polyethylene charging and fluidized bed fouling is mitigated when parameter such as fluidization gas velocity and pressure are reduced while that of the temperature is increased. Transition from bubbling to turbulent flow regime was found to significantly aggravate bed charging and fouling [35] while addition of antistatic agents of certain chemistry and at an optimum concentration was found beneficial [39].

A patent by Fulks et al. (1989) [40] concluded that the potential required to initiate sheeting in a commercial polyethylene reactor is a function of reactant gas composition (i.e., they varied H_2 concentration in the reactor), particle size distribution, sintering temperature and the drag forces in play. Recently, Hou et al. [41] looked into on charging of glass beads and HDPE particles while studying the effects of fluidization gas type including argon, nitrogen and air. Their study made use of only one sampling port to collect and measure the charge of a small sample of fluidization particles located near the column wall. The study concluded that argon

decreases the specific charge (charge to mass ratio expressed as Q/m) of HDPE and glass beads in single samples taken from the wall compared to air and nitrogen. However, no results with respect to the degree of wall fouling was measured. Apart from this, in a patent published in 2003 by Gupte et al. [42] the impact of inert gases in pneumatic conveying of amorphous silica (a commonly used catalyst support for polyethylene process) was studied. The work only reported a decline in static charge of calcined silica particles, conveyed through a 0.0635 m inner diameter stainless-steel tube for 30 to 60 minutes using pure helium, argon, and nitrogen as the conveying gas. The static values were obtained by measuring voltage across a small, isolated section of the conveying tube. The patent concluded that helium performed the best, followed by argon and finally nitrogen. Although no experimental results on the impact on polyethylene resin charging and sheeting downstream of the conveying tube was shown, the authors claimed that feeding catalyst particles into a gas-phase polyethylene fluidized bed reactor using a stream of 75% noble gas (helium or argon) could reduce static in the reactor. Although the study did not test the charges within the reactor, the authors speculated that lower voltage read off the tube during conveying is an indication of lower charge on particles and this would have a subsequent impact on charging inside the polyethylene reactor. Besides aforementioned studied, no other work has looked into the effects of gas type on particle charging and fouling behaviours in a fluidized bed.

1.3 Electrostatic Charging in Pneumatic Conveying

Pneumatic conveying systems are employed in pharmaceutical, fertilizer, mineral processing, and other manufacturing industries to handle a variety of particle handling and transportation requirements. The particles in these industries display a wide range of characteristics and vary in their mass flow, size, surface properties, geometry, etc. For instance, in polyethylene manufacturing, certain catalysts are transported and introduced into the reactor system using a conveying tube that makes use of nitrogen as the carrier gas. These tubes can range between 3.18 mm ($1/8^{th}$ inch) to 6.35 mm ($1/4^{th}$ inch) in diameter and include bends and fittings that contribute to contact electrification of the particles being transported. The introduction of catalysts play an important role in maintaining the productivity of the reactor, thus entails economic consequences if failures arise.

Particles conveyed in tubes tend to collide more often with each other and the tube wall owing to the high transport velocity. Thus, triboelectrification in the gaseous environment can occur. In solids conveying systems, it is understood that the magnitude of specific charge is directly related to the solid mass loading [43,44], velocity of the conveying gas [5,43,45], length of the

conveying line [46] and its material of construction [2], mean diameter of the particle and its shape [43], and relative humidity of the conveying gas [2,43]. Sufficiently high specific charge on conveyed particles could disrupt process productivity through particle agglomeration and adhesion on surfaces in contact, and even pose a serious risk of electrostatic discharge and subsequent explosions. Particle agglomeration might even change the particle characteristics which impacts the conveying efficiency, increasing the power demand. Particle fouling might also plug the conveying tube, causing material loss and a drop in productivity. Furthermore, introduction of charged particles might also hinder downstream processes reducing the productivity even more. In polyethylene manufacturing, charged catalyst particles are anticipated to contribute to challenges with their dry feeling flowability in addition to induce an image force [47] within the reactor system which aggravates reactor fouling and compromises the operation.

Aforementioned studies utilize various tube diameters, particles, and operating parameters. Hence, applicability of these results to catalyst conveying in polyethylene manufacturing can only be established through experimentation. The research group at the University of Ottawa has investigated the influence of above-mentioned parameters on the charging behaviour displayed by amorphous silica, which is used as a catalyst support in polyethylene manufacturing [48–51]. Apart from these, studies looking into the impact of catalyst charging on fluidization behaviour are limited.

It is established in section 1.1.5 that triboelectrification of insulators can be reduced under certain gases. Applicability of these findings in pneumatic conveying system however is not thoroughly studied. Studies investigating the impact of different gases on the charging behaviour of conveyed particles aren't available. The patent mentioned in section 1.2.3 [42] is the only study relating the usage of inert gases in reducing static electricity in pneumatic conveying of catalysts in polyethylene manufacturing. Thus, experimentation would be worthwhile in establishing the applicability of low dielectric strength gases on charge regulation in solid handling systems.

1.4 Thesis objective

The motivation that drives this research is to determine ways to mitigate and control the electrostatic charging of solids in gas-solid fluidization and pneumatic conveying. In particular, the goal of this study was to determine how various gases affect the electrostatic charging and subsequent fouling of solid particles on the reactor/conveying tube walls during fluidization

and pneumatic conveying. It was hypothesized that the lower is the dielectric strength of a gas, the less charge is generated on the particles and in turn less fouling is formed.

The specific objectives of this study were to:

- Perform gas-solid fluidization experiments with LLDPE resin using fluidization gases including nitrogen and argon, as well as their mixtures of different compositions. This objective focused on determining the effect of fluidization gas type on the degree of charging of the LLDPE resin, and the resulting fluidization column wall fouling was studied.
- Carry out pneumatic conveying experiments using dehydrated amorphous silica, as a common catalyst base used in the polyethylene process. This objective aimed at investigating the extent of the charging of the conveyed solids and their fouling on the conveying tube walls while using conveying gases that have different dielectric strengths. Argon, which has a lower dielectric strength was compared against nitrogen in controlled trials.
- Conduct bench-scale shake test with LLDPE resin under controlled environment using a single large particle and multiple smaller particles. The objective was to understand, at small-scale, the relation between dielectric strength of gases and the maximum charge attained by particles constantly undergoing collisions.

This research was carried out in relation to the gas-phase polyethylene production process and pneumatic conveying. However, results obtained are applicable to any other gas-solid handling and processing system that experiences electrostatic charging.

1.5 Thesis outline

This thesis includes five chapters of which one chapter is prepared in manuscript form for publication in refereed journals.

The second chapter of this thesis presents the results of gas solid fluidization trials undertaken using various gases. The fluidization experiment was set up with a commercially produced LLDPE resin as the solid particles. Two gases, argon and nitrogen, were considered for the study based on their electrical breakdown voltage. The degree of particles charging and wall fouling of the resin was measured using reliable measurement techniques. This chapter is a

manuscript to be submitted to the Powder Technology journal. This chapter serves as a basis for a patent under evaluation.

The third chapter of this thesis presents the results of pneumatic conveying trials using two gases. The pneumatic injection apparatus was set up with the same objective in mind. Dehydrated amorphous silica was chosen for the study, while the carrier gases remained the same as in Chapter 2. The specific charge of the particles and the fouling of these particles on the conveying tube walls were measured.

The fourth chapter of this thesis presents the results of bench-scale shake tests performed under controlled environment of temperature and relative humidity. The trial studied charging behaviour of large single LLDPE resin and fixed mass of smaller particles of the same resin shaken in an orbital shaker, under the same gases used in Chapter 2.

The fifth chapter collates the results of all the experiments and concludes on the hypothesis presented in the thesis objective. Future scope and recommendations to improve on and validate the findings are also listed out in this final chapter.

References

[1] G. Hendrickson, Electrostatics and gas phase fluidized bed polymerization reactor wall sheeting, Chem. Eng. Sci. 61 (2006) 1041–1064. https://doi.org/10.1016/j.ces.2005.07.029.

[2] G.E. Klinzing, A review of pneumatic conveying status, advances and projections, Powder Technol. 333 (2018) 78–90. https://doi.org/10.1016/j.powtec.2018.04.012.

[3] M.B. John, E.P. John, Using inert gases for pneumatic conveymg, Powder Bulk Eng. (1989) 17–19.

[4] G.E. Klinzing, F. Rizk, R. Marcus, L.S. Leung, Pneumatic Conveying of Solids: A theorical and practical approach, 2010.

[5] M. Nifuku, H. Katoh, A study on the static electrification of powders during pneumatic transportation and the ignition of dust cloud, Powder Technol. 135–136 (2003) 234–242. https://doi.org/10.1016/S0032-5910(03)00163-3.

[6] P. Mehrani, M. Murtomaa, D.J. Lacks, An overview of advances in understanding electrostatic charge buildup in gas-solid fluidized beds, J. Electrostat. 87 (2017) 64–78. https://doi.org/10.1016/j.elstat.2017.03.005.

[7] J. Cross, Electrostatics: Principles, Problems and Applications, 1987. https://doi.org/10.1088/0031-9112/38/11/030.

[8] S. Matsusaka, H. Maruyama, T. Matsuyama, M. Ghadiri, Triboelectric charging of powders: A review, Chem. Eng. Sci. 65 (2010) 5781–5807. https://doi.org/10.1016/j.ces.2010.07.005.

[9] J. Lowell, A.C. Rose-Innes, Contact electrification, Adv. Phys. 29 (1980) 947–1023. https://doi.org/10.1080/00018738000101466.

[10] J.H. Anderson, A comparison of experipmental data and model predictions for tribocharging of two-component electrophotographic developers, J. Imaging Sci. Technol. 38 (n.d.) 378–382. http://cat.inist.fr/?aModele=afficheN&cpsidt=3376350.

[11] F.R. Ruckdeschel, L.P. Hunter, Contact electrification between insulators:

Phenomenological aspects, J. Appl. Phys. 46 (1975) 4416–4430. https://doi.org/10.1063/1.321469.

[12] L.H. Lee, Dual mechanism for metal-polymer contact electrification, J. Electrostat. 32 (1994) 1–29. https://doi.org/10.1016/0304-3886(94)90026-4.

[13] L.S. McCarty, G.M. Whitesides, Electrostatic charging due to separation of ions at interfaces: Contact electrification of ionic electrets, Angew. Chemie - Int. Ed. 47 (2008) 2188–2207. https://doi.org/10.1002/anie.200701812.

[14] P. Jiang, H. Bi, S. -C Liang, L. -S Fan, Hydrodynamic behavior of circulating fluidized bed with polymeric particles, AIChE J. 40 (1994) 193–206. https://doi.org/10.1002/aic.690400202.

[15] M.E. Abdel-kader, W.H. Gaber, F.A. Ebrahim, M.A. Abd Al-Halim, Characterization of the electrical breakdown for DC discharge in Ar-He gas mixture, Vacuum. 169 (2019) 108922. https://doi.org/10.1016/j.vacuum.2019.108922.

[16] K.P. Brand, Dielectric Strength, Boiling Point and Toxicity of Gases - Different: Aspects of the Same Basic Molecular Properties, IEEE Trans. Electr. Insul. EI-17 (1982) 451–456. https://doi.org/10.1109/TEI.1982.298489.

[17] A.E.D. Heylen, Maximization of argon-hydrocarbon Penning mixtures, J. Phys. D. Appl. Phys. 3 (1970) 789–796. https://doi.org/10.1088/0022-3727/3/5/321.

[18] H.R. Hiziroglu, M.S. Dincer, T.D. Nguyen, Breakdown voltages in SF6+argon mixtures under nonuniform electrostatic fields, Conf. Electr. Insul. Dielectr. Phenom. (CEIDP), Annu. Rep. 2 (1997) 579–582. https://doi.org/10.1109/ceidp.1997.641140.

[19] T. Miura, Observation of charge separation and gas discharge during sliding friction between metals and insulators, J. Phys. Conf. Ser. 646 (2015) 0–4. https://doi.org/10.1088/1742-6596/646/1/012057.

[20] T. Miura, I. Arakawa, Gas discharge caused by triboelectricity around a contact during friction between insulators, IEEE Trans. Dielectr. Electr. Insul. 14 (2007) 560–565. https://doi.org/10.1109/TDEI.2007.369513.

[21] T. Matsuyama, H. Yamamoto, Charge relaxation process dominates contact charging of

a particle in atmospheric conditions, J. Phys. D. Appl. Phys. 28 (1995) 2418–2423. https://doi.org/10.1088/0022-3727/28/12/005.

[22] T. Matsuyama, H. Yamamoto, Charge-relaxation process dominates contact charging of a particle in atmospheric condition: II. the general model, J. Phys. D. Appl. Phys. 30 (1997) 2170–2175. https://doi.org/10.1088/0022-3727/30/15/008.

[23] J.R. Grace, H. Bi, Introduction to Circulating Fluidized Beds, Circ. Fluid. Beds. (1997) 1–20. https://doi.org/10.1007/978-94-009-0095-0_1.

[24] A. Peacock, Use and Fabrication of Polyethylene Products, Handb. Polyethyl. (2020) 469–518. https://doi.org/10.1201/9781482295467-20.

[25] T. Xie, K.B. McAuley, J.C.C. Hsu, D.W. Bacon, Gas Phase Ethylene Polymerization: Production Processes, Polymer Properties, and Reactor Modeling, 1994. https://doi.org/10.1021/ie00027a001.

[26] T.E. Nowlin, Business and Technology of the Global Polyethylene Industry, 2014. https://doi.org/10.1002/9781118946039.

[27] Data from www.sriconsulting.com/, (n.d.).

[28] A. Peacock, Commercial Development of Polyethylene, Handb. Polyethyl. (2020) 37–52. https://doi.org/10.1201/9781482295467-4.

[29] S.E. Horne Jr., J.P. Kiehl, J.J. Shipman, V.L. Folt, C.F. Gibbs, Ameripol SN — A C is-1 , 4-Poly isoprene : V, Ind. Eng. Chem. Res. 48 (1956) 784–791.

[30] T.E. Nowlin, Low pressure manufacture of polyethylene, Prog. Polym. Sci. 11 (1985) 29–55. https://doi.org/10.1016/0079-6700(85)90007-3.

[31] Y. Rao, P. Cai, K.J. Cann, F.D. Hussein, W.R. Mariott, P.A. Cao, Patent Issued for Supported Catalyst With Improved Flowability (USPTO 10,676,588), 2020.

[32] A. Sowinski, The Study of Reactor Wall Fouling in Gas-Solid Fluidized Beds Caused by Electrostatic Charge Generation, Dr. Thesis Diss. Univ. Ottawa. (2012).

[33] A. Sowinski, A. Mayne, P. Mehrani, Effect of fluidizing particle size on electrostatic

charge generation and reactor wall fouling in gas-solid fluidized beds, Chem. Eng. Sci. 71 (2012) 552–563. https://doi.org/10.1016/j.ces.2011.11.031.

[34] A. Sowinski, L. Miller, P. Mehrani, Investigation of electrostatic charge distribution in gas-solid fluidized beds, Chem. Eng. Sci. 65 (2010) 2771–2781. https://doi.org/10.1016/j.ces.2010.01.008.

[35] D. Song, P. Mehrani, Comparison of electrostatic charge generation in gas-solid fluidized beds in turbulent versus pre-turbulent flow regime, Powder Technol. 319 (2017) 426–433. https://doi.org/10.1016/j.powtec.2017.07.013.

[36] D. Song, P. Mehrani, Effect of Fluidization Pressure on Electrostatic Charge Generation of Polyethylene Particles, Ind. Eng. Chem. Res. 56 (2017) 14716–14724. https://doi.org/10.1021/acs.iecr.7b04056.

[37] A. Giffin, P. Mehrani, Effect of gas relative humidity on reactor wall fouling generated due to bed electrification in gas-solid fluidized beds, Powder Technol. 235 (2013) 368–375. https://doi.org/10.1016/j.powtec.2012.10.037.

[38] M.I. Nimvari, A. Sowinski, P. Mehrani, Effect of temperature on triboelectrifcation of polyethylene particles in a pilot-scale pressurized gas-solid fluidized bed, Powder Technol. 405 (2022) 117524. https://doi.org/10.1016/j.powtec.2022.117524.

[39] M. Taghavivand, A. Sowinski, P. Mehrani, Triboelectric effects of continuity additives and a silica catalyst support on polyethylene fluidized bed wall fouling, Chem. Eng. Sci. 245 (2021) 116882. https://doi.org/10.1016/j.ces.2021.116882.

[40] B.D. Fulks, S.P. Sawin, C.D. Aikman, J.M. Jenkins III, Process for reducing sheeting during polymerization of alpha-olefins (USPTO 4,876,320-A), 1989.

[41] J. Hou, X. Liu, M.H. Rahman, H. Li, S. Sundaresan, J.R. Grace, X. Bi, Effect of gas properties and wall materials on particle charging in gas–solid fluidized beds, Can. J. Chem. Eng. (2022) 1–12. https://doi.org/10.1002/cjce.24568.

[42] M.K. Gupte, K. Tolley, A. Mutchler, S. Holland, Static reduction (USPTO 6,630,548 B1), 2003.

[43] K. Saleh, A. Traore Ndama, P. Guigon, Relevant parameters involved in tribocharging

of powders during dilute phase pneumatic transport, Chem. Eng. Res. Des. 89 (2011) 2582–2597. https://doi.org/10.1016/j.cherd.2011.06.001.

[44] E.E. Smeltzer, M.L. Weaver, G.E. Klinzing, Individual electrostatic particle interaction in pneumatic transport, Powder Technol. 33 (1982) 31–42. https://doi.org/10.1016/0032-5910(82)85036-5.

[45] N. Schwindt, U. von Pidoll, D. Markus, U. Klausmeyer, M. V. Papalexandris, H. Grosshans, Measurement of electrostatic charging during pneumatic conveying of powders, J. Loss Prev. Process Ind. 49 (2017) 461–471. https://doi.org/10.1016/j.jlp.2017.05.028.

[46] S. Matsusaka, H. Umemoto, M. Nishitani, H. Masuda, Electrostatic charge distribution of particles in gas-solids pipe flow, J. Electrostat. 55 (2002) 81–96. https://doi.org/10.1016/S0304-3886(01)00185-1.

[47] D. Song, P. Mehrani, Mechanism of particle build-up on gas-solid fluidization column wall due to electrostatic charge generation, Powder Technol. 316 (2017) 166–170. https://doi.org/10.1016/j.powtec.2017.01.031.

[48] M. Taghavivand, B. Elchamaa, A. Sowinski, P. Mehrani, Study of electrostatic charging of single particles during pneumatic conveying, Powder Technol. 355 (2019) 242–250. https://doi.org/10.1016/j.powtec.2019.07.046.

[49] M. Taghavivand, B.J. Cho, P. Mehrani, A. Sowinski, Electrostatic charging behaviour of a silica powder during pulse pneumatic conveying, Powder Technol. 366 (2020) 119–129. https://doi.org/10.1016/j.powtec.2020.02.031.

[50] M. Taghavivand, P. Mehrani, A. Sowinski, Triboelectric effects of a pneumatically injected silica catalyst support on polyethylene fluidized bed wall fouling, Powder Technol. 385 (2021) 287–298. https://doi.org/10.1016/j.powtec.2021.03.002.

[51] M.I. Nimvari, M. Taghavivand, K. Choi, A. Sowinski, P. Mehrani, Velocity measurement of pneumatically conveyed particles via a simple current signal technique and the influence of electrostatic charge, Powder Technol. 413 (2023) 118018. https://doi.org/10.1016/j.powtec.2022.118018.

[52] J. Guardiola, V. Rojo, G. Ramos, Influence of particle size, fluidization velocity and relative humidity on fluidized bed electrostatics, J. Electrostat. 37 (1996) 1–20. https://doi.org/10.1016/0304-3886(96)00002-2.

[53] F. Wang, J. Wang, Y. Yang, Distribution of electrostatic potential in a gas-solid fluidized bed and measurement of bed level, Ind. Eng. Chem. Res. 47 (2008) 9517–9526. https://doi.org/10.1021/ie800805t.

[54] W.O. Moughrabiah, J.R. Grace, X.T. Bi, Effects of pressure, temperature, and gas velocity on electrostatics in gas-solid fluidized beds, Ind. Eng. Chem. Res. 48 (2009) 320–325. https://doi.org/10.1021/ie800556y.

[55] A.C. Hoffmann, J.G. Yates, Experimental Observations of Fluidized Beds at Elevated Pressures, Chem. Eng. Commun. 41 (1986) 133–149. https://doi.org/10.1080/00986448608911716.

[56] X. Liu, S. Sundaresan, The effect of gas on tribocharging of particles in a vibrated bed, Powder Technol. 401 (2022) 117272. https://doi.org/10.1016/j.powtec.2022.117272.

[57] C.Y. Wen, Y.H. Yu, A generalized method for predicting the minimum fluidization velocity, AIChE J. 12 (1966) 610–612. https://doi.org/10.1002/aic.690120343.

[58] F. Chowdhury, A. Sowinski, M. Ray, A. Passalacqua, P. Mehrani, Charge generation and saturation on polymer particles due to single and repeated particle-metal contacts, J. Electrostat. 91 (2018) 9–15. https://doi.org/10.1016/j.elstat.2017.11.004.

[59] F. Chowdhury, B. Elchamaa, M. Ray, A. Sowinski, A. Passalacqua, P. Mehrani, Apparatus design for measuring electrostatic charge transfer due to particle-particle collisions, Powder Technol. 361 (2020) 860–866. https://doi.org/10.1016/j.powtec.2019.11.013.

[60] F. Chowdhury, M. Ray, A. Passalacqua, P. Mehrani, A. Sowinski, Electrostatic charging due to individual particle-particle collisions, Powder Technol. 381 (2021) 352–365. https://doi.org/10.1016/j.powtec.2020.12.012.

Chapter 2 Effect of Dielectric Strength of Gases on the Degree of Wall Fouling and Electrostatic Charge Generation in an Atmospheric Gas-Solid Fluidized Bed

Nikhil Sridhar, Poupak Mehrani

Department of chemical and biological engineering, University of Ottawa, 161 Louise Pasteur, Ottawa, ON K1N 6N5, Canada

Manuscript to be submitted to the Journal of Powder Technology

Abstract

The aim of this work was to study the impact of dielectric strength of the gas on charging of a commercially produced polyethylene resin fluidized in a stainless-steel column and its subsequent fouling on the column inner surface. The study utilized nitrogen, argon, and binary mixtures of the two in varying concentrations to fluidize polyethylene resin. Successive fluidizations where the bed was fluidized with argon for a short period after fluidization with nitrogen were also carried out to explore the feasibility of using argon in commercial reactors to mitigate sheeting. Fluidization with pure argon resulted in the lowest specific charge and reduced the fouling by 90% relative to pure nitrogen. The fouling and net charge of the particles in the mixture trials were in between the two pure gases showing a decreasing non-linear trend as the concentration of argon increased. Even presence of 10 vol.% argon in the mixture reduced the wall fouling by 50%. Successive fluidization also yielded a positive result with fouling and specific charge values comparable to pure argon. The results showcased by argon and the mixtures are attributed to argon's relatively low dielectric strength. Localized gas discharge within the particle-dense section of the fluidized bed is assumed to dissipate and limit the charges on the polyethylene particles; thereby reducing fouling.

Keywords: Fluidization, triboelectrification, electrostatics, gas type, polyethylene, dielectric strength.

2.1 Introduction

Industries that employ solids and particulates in their processes at times report electrostatic charge generation while processing and handling them. These charges are generated when solid particles collide with each other and nearby surfaces. The charged particles are susceptible to

electrostatic forces that hinder the process and introduce risks which mandate additional controls to maintain efficiency and prevent economic loss. Examples of processes where electrostatic charge generation can be detrimental include pneumatic conveying, size reduction (e.g., grinding), gas-phase fluidization, etc. Fluidization technology is widely applied in many industries including oil and gas, petrochemical, pharmaceutical, agriculture and food. In the polymer sector, fluidized bed reactors are used to carry out polymerization reaction. For example, polyethylene (PE) which is a commercially significant product, is manufactured through the polymerization of ethylene monomers in gas-phase catalytic fluidized bed reactors. The vigorous solids mixing patterns in gas-solid fluidized beds makes them highly susceptible to electrostatic charge generation. For instance, electrostatic charge generation is a common cause of concern in gas-phase polyethylene fluidization process. In these reactors, the significant contacts among the polyethylene particles, as well as their contacts with the reactor wall and catalyst particles generate electrostatic charges through triboelectric charging. This in turn leads to adherence of highly charged polyethylene and catalyst particles onto the reactor wall. Prolonged adhesion then causes localized polymerization reaction to occur without any reaction heat being removed from the region. This leads to formation of melted and fused polymer particles knowns as “sheets” [1]. These sheets, subsequently dislodge from the reactor wall and fall onto the gas distributor plate, thereby destabilizing the bed hydrodynamics and in turn causing a drop in productivity and mandating reactor shutdown. Sowinski [32] as well as Song and Mehrani [47] proposed that fluidizing particles migrate and adhere onto the column wall when the net sum of horizontal forces imparted due to electrostatic forces are greater than the net of vertical forces which consists of the weight of the particle and the drag force exerted by the upward flowing gas.

Electrostatic charging of insulators, such as polymers, have been extensively studied and multiple theories are put forth to explain the mechanisms at work behind charge generation, accumulation, and transfer. Mechanisms behind charge dissipation, however, are still not completely understood. In relation to polyethylene industry, prevention, or regulation of sheeting and electrostatic charge generation within the system is of utmost importance. The research group at the University of Ottawa has studied electrostatics in fluidized beds to better understand the underlying mechanisms involved. Their studies, as well as others, include the influence of fluidization gas velocity, fluidization particle properties, and system operating parameters on the degree of electrostatic charge generation and the extent of wall fouling [6]. Thus far, the effects of particle size and distribution [33,52,53], gas humidity [37,52], gas

velocity [34,52,54], fluidization flow regime [35], fluidization pressure [36,54,55], temperature [38,54], and addition of continuity additives [39], have been studied.

One parameter that has received limited attention but is of significant importance is the type of fluidizing gas and its effect on the degree of particles charging and fluidization column wall fouling. Couple of studies have reported that electrostatic charge generation is lower in an argon atmosphere compared to air or nitrogen. These studies are not related to fluidization, yet their results are very much relevant. Miura [19] measured the electrostatic charge on a metal pin (conductor) sliding on a quartz disc (insulator) in a closed chamber under vacuum and various gaseous environments. In vacuum, he observed that the charge on the pin rose without any dissipation. However, under argon, the charge generated underwent dissipation frequently. Frequency of charge dissipation and the magnitude of charge dissipation was lower in dry air, ambient air, and nitrogen in comparison to argon. Miura attributed this dissipation to the breakdown of the gas molecules around the pin. When reviewing literature to find the maximum charge that a particle can possess, we find that it is limited by the breakdown strength of the surrounding gas [7]. If the charge and the subsequent electric field applied by the charge exceed the gas breakdown strength, the gas molecules ionize and neutralize the surface charge of the neighbouring objects. Thus, the findings of Miura are in line with literature, considering argon's lower breakdown voltage relative to air and nitrogen as shown in Table 2-1. A second study by Miura and Arakawa [20] made use of an insulator pin sliding on a quartz and a diamond disc (insulator) under nitrogen, neon and krypton atmospheres. In addition to observing the same results, they were also able to photograph the micro-gap discharge during the experiment.

Table 2-1. Dielectric strength of various gases at 0.1 MPa and 20°C.

Gas	**Dielectric strength** [16] **kV/mm**
Neon (Ne)	0.05
Argon (Ar)	0.6
Air (Calculated)	3.25
Nitrogen (N_2)	3.4
Sulfur hexafluoride (SF_6)	8.86

In another work, Matsuyama and Yamamoto [21,22] contacted single particles of various polymers against a metal plate in a closed chamber filled with air or argon. The study measured the charge on the particle before and after collision to understand the degree of charge generation due to contact. Their results showed a smaller charge generation in argon compared to air and the authors concluded that the lower breakdown voltage of argon contributed to the lower charge generation on the particles. The Matsuyama and Yamamoto study also outlines a charge relaxation model that considers the change in potential difference between two charged objects after contact. Matsusaka [8] reported the usage of the condenser model as a possible mechanism of polymer particle charging wherein the region between the two objects is considered to represent a capacitor. According to the condenser model, if the capacitance of the imaginary capacitor is *C*, then the charge transferred is related to the potential difference as:

$$V = \frac{\Delta q}{k_C C} \qquad \text{Equation 2-1}$$

$$C = \frac{\varepsilon_0 S}{z_0} \qquad \text{Equation 2-2}$$

where, Δq is the charge difference, k_c is the charging efficiency, ε_0 is the absolute permittivity of the gas, S is the area of contact, and z_0 is the gap distance.

Assuming the condenser model is valid, when two charged surfaces make contact and then separate, the potential difference between the surfaces increases as the gap between them increases, eventually reaching the limit imposed by the breakdown of the surrounding gas. This increase in potential is due to reduction of the capacitance as shown in equation 2-1. Thus, the possibility of gas breakdown is highest after particles make contact and separate.

In a recent work, Liu and Sundaresan [56] studied the charging of soda lime (mean diameter of 1.46 mm and 2.2 mm) and polyethylene particles (mean diameter of 2.1 mm) under pure argon and pure nitrogen in a small bench-scale (50.8 × 50.8 × 114.3 mm) vibratory bed made of PMMA. The study made a similar conclusion in attributing the lower breakdown voltage of argon for the lower magnitude of charge observed on both particles at different mass loadings.

Although the studies listed above provide some very relevant information regarding the influence of gas type, the usage of different gases in a fluidization setup yielded minimal results. Only one study [41] investigated the effects of gas type on charge generation, but no

study reviewed the effect of gas type on degree of fluidization column wall fouling. Hou et al., studied the influence of pure gases including argon, nitrogen, and air (dry and humid) on the charging behavior of high-density polyethylene (HDPE) particles and soda lime glass beads fluidized in a stainless steel and acrylic columns [41]. The study makes use of only one sampling port to collect and measure the charge of the small amount of particles located near the fluidization column wall. The study concluded that argon decreases the specific charge (charge to mass ratio expressed as Q/m) of HDPE particles and glass beads compared to air and nitrogen in both the columns. However, no data with respect to the degree of wall fouling was measured. The study also employed a single sampling port, which may not yield a representative sample for analysis and might not give an accurate indication of the extent of charging of particles within the fluidized bed.

The only other work listed in open literature which relates the effect of gas type, and a gas-phase polyethylene fluidization system is a patent by Gupte et al. [42]. The work only reported a decline in static charge of calcined silica particles, used as a catalyst base, conveyed through a 6.35 mm inner diameter stainless-steel tube for 30 to 60 minutes using pure helium, argon, and nitrogen as the conveying gas. The static values were obtained by measuring voltage across a small, isolated section of the conveying tube. The patent concluded that helium performed the best, followed by argon and finally nitrogen. Although no experimental results on the impact on polyethylene resin charging and sheeting downstream of the conveying tube was shown, the authors claimed that feeding catalyst particles into a gas-phase polyethylene fluidized bed reactor using a stream of 75% noble gas (helium or argon) could reduce static in the reactor.

The gas-solid fluidization apparatus at the University of Ottawa is equipped with a unique charge measurement technique, which provides a clear picture of fluidizing particles charge distribution inside the bed in three regions (i.e., in the bulk, fouled layer on the column wall, and entrained particles). Most importantly, this apparatus uniquely provides comprehensive information regarding the amount of the wall fouling (i.e., fouled layer mass, charge, and particle size distribution). Thus, using this apparatus, the aim of this study was to investigate the degree of charge generation and subsequent adhesion of particles to the column wall using various pure fluidizing gases in addition to their mixtures with various composition.

2.2 Materials and methods

The fluidization apparatus used in this study is shown in Fig. 2-1. The setup consists of a stainless-steel fluidization column, 1.2 m in height and 0.1 m in diameter. The column is fitted with two Faraday cages, one at the top of the column and one at the bottom below the distributor plate. A filter bag is affixed to the top of the column, inside the top Faraday cage, to capture fine particles entrained by the fluidizing gas. A knife gate valve located at the bottom of the column, just above the bottom Faraday cage acts as a removable distributor plate. The gate of the valve is a stainless-steel plate that is perforated to act as a distributor plate. A mass flow controller was used to measure and regulate the flow of gas into the column. The relative humidity and temperature of the fluidizing gases were measured using a hygrometer located on the inlet gas piping. A second hygrometer was placed near the fluidization column to monitor and record the laboratory's relative humidity and temperature. The electrostatic charge of the fluidizing particles was measured via the two Faraday cages each connected to a digital electrometer (Keithley 6514). LabVIEW software was used to control and record critical parameters during and after each experimental trial.

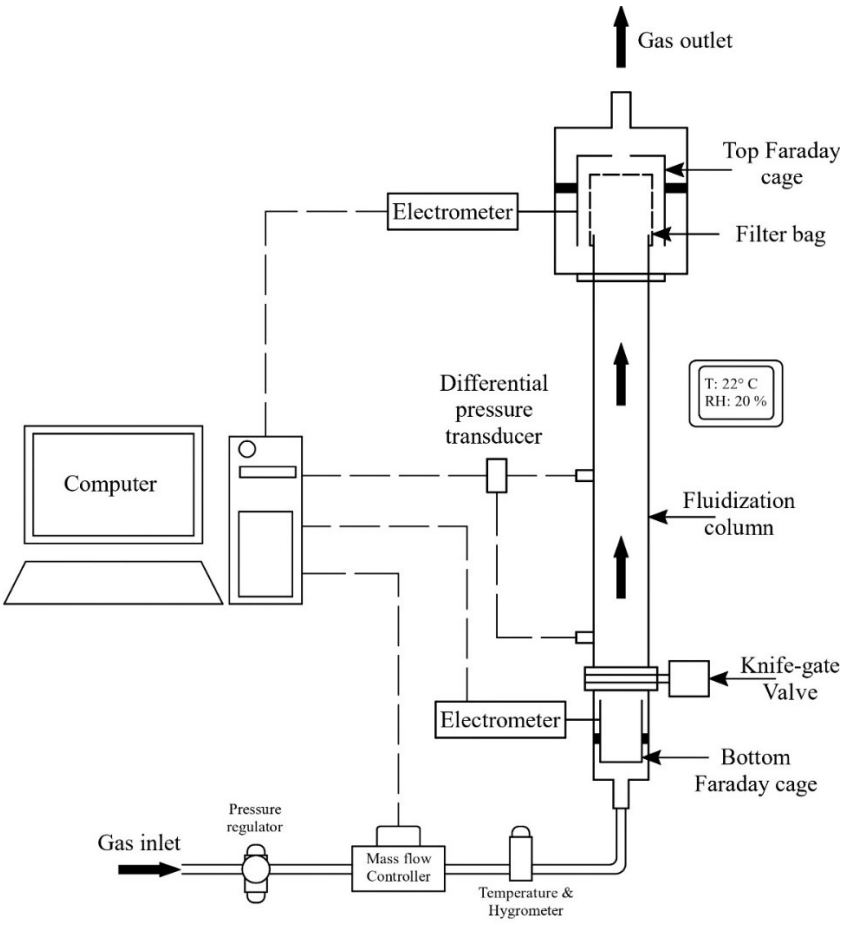

Fig. 2-1. Fluidization apparatus used in this study.

The particles used in this work were metallocene based linear low-density polyethylene (LLDPE) resin received directly from commercial reactors. Table 2-2 outlines the critical properties of the particles. Pure argon and nitrogen were tested as the fluidizing gases in addition to their mixtures with various composition. Table 2-3 summarizes the critical parameters for the gases used.

Prior to the commencement of the trials, the minimum fluidization velocity (U_{mf}) corresponding to the gases used and the particle size distribution of the resin were experimentally measured and cross verified using the Wen-Yu correlation [57]. The measurements were carried out by gradually increasing the flow rate of the gas used and measuring the pressure drop across the fluidized bed.

Table 2-2. Particle characteristics

Particle Type	LLDPE Resin
Particle Size distribution (μm)	20-2000
Particle Sauter-mean diameter (μm)	947
Particle density (kg/m^3)	917

Table 2-3. Pure gas and binary gas mixture properties at 23 ± 2°C and 1 atm pressure.

Gas type	**Density (kg/m^3)**	**Viscosity (Pa. s)**	**Minimum Fluidization Velocity (m/s)**
Pure Nitrogen	1.16	1.76×10^{-5}	0.219
Pure Argon	1.64	2.23×10^{-5}	0.182
10 vol% Argon + 90 vol% Nitrogen	1.21	1.81×10^{-5}	0.215
25 vol% Argon + 75 vol% Nitrogen	1.28	1.89×10^{-5}	0.210
50 vol% Argon + 50 vol% Nitrogen	1.41	2.01×10^{-5}	0.201

Fresh batches of LLDPE resin were weighed and poured into the column from the top after ensuring that the knife gate valve was fully closed. For each trial, 1 kg of resin was used. The filter bag was attached to the top of the column and the top Faraday cage was then mounted. The superficial velocity of the fluidizing gas was set to be 0.1 m/s higher than the U_{mf} (U- U_{mf} = 0.1 m/s). Gas flowrate was changed by a set increment of 10-15 SLPM until the desired flowrate was reached. 1 minute interval was provided between each flowrate increment. Once

the desired gas flowrate was reached, fluidization was performed for 50 minutes. During the fluidization period, the charge of the entrained fines was cumulatively measured via the top Faraday cage. After the completion of the fluidization period, gas supply was stopped. The top Faraday cage and the filter bag were removed, and the mass of fines collected in the top filter bag was measured. The electrostatic charge on the particles in the bulk of the bed was then measured by opening the knife gate valve and allowing the particles to fall into the bottom Faraday cage. The Faraday cage was then removed, and the collected particles mass measured. Thus, the charge-to-mass ratio (Q/m) of the bulk particles was calculated. After removing the bottom Faraday cage, the inner fluidization column wall was inspected for any wall fouling. Images were taken from the fouled layer for qualitative evaluation of the extent of the wall fouling due to electrostatics. Fig. 2-2 shows an example of such image. The Faraday cage was cleaned and reattached. The particles adhering on to the column wall were then dislodged into the bottom Faraday cage using jets of compressed dry air via a narrow tube inserted into the column from its top. The particles fell into the bottom Faraday cage and subsequently, their charge and mass were measured, and their Q/m was calculated. The inner walls of the column were then cleaned from any residual particles left and the column was vented with dry air for at least an hour before the next trial was conducted. Fig. 2-3 shows the classification of fouled particles and distribution along the column inner surface. Region 1 encompassed the column wall in contact with the static bed height, and region 2 encompassed the column wall from the static bed height to the column exit. Each trial was repeated at least twice to establish reproducibility.

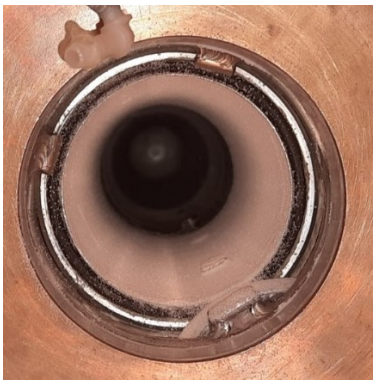

Fig. 2-2. Polyethylene resin fouled onto the inner wall of the fluidization column (*white layer of coating from the bottom of the column to the expanded bed height*) after 50 minutes of fluidization with nitrogen. Image taken from the bottom of the column after the removal of bulk particles.

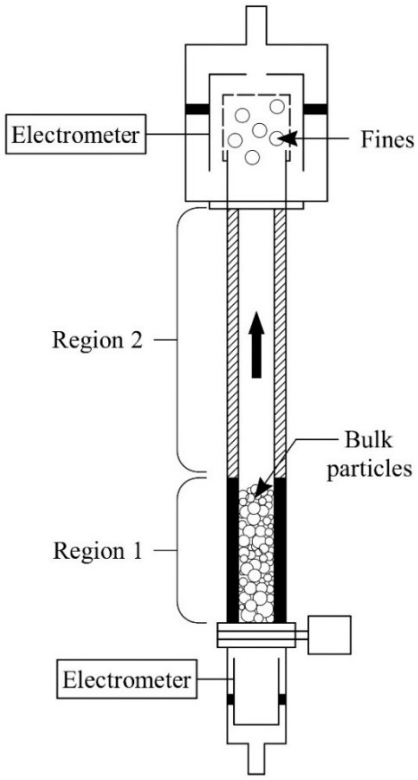

Fig. 2-3. Column schematic representing the distribution of fouled particles and their classification.

2.3 Results and discussions

The net specific charge of the resin was measured prior to pouring the particles inside the fluidization column for each trial. This specific charge was on average 0.22 ± 0.1 nC/g.

2.3.1 Pure gases

Fig. 2-4 shows the net specific charge of the bulk particles and the particles that adhered to the column wall in region 1. For the bulk of the particles, argon resulted in a significantly lower specific charge of 0.16 nC/g compared to 0.37 nC/g in nitrogen. Although the average net specific charge of fouled particles in region 1 was lower in argon, the standard deviation was significantly higher. This was attributed to the minute magnitude of charge and the equally small mass of particles in region 1 when fluidized with argon. The charges were -13 nC and 69 nC and the corresponding masses were 1.32 g and 0.5 g for the two repeated trials. The negative polarity of the first trial could be due to the presence of finer particles on the wall surface as bipolar charging is usually observed among particles with a wide size distribution.

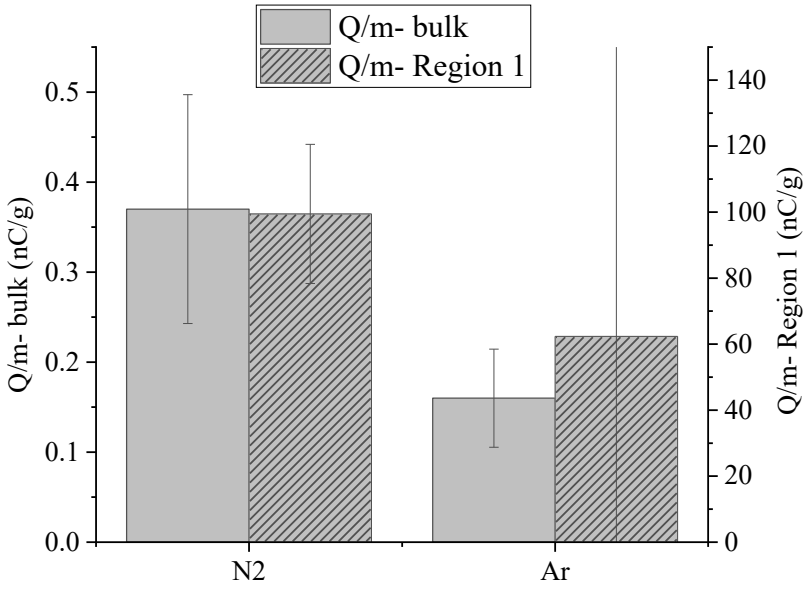

Fig. 2-4. Degree of charging expressed as specific charge (Q/m) of bulk particles and fouling in region 1 as a function of gas type.

Images of the column inner wall taken after fluidization with nitrogen (Fig. 2-5a) and argon (Fig. 2-5b) give a visual comparison between the two conditions. The white layer seen in Fig. 2-5a stretching from the bottom of the column to the expanded bed height is the fouled resin while in Fig. 2-5b the same region is almost clear of any particles. Analogous to the net specific charge results, total fouling (i.e., fouling in region 1, plus region 2) observed when using pure argon gas were significantly less compared to pure nitrogen with a reduction close to 90% observed (Fig. 2-6).

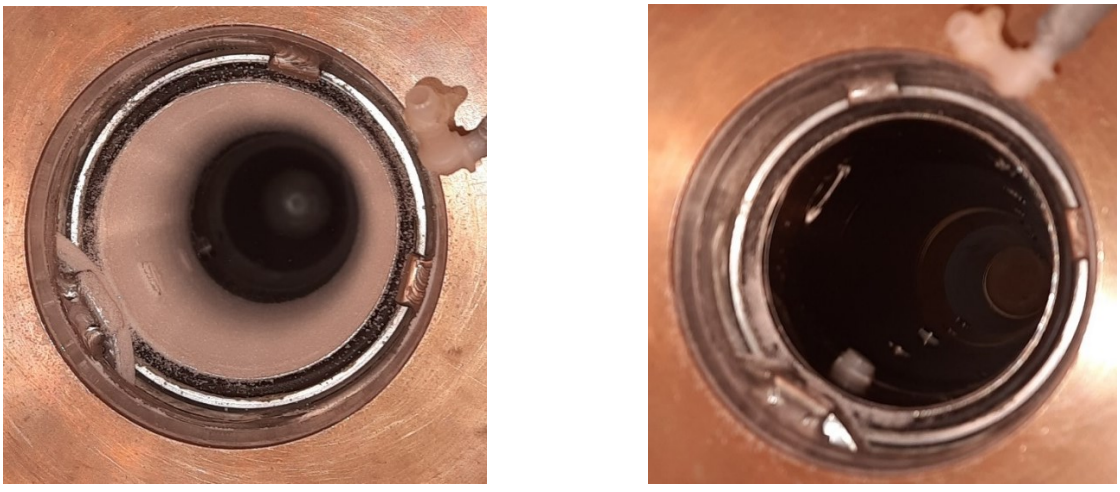

(a) (b)

Fig. 2-5. Image showing the degree of particle fouling on the inner column wall after a 50-minute fluidization trial with (a) nitrogen; and (b) argon.

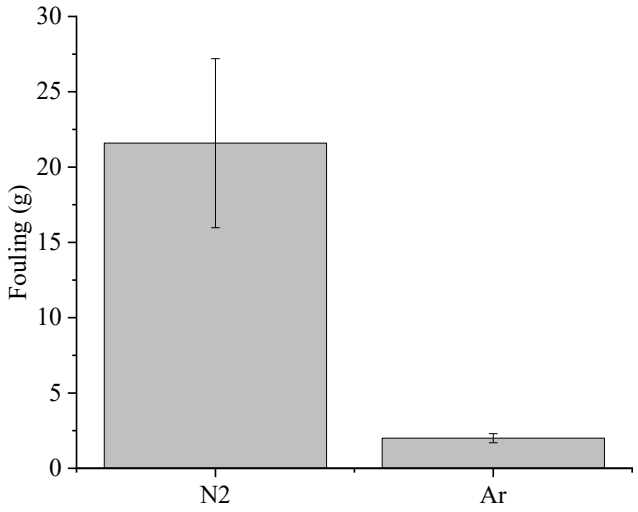

Fig. 2-6. Degree of total column wall fouling with different fluidization gases.

The distribution of the total mass of fouled particles and entrained fines is shown in Fig. 2-7. Results clearly imply that argon influenced the degree of fouling in region 1, while neither region 2 nor the entrainment of fines were impacted.

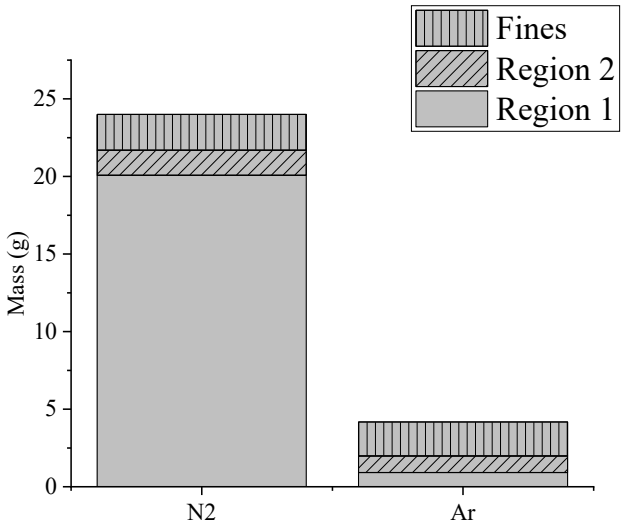

Fig. 2-7. Mass distribution of total column wall fouling observed along with the mass of entrained fine particles with different fluidization gases.

2.3.2 Gas mixtures and successive fluidization

Upon observing a significant reduction in the magnitude of wall fouling when fluidization was carried out with argon gas, experiments with mixture of argon and nitrogen were conducted to identify whether small amounts of argon will be beneficial in reducing charge generation and column wall fouling. In addition to mixture fluidization where the binary gases were fed simultaneously, successive fluidization was also carried out wherein the particles were fluidized by pure nitrogen first and then switched over to pure argon gas for a predetermined interval of time. The reasoning behind this approach was to explore the possibility of using argon in industrial reactors as soon as deviations arise in operating parameters (change in reactor temperature or voltage) due to sheeting formation. Ideally, switching over to argon would resolve the deviations and normal operations can be resumed.

The results for the net specific charge of bulk particles obtained for pure gas fluidization trials are compared with that of the gas mixture trials and successive fluidization trials in Fig. 2-8. Bulk particles consist of larger particles that would not foul onto the column wall, in addition to particles that are charged insufficiently to adhere to the wall. Thus, it is assumed that a major chunk of particles fouled in region 1 in nitrogen, would end up in the bulk when fluidized by gas mixtures.

Adhesion of particles to the column wall implies the presence of sufficient electrostatic forces within the column. Thus, region 1 particles specific charging results shown in Fig. 2-8 offer a better perspective into the influence of argon in charge reduction. Although pure argon and pure nitrogen trials show a stark difference in their results, mixture trials fall in between the two ends. 10% trial and 50% trials, however, show a slight deviation. In addition to the two mixtures, successive fluidization also showed a deviation from the expected trend. Thus, results were further evaluated by plotting the net charge (Q) held by the particles in region 1, as shown in Fig. 2-9, which showed a decline in charge values as the concentration of argon in the mixture increased. Additionally, successive fluidization exhibited a considerably lower net charge in region 1 compared to corresponding volume-split binary gas mixture trials.

Since the specific charge is dependent on the mass of the particles collected, a lower mass would result in a larger specific charge, even if the absolute charges are the same. Thus, considering the variability in the mass of the bulk and fouled particles collected for different gas mixtures and the slight discrepancies in collecting said particles, this deviation can be justified.

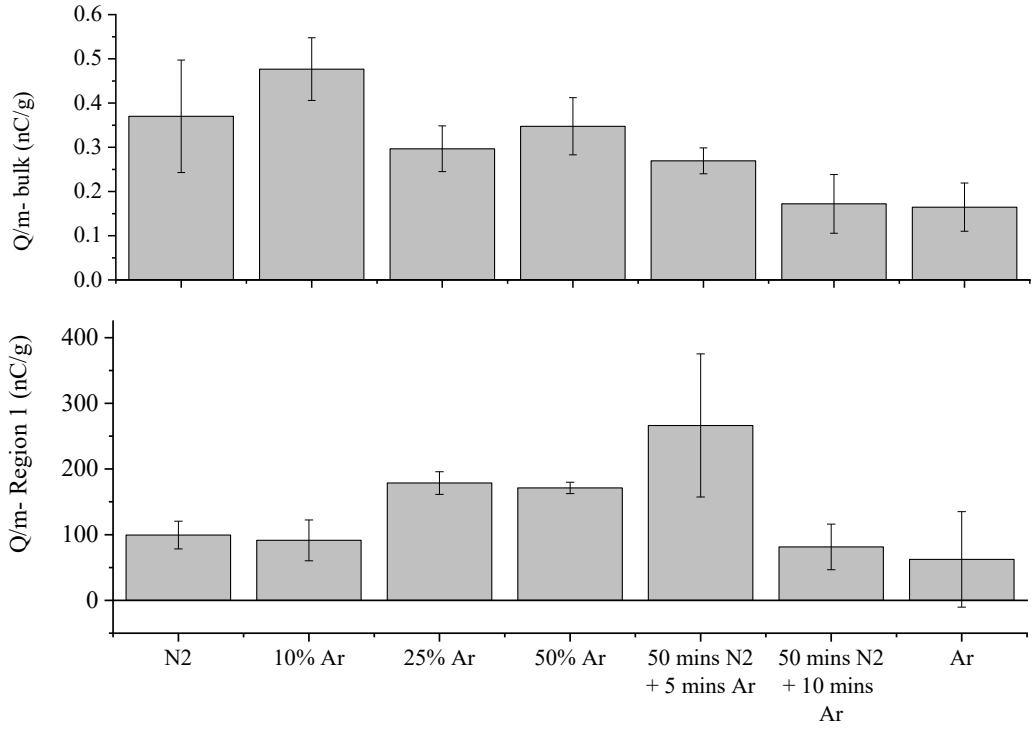

Fig. 2-8. Degree of charging expressed as specific charge (Q/m) of bulk and region 1 particles as a function of gas composition for gas mixtures and successive fluidization trials.

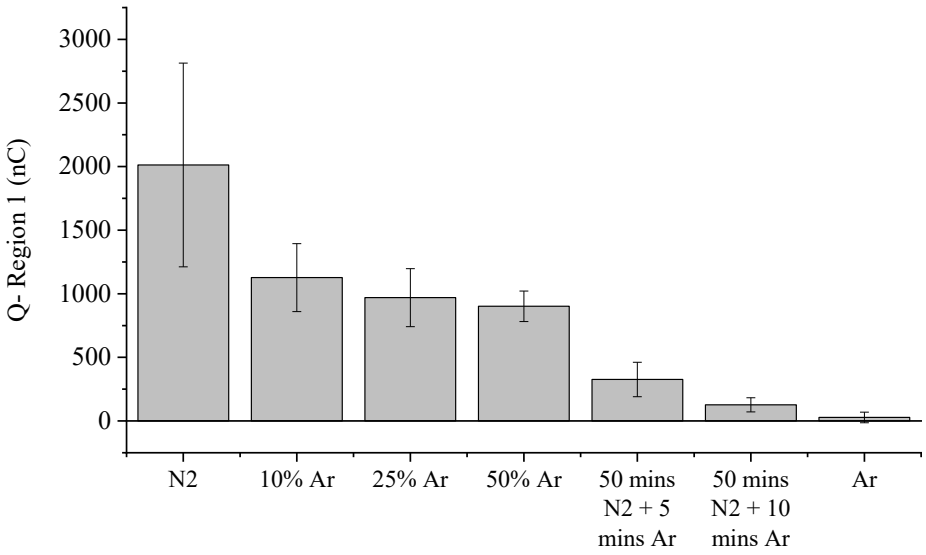

Fig. 2-9. Degree of charging expressed as net charge (Q) of region 1 particles for pure gases and mixtures, and successive fluidization trials.

Significant results were obtained with respect to the degree of column wall fouling. Fig. 2-10a shows a decline with a non-linear trend in the total fouling for the mixture trials with the majority of the decline being observed in region 1. The trial with 10 volume % argon mixture

showed an approximate 50% reduction, and trial with 25 volume % argon showed an 80% reduction in fouling compared to testing with pure nitrogen. The 50 volume % argon trial, however, was only marginally better than 25 volume % in terms of fouling reduction. On an industrial scale, 50% reduction in fouling is quite attractive particularly when using only 10% of argon to reduce static.

In addition to the mixture trials, successive fluidization (Fig. 2-10b) showed a similar disposition. This is noteworthy since the overall volume of argon used in the two trials correspond to 8% and 15% of the total volume of gas. Moreover, compared to binary gas fluidization, successive fluidization even at the lowest tested argon volumes (8%) performed much better and on a range closer to pure argon. From the trials so far, it is evident that the relationship between concentration of argon and the degree of fouling is not linear. These results are of significant importance because they imply that even small quantities of argon (e.g., successive fluidization or 10% argon volume mixtures) might be beneficial in reducing the extent of solids charging and consequently their deposition on surfaces. Furthermore, argon's inertness would not severely impact established processes, making it suitable for a variety of industrial applications. In relation to commercial gas-phase polyethylene process such approach will be of great impact in improving reactor productivity while simultaneously being cost-effective.

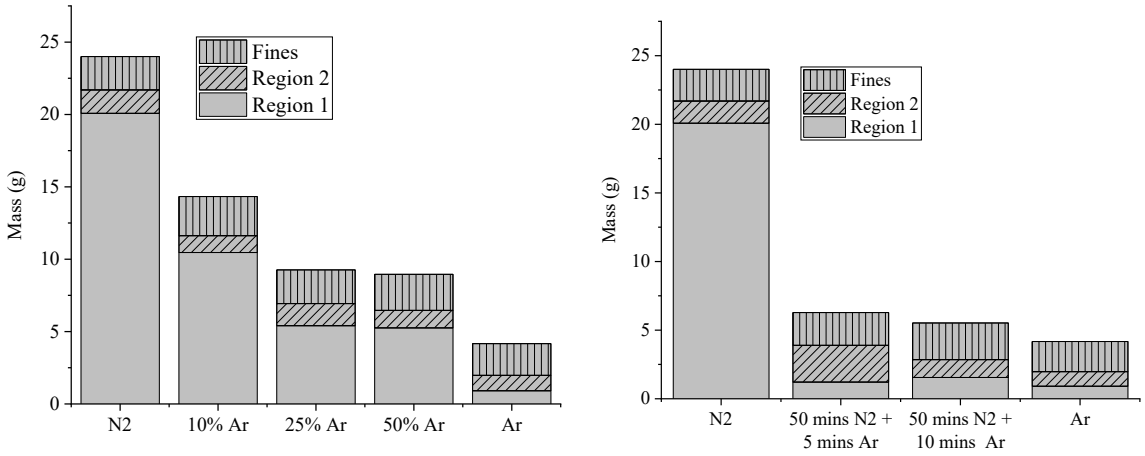

Fig. 2-10. Distribution of degree of wall fouling between regions 1 and 2, and amount of fines entrained for (a) pure gases and mixtures; and (b) successive fluidization trials.

2.4 Discussions

The influence of argon was clearly observed in the trials undertaken, even in small volumes. The consensus regarding the observation is directed at argon's lower breakdown voltage relative to nitrogen. Previous studies have supported this line of thought and the current study produces agreeable data. The mass distribution within the total wall fouling observed among nitrogen and argon trials as well as the gas mixture trials, support the hypothesis of substantial gas breakdown occurring in region 1 since the majority of the decline is observed in this region. The degree of particle contacts and separation is largest in region 1 that corresponds to the height between the distributor plate and static bed height, thus it can be assumed to house the largest density of electrostatic potential differences. Hence, it would be satisfactory to assume that the majority of charge dissipation occurs in region 1. Furthermore, it appears that a lower bulk particle charge implies a lower degree of fouling. The pure gases and the mixture trials showcased a direct relationship between fouling and bulk particle charge. Even though the particles adhering to the column wall display a larger and sometimes unexpected specific charge, the distribution of net charge on these particles further support the findings.

Upper region 2 that includes the splash zone and the freeboard, show limited charge dissipation due to infrequent contacts between the particles, thereby generating small electric fields that cannot sustain gas breakdown. As finer particles pass through region 1, they accumulate charge, but this charge does not get dissipated in region 2, thereby the particles hold on to the charge. Successive fluidization results agree with this justification as they showed tremendous decline in fouling while considering just 8 – 15% of the total fluidizing gas volume was argon. A pure argon environment within the region with the highest electric field and charge generation probability significantly reduces particle adhesion, even if introduced for a small duration of time.

Another substantial observation was the non-linear decline observed in mixture trials, wherein the 50% and 25% volume trials showed comparable results with respect to both degree of fouling and charging. On a commercial scale, complete removal of reactants and other gases might not be feasible; hence, gas mixture ensuring 25% argon in the system might yield desirable results.

2.5 Conclusions

The results presented in this study are comprehensive and extremely relevant to the objective undertaken. The charge measurement technique, in particular the measurement of the

magnitude of wall fouling, and the parameters under observation make the results reliable and sets up a basis to implement a similar approach towards solving the problem of sheeting in commercial gas-phase PE reactors. In addition to presenting data regarding the pure gases, this study has experimented with gas mixtures to determine a minimum gas concentration with respect to argon, considering financial implications involved if the process is commercialized. Pure argon was found to immensely reduce the bulk particle charge and subsequently, the degree of particle fouling on the inner column wall. Furthermore, even addition of 10% argon substantially reduced the column fouling and net charge of fouled particles. Successive fluidization, if emulated in a commercial scale, might also prove to be beneficial in maintaining column health. Mixtures of nitrogen and argon performed on a non-linear scale with 10% argon showing a 50% reduction in fouling and higher argon concentrations performing better. Lastly, successive fluidization performed better than the gas mixture trials, being comparable to pure argon in terms of specific charge of the bulk particles and the degree of fouling.

Acknowledgements

Financial support from Univation Technologies, LLC (USA) and The Natural Sciences and Engineering Research Council of Canada (NSERC) is acknowledged with gratitude.

References

[1] G. Hendrickson, Electrostatics and gas phase fluidized bed polymerization reactor wall sheeting, Chem. Eng. Sci. 61 (2006) 1041–1064. https://doi.org/10.1016/j.ces.2005.07.029.

[2] G.E. Klinzing, A review of pneumatic conveying status, advances and projections, Powder Technol. 333 (2018) 78–90. https://doi.org/10.1016/j.powtec.2018.04.012.

[3] M.B. John, E.P. John, Using inert gases for pneumatic conveymg, Powder Bulk Eng. (1989) 17–19.

[4] G.E. Klinzing, F. Rizk, R. Marcus, L.S. Leung, Pneumatic Conveying of Solids: A theorical and practical approach, 2010.

[5] M. Nifuku, H. Katoh, A study on the static electrification of powders during pneumatic transportation and the ignition of dust cloud, Powder Technol. 135–136 (2003) 234–242. https://doi.org/10.1016/S0032-5910(03)00163-3.

[6] P. Mehrani, M. Murtomaa, D.J. Lacks, An overview of advances in understanding electrostatic charge buildup in gas-solid fluidized beds, J. Electrostat. 87 (2017) 64–78. https://doi.org/10.1016/j.elstat.2017.03.005.

[7] J. Cross, Electrostatics: Principles, Problems and Applications, 1987. https://doi.org/10.1088/0031-9112/38/11/030.

[8] S. Matsusaka, H. Maruyama, T. Matsuyama, M. Ghadiri, Triboelectric charging of powders: A review, Chem. Eng. Sci. 65 (2010) 5781–5807. https://doi.org/10.1016/j.ces.2010.07.005.

[9] J. Lowell, A.C. Rose-Innes, Contact electrification, Adv. Phys. 29 (1980) 947–1023. https://doi.org/10.1080/00018738000101466.

[10] J.H. Anderson, A comparison of experipmental data and model predictions for tribocharging of two-component electrophotographic developers, J. Imaging Sci. Technol. 38 (n.d.) 378–382. http://cat.inist.fr/?aModele=afficheN&cpsidt=3376350.

[11] F.R. Ruckdeschel, L.P. Hunter, Contact electrification between insulators: Phenomenological aspects, J. Appl. Phys. 46 (1975) 4416–4430. https://doi.org/10.1063/1.321469.

[12] L.H. Lee, Dual mechanism for metal-polymer contact electrification, J. Electrostat. 32 (1994) 1–29. https://doi.org/10.1016/0304-3886(94)90026-4.

[13] L.S. McCarty, G.M. Whitesides, Electrostatic charging due to separation of ions at interfaces: Contact electrification of ionic electrets, Angew. Chemie - Int. Ed. 47 (2008) 2188–2207. https://doi.org/10.1002/anie.200701812.

[14] P. Jiang, H. Bi, S. -C Liang, L. -S Fan, Hydrodynamic behavior of circulating fluidized bed with polymeric particles, AIChE J. 40 (1994) 193–206. https://doi.org/10.1002/aic.690400202.

[15] M.E. Abdel-kader, W.H. Gaber, F.A. Ebrahim, M.A. Abd Al-Halim, Characterization of the electrical breakdown for DC discharge in Ar-He gas mixture, Vacuum. 169 (2019) 108922. https://doi.org/10.1016/j.vacuum.2019.108922.

[16] K.P. Brand, Dielectric Strength, Boiling Point and Toxicity of Gases - Different:

Aspects of the Same Basic Molecular Properties, IEEE Trans. Electr. Insul. EI-17 (1982) 451–456. https://doi.org/10.1109/TEI.1982.298489.

[17] A.E.D. Heylen, Maximization of argon-hydrocarbon Penning mixtures, J. Phys. D. Appl. Phys. 3 (1970) 789–796. https://doi.org/10.1088/0022-3727/3/5/321.

[18] H.R. Hiziroglu, M.S. Dincer, T.D. Nguyen, Breakdown voltages in SF6+argon mixtures under nonuniform electrostatic fields, Conf. Electr. Insul. Dielectr. Phenom. (CEIDP), Annu. Rep. 2 (1997) 579–582. https://doi.org/10.1109/ceidp.1997.641140.

[19] T. Miura, Observation of charge separation and gas discharge during sliding friction between metals and insulators, J. Phys. Conf. Ser. 646 (2015) 0–4. https://doi.org/10.1088/1742-6596/646/1/012057.

[20] T. Miura, I. Arakawa, Gas discharge caused by triboelectricity around a contact during friction between insulators, IEEE Trans. Dielectr. Electr. Insul. 14 (2007) 560–565. https://doi.org/10.1109/TDEI.2007.369513.

[21] T. Matsuyama, H. Yamamoto, Charge relaxation process dominates contact charging of a particle in atmospheric conditions, J. Phys. D. Appl. Phys. 28 (1995) 2418–2423. https://doi.org/10.1088/0022-3727/28/12/005.

[22] T. Matsuyama, H. Yamamoto, Charge-relaxation process dominates contact charging of a particle in atmospheric condition: II. the general model, J. Phys. D. Appl. Phys. 30 (1997) 2170–2175. https://doi.org/10.1088/0022-3727/30/15/008.

[23] J.R. Grace, H. Bi, Introduction to Circulating Fluidized Beds, Circ. Fluid. Beds. (1997) 1–20. https://doi.org/10.1007/978-94-009-0095-0_1.

[24] A. Peacock, Use and Fabrication of Polyethylene Products, Handb. Polyethyl. (2020) 469–518. https://doi.org/10.1201/9781482295467-20.

[25] T. Xie, K.B. McAuley, J.C.C. Hsu, D.W. Bacon, Gas Phase Ethylene Polymerization: Production Processes, Polymer Properties, and Reactor Modeling, 1994. https://doi.org/10.1021/ie00027a001.

[26] T.E. Nowlin, Business and Technology of the Global Polyethylene Industry, 2014. https://doi.org/10.1002/9781118946039.

[27] Data from www.sriconsulting.com/, (n.d.).

[28] A. Peacock, Commercial Development of Polyethylene, Handb. Polyethyl. (2020) 37–52. https://doi.org/10.1201/9781482295467-4.

[29] S.E. Horne Jr., J.P. Kiehl, J.J. Shipman, V.L. Folt, C.F. Gibbs, Ameripol SN — A C is-1 , 4-Poly isoprene : V, Ind. Eng. Chem. Res. 48 (1956) 784–791.

[30] T.E. Nowlin, Low pressure manufacture of polyethylene, Prog. Polym. Sci. 11 (1985) 29–55. https://doi.org/10.1016/0079-6700(85)90007-3.

[31] Y. Rao, P. Cai, K.J. Cann, F.D. Hussein, W.R. Mariott, P.A. Cao, Patent Issued for Supported Catalyst With Improved Flowability (USPTO 10,676,588), 2020.

[32] A. Sowinski, The Study of Reactor Wall Fouling in Gas-Solid Fluidized Beds Caused by Electrostatic Charge Generation, Dr. Thesis Diss. Univ. Ottawa. (2012).

[33] A. Sowinski, A. Mayne, P. Mehrani, Effect of fluidizing particle size on electrostatic charge generation and reactor wall fouling in gas-solid fluidized beds, Chem. Eng. Sci. 71 (2012) 552–563. https://doi.org/10.1016/j.ces.2011.11.031.

[34] A. Sowinski, L. Miller, P. Mehrani, Investigation of electrostatic charge distribution in gas-solid fluidized beds, Chem. Eng. Sci. 65 (2010) 2771–2781. https://doi.org/10.1016/j.ces.2010.01.008.

[35] D. Song, P. Mehrani, Comparison of electrostatic charge generation in gas-solid fluidized beds in turbulent versus pre-turbulent flow regime, Powder Technol. 319 (2017) 426–433. https://doi.org/10.1016/j.powtec.2017.07.013.

[36] D. Song, P. Mehrani, Effect of Fluidization Pressure on Electrostatic Charge Generation of Polyethylene Particles, Ind. Eng. Chem. Res. 56 (2017) 14716–14724. https://doi.org/10.1021/acs.iecr.7b04056.

[37] A. Giffin, P. Mehrani, Effect of gas relative humidity on reactor wall fouling generated due to bed electrification in gas-solid fluidized beds, Powder Technol. 235 (2013) 368–375. https://doi.org/10.1016/j.powtec.2012.10.037.

[38] M.I. Nimvari, A. Sowinski, P. Mehrani, Effect of temperature on triboelectrifcation of

polyethylene particles in a pilot-scale pressurized gas-solid fluidized bed, Powder Technol. 405 (2022) 117524. https://doi.org/10.1016/j.powtec.2022.117524.

[39] M. Taghavivand, A. Sowinski, P. Mehrani, Triboelectric effects of continuity additives and a silica catalyst support on polyethylene fluidized bed wall fouling, Chem. Eng. Sci. 245 (2021) 116882. https://doi.org/10.1016/j.ces.2021.116882.

[40] B.D. Fulks, S.P. Sawin, C.D. Aikman, J.M. Jenkins III, Process for reducing sheeting during polymerization of alpha-olefins (USPTO 4,876,320-A), 1989.

[41] J. Hou, X. Liu, M.H. Rahman, H. Li, S. Sundaresan, J.R. Grace, X. Bi, Effect of gas properties and wall materials on particle charging in gas–solid fluidized beds, Can. J. Chem. Eng. (2022) 1–12. https://doi.org/10.1002/cjce.24568.

[42] M.K. Gupte, K. Tolley, A. Mutchler, S. Holland, Static reduction (USPTO 6,630,548 B1), 2003.

[43] K. Saleh, A. Traore Ndama, P. Guigon, Relevant parameters involved in tribocharging of powders during dilute phase pneumatic transport, Chem. Eng. Res. Des. 89 (2011) 2582–2597. https://doi.org/10.1016/j.cherd.2011.06.001.

[44] E.E. Smeltzer, M.L. Weaver, G.E. Klinzing, Individual electrostatic particle interaction in pneumatic transport, Powder Technol. 33 (1982) 31–42. https://doi.org/10.1016/0032-5910(82)85036-5.

[45] N. Schwindt, U. von Pidoll, D. Markus, U. Klausmeyer, M. V. Papalexandris, H. Grosshans, Measurement of electrostatic charging during pneumatic conveying of powders, J. Loss Prev. Process Ind. 49 (2017) 461–471. https://doi.org/10.1016/j.jlp.2017.05.028.

[46] S. Matsusaka, H. Umemoto, M. Nishitani, H. Masuda, Electrostatic charge distribution of particles in gas-solids pipe flow, J. Electrostat. 55 (2002) 81–96. https://doi.org/10.1016/S0304-3886(01)00185-1.

[47] D. Song, P. Mehrani, Mechanism of particle build-up on gas-solid fluidization column wall due to electrostatic charge generation, Powder Technol. 316 (2017) 166–170. https://doi.org/10.1016/j.powtec.2017.01.031.

[48] M. Taghavivand, B. Elchamaa, A. Sowinski, P. Mehrani, Study of electrostatic charging of single particles during pneumatic conveying, Powder Technol. 355 (2019) 242–250. https://doi.org/10.1016/j.powtec.2019.07.046.

[49] M. Taghavivand, B.J. Cho, P. Mehrani, A. Sowinski, Electrostatic charging behaviour of a silica powder during pulse pneumatic conveying, Powder Technol. 366 (2020) 119–129. https://doi.org/10.1016/j.powtec.2020.02.031.

[50] M. Taghavivand, P. Mehrani, A. Sowinski, Triboelectric effects of a pneumatically injected silica catalyst support on polyethylene fluidized bed wall fouling, Powder Technol. 385 (2021) 287–298. https://doi.org/10.1016/j.powtec.2021.03.002.

[51] M.I. Nimvari, M. Taghavivand, K. Choi, A. Sowinski, P. Mehrani, Velocity measurement of pneumatically conveyed particles via a simple current signal technique and the influence of electrostatic charge, Powder Technol. 413 (2023) 118018. https://doi.org/10.1016/j.powtec.2022.118018.

[52] J. Guardiola, V. Rojo, G. Ramos, Influence of particle size, fluidization velocity and relative humidity on fluidized bed electrostatics, J. Electrostat. 37 (1996) 1–20. https://doi.org/10.1016/0304-3886(96)00002-2.

[53] F. Wang, J. Wang, Y. Yang, Distribution of electrostatic potential in a gas-solid fluidized bed and measurement of bed level, Ind. Eng. Chem. Res. 47 (2008) 9517–9526. https://doi.org/10.1021/ie800805t.

[54] W.O. Moughrabiah, J.R. Grace, X.T. Bi, Effects of pressure, temperature, and gas velocity on electrostatics in gas-solid fluidized beds, Ind. Eng. Chem. Res. 48 (2009) 320–325. https://doi.org/10.1021/ie800556y.

[55] A.C. Hoffmann, J.G. Yates, Experimental Observations of Fluidized Beds at Elevated Pressures, Chem. Eng. Commun. 41 (1986) 133–149. https://doi.org/10.1080/00986448608911716.

[56] X. Liu, S. Sundaresan, The effect of gas on tribocharging of particles in a vibrated bed, Powder Technol. 401 (2022) 117272. https://doi.org/10.1016/j.powtec.2022.117272.

[57] C.Y. Wen, Y.H. Yu, A generalized method for predicting the minimum fluidization

velocity, AIChE J. 12 (1966) 610–612. https://doi.org/10.1002/aic.690120343.

[58] F. Chowdhury, A. Sowinski, M. Ray, A. Passalacqua, P. Mehrani, Charge generation and saturation on polymer particles due to single and repeated particle-metal contacts, J. Electrostat. 91 (2018) 9–15. https://doi.org/10.1016/j.elstat.2017.11.004.

[59] F. Chowdhury, B. Elchamaa, M. Ray, A. Sowinski, A. Passalacqua, P. Mehrani, Apparatus design for measuring electrostatic charge transfer due to particle-particle collisions, Powder Technol. 361 (2020) 860–866. https://doi.org/10.1016/j.powtec.2019.11.013.

[60] F. Chowdhury, M. Ray, A. Passalacqua, P. Mehrani, A. Sowinski, Electrostatic charging due to individual particle-particle collisions, Powder Technol. 381 (2021) 352–365. https://doi.org/10.1016/j.powtec.2020.12.012.

Chapter 3 A Preliminary Study on the Effect of Gas Dielectric Strength on the Degree of Electrostatic Charge Generation in Solids Pneumatic Conveying

3.1 Introduction

Commercial sectors that handle and process solids report operability issues caused by electrostatic charge generation. Pneumatic conveying of solids is a prime example of such operations where electrostatics could play a role in limiting system efficiency. In general, the impact of electrostatic charge generation could disrupt process productivity through particle agglomeration and adhesion on surfaces in contact, and even pose a serious risk of electrostatic discharge and subsequent explosions [2,5]. Particle agglomeration might even change particle characteristics including size distribution, which impacts the conveying efficiency, increases the power demand and change the flow pattern of the system [4]. Particle fouling might also plug the conveying tube, causing material loss and a drop in efficiency [2,4]. Pneumatic conveying is thought to generate the largest amount of charges in solid handling systems [2]. Thus, it is pertinent to understand the impact of introducing highly charged particles into a well-established system.

Catalyst transport is a key operation in manufacturing industries that is fulfilled using a pneumatic conveying system. Polyethylene manufacturing uses pneumatic conveying, among other systems, to introduce catalyst into the catalytic gas-solid fluidized bed reactor. The feed-rate of the catalyst and its flowability influence the productivity of the reactor. The catalyst particles are stored under a nitrogen blanket and injected into the reactors on a continuous basis through narrow stainless-steel tubes (e.g., 6.35 mm in diameter) [25]. Inside the reactor, collisions between polymer particles, and polymers and catalyst particles contribute to the generation of electrostatic charge, which subsequently lead to the formation of fused mass of polymer and catalyst particles called sheets [1]. In addition to the charges generated within the reactor, one must also consider the influence of already-charged catalyst particles entering the fluidized bed. A study on polyethylene processing by Song and Mehrani [47] reported the presence of an image force that supplemented the established electrostatic forces present within the fluidized bed. Thus, charged catalyst particles freshly introduced into the system could participate in promoting a corresponding image force that compounds electrostatic adhesion. In addition to electrostatic effects, surface chemistry of these complex catalysts may also play a role in their adhesion.

A number of works have reported the influence of various system parameters on the specific charge of the conveyed solids in dilute systems. It is understood that the magnitude of specific charge is dependent to the solid mass loading [43,44], the conveying gas velocity [5,43,45] and relative humidity [2,43], length of the conveying line [46] and its material of construction [2], and mean diameter of the particle and its shape [43]. It is noteworthy that the results of aforementioned studies are mainly applicable to systems with similar characteristics (i.e., of similar particle size and characteristics, tube diameters, and operating parameters). Hence, to understand electrostatics in catalyst conveying in polyethylene manufacturing, results must be established through experimentation. The research group at the University of Ottawa studied the influence of previously stated parameters on the specific charge of industry relevant catalyst supports, namely amorphous silica. These studies re-established the findings with respect to conveying line length, moisture content of the particles, and subsequent impact of gas velocity [48–51].

The possibility of other system parameters, like gas properties, among others, influencing the charging behaviour of conveyed particles must also be entertained. Cross [7] demonstrated that the maximum charge possessable by a particle of a given surface area is dependant on the breakdown strength of the surrounding gas.

$$q_{max} = E\varepsilon_0 S = 2.64 \times 10^{-5}(\pi d_p)p \qquad \text{Equation 3-1}$$

Where E is the electric field strength generated by the charge, ε_0 is the permittivity of free space, S is the surface area that encloses all the charges and $p = 3\epsilon_r / (\epsilon_r+2)$, ϵ_r is the dielectric constant of the particle and d_p is the particle diameter. Evident from equation 3-1, as the maximum charge increases, the resulting electric field increases accordingly. The rising electric field reaches the dielectric strength of the surrounding medium, which then serves to limit the maximum charge on the surface of a particle. Under normal conditions gases are electrically insulative and do not conduct electrons. However, under sufficiently high electric fields, gases may undergo ionization, forming a positive ion and an electron. Potential difference that generates strong electric fields can be formed between electrodes within a system or even between highly charged surfaces that develop a temporary potential between each other after a collision. The resulting free electrons accelerate in the electric field leading to the generation of large number of charge carriers. This results in a conducive path being formed by the charge carries, increasing the conductivity of the gas and bridging the two electrodes or potential differences. This phenomenon is termed as *gas discharge*. Nitrogen, a commonly used carrier

gas, has a dielectric strength of 3.4 kV/mm at 20°C and 0.1 MPa pressure. Under similar conditions, argon displays a dielectric strength of 0.6 kV/mm, roughly 6 times lower. Thus, considering the ease of ionization, the possibility of using gases with low dielectric strengths must be explored.

A review on available literature investigating the influence of gases on particle charging in pneumatic conveying yielded limited results. Matsuyama and Yamamoto [21,22] in a study, unrelated to pneumatic conveying, via experimentation and modeling reported that usage of argon as the gaseous medium reduced the magnitude of impact charging of solids. Their study compared the impact charge gained by a single polymer particle in air and argon after it collides with a metal plate placed at an angle. A similar study by Miura [19] showed the influence of gases on charge generation between a stainless-steel pin sliding along a quartz disk. Argon, nitrogen, and ambient air were studied and compared to charge generation in vacuum. Gas discharge occurring in a micro-gap around the point of contact was attributed to the lower charge values observed in argon. Subsequently, Miura and Arakawa [20] photographed micro-gap discharge occurring between the materials in contact. The study employed a similar pin-and-disk technique to generate triboelectric charges on either an insulating or conducting pin sliding on an insulator disk under various gases including air, nitrogen, argon, neon, and krypton. Ring shaped gas discharges were observed in insulator-insulator contact while no such shapes were observed when using a conducting pin.

The only work in relation to pneumatic conveying is a patent filed in 2003 [42]. The work only reported a decline in static charge of calcined silica particles, used as a catalyst base, conveyed through a 6.35 mm inner diameter stainless-steel tube for 30 to 60 minutes using pure helium, argon, and nitrogen as the conveying gas. The static values were obtained by measuring voltage across a small, isolated section of the conveying tube. The patent concluded that helium performed the best in reducing static charge, followed by argon and finally nitrogen. Although no experimental results on the impact on polyethylene resin charging and sheeting downstream of the conveying tube was shown, the authors claimed that feeding catalyst particles into a gas-phase polyethylene fluidized bed reactor using a stream of 75% noble gas (helium or argon) could reduce static in the reactor.

In addition to parameters already studied, the effect of gas type on electrostatic charging of solids conveyed pneumatically must further be investigated. Hence, the objective of this study was to understand the effect of different gases including nitrogen and argon, on the extent of

generation, accumulation, and dissipation of charges on particles conveyed pneumatically and to compare the usage of these gases in reducing electrostatic charge. The study was carried out in continuation of our earlier works by Taghavivand et al. [48–50] and Nimvari et al. [51]. Although polyethylene manufacturing was used as a basis for particle selection and operating parameters, results obtained are applicable to other solids conveying systems as well.

3.2 Materials and methods

The pneumatic conveying apparatus used in this study is shown in Fig. 3-1 and is in continuation from our earlier work by Taghavivand et al. [48–50]. The setup consisted of a particle injection section, a conveying section, and an electrostatic charge measurement section. Particle injection section was placed inside a glove box filled with nitrogen under controlled temperature and relative humidity (RH) conditions (22°C – 24°C and < 8%). The particles were introduced into the conveying tube using a union tee, and a plug was fixed to ensure no gas leakage during the operation. A stainless-steel tube with an inner diameter of 4.57×10^{-3} m was used to convey the particles. The conveying line was 5 m in length including two smooth bends with radii of 0.25 and 0.33 m. To determine the extent of charging of the conveyed particles, a cyclone separator was attached to the exit of the conveying line. An electrometer (Keithley model 6514) was connected to the cyclone which acted as a Faraday cage. A filter was fixed on the outlet of the cyclone to trap the conveyed particles. Two insulator fittings isolated the conveying section in order to measure the current generated by the transport of the charged particles within the tube. The current signal was measured directly from the conveying tube during the operation using a second electrometer (Keithley model 6514). The measured current signal was then converted to charge. Our previous work by Taghavivand et al. [48–50] provides further details of this measurement. LabVIEW software was used to control and record the operating parameters, and the current and charge signals during each trial. Gas cylinders served as sources for the two gases used.

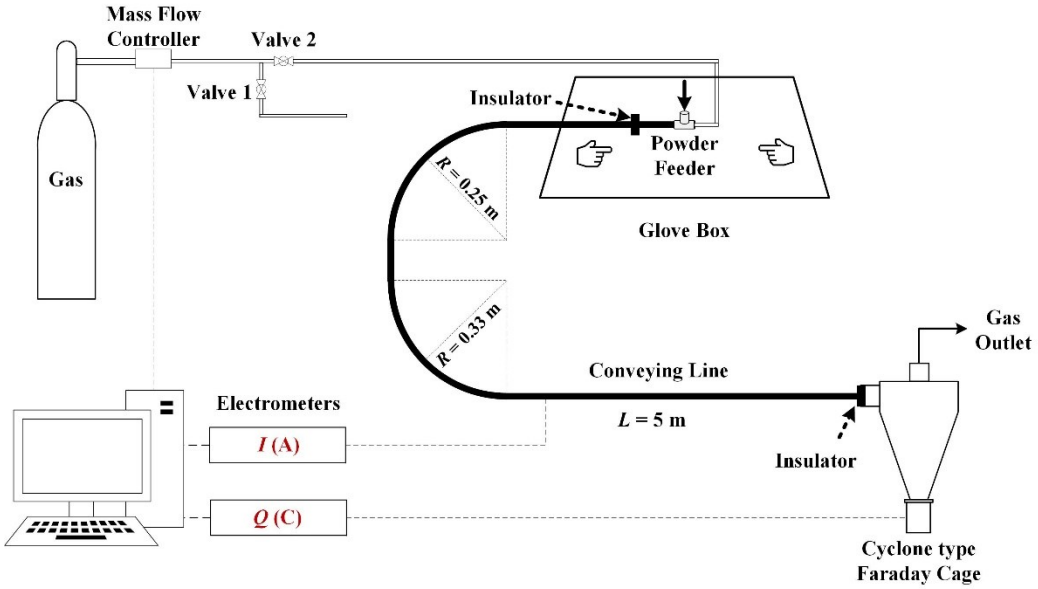

Fig. 3-1. Schematic of the conveying apparatus used.

The gas flowrate was controlled using a mass flow meter. Since the density and viscosity of the two gases are different, trials were performed at gas velocities that ensured similar Stokes number and flow regime (Table 3-1). Thus, argon trials were run at 21 m/s and nitrogen trials were run at 15 m/s. This ensured the flow a pattern was turbulent, and the results were comparable. One set of nitrogen trial at 21 m/s was also performed to correlate charging under the same gas velocities.

Table 3-1. Gas properties and operating parameters

Properties	**Argon**	**Nitrogen**
Gas density (kg/m^3)	1.64	1.16
Gas viscosity (Pa. s)	2.23×10^{-5}	1.76×10^{-5}
Gas velocity (m/s)	21	15/ 21
Reynold's number	7062	4518/ 6325
Stokes number	14	13/ 18

Once the particles were weighed and loaded into the conveying line, the flowrate of the gas was ramped to the desired value while being purged through valve 1. Once the flowrate set point was reached, particle conveying was commenced when valve 2 was opened and valve 1 was closed simultaneously. The gas flow was maintained until the current signal read zero and the charge signal remained unchanged, which was an indication of the full withdrawal of the

particles from the conveying tube. The current signal was measured from the conveying tube and the net charge of the conveyed particles was measured at the cyclone separator. The cyclone was then detached and weighed to measure the mass of the particles collected to determine the particles mass recovery (i.e., higher mass recovery implies a lower tube wall fouling). Each trial included 5 consecutive injections with no cleaning or purging performed between injections to recreate industrial scenarios.

Dehydrated amorphous silica was chosen for this study because it serves as a base for a variety of industrial catalysts, including PE industries. Furthermore, it has a tendency to generate large specific charge and conveying tube fouling [49–51]. Table 3-2 outlines the critical properties of the particles.

Table 3-2. Particle characteristics

Particle type	Amorphous Silica
Mean diameter, d_{50} (μm)	54
Particle density (kg/m^3)	2170 - 2200
Mass of particles used per injection (g)	0.103 ± 0.003

3.3 Results and discussions

A typical current versus time plot obtained from the conveying tube during particle injections is shown in Fig. 3-2. For this trial presented, the area under the curve that represents the net charge of the particles as they leave the conveying line was calculated at 966.36 nC and the corresponding net charge measured by the electrometer connected to the cyclone read - 968.74 nC. The reversal in polarity is due to charge transfer occurring between the conveying tube and the particles. Conveyed particles charged negatively, thus the tube acquired positive charges. Since both results are in good agreement, it is concluded that the current signal measurement is reliable and could be used as an online technique for such application. Previous studies elaborate on the validity [48]. Results presented from here onwards are that measured by the cyclone.

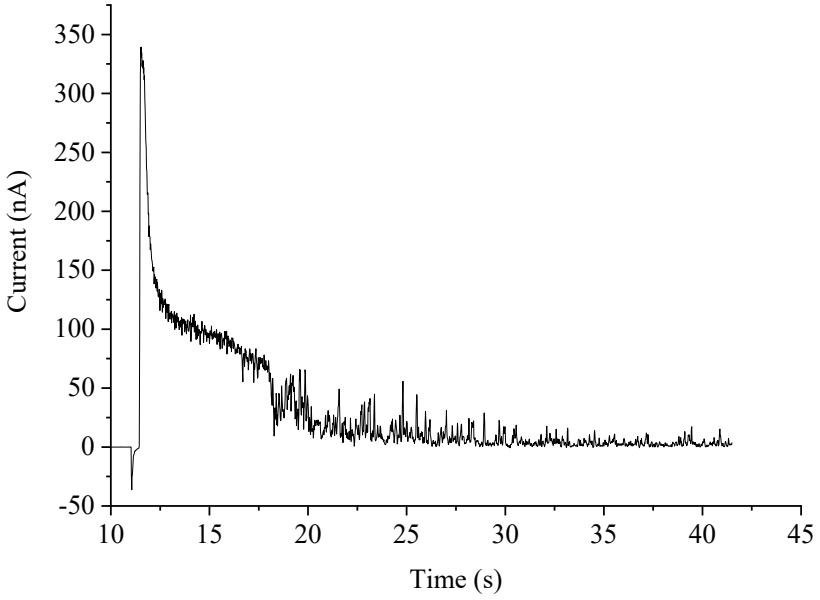

Fig. 3-2. Current signal received from the conveying tube during conveying of amorphous silica particles using nitrogen.

Fig. 3-3 shows the results for amorphous silica plotted with respect to the degree of particle net specific charge and the tube fouling for consecutive injections. The results shown are for trials operated at constant Stokes number. Fig. 3-3a correlates the mass of particles recovered against the total 0.1 g introduced into the conveying line per injection. Thus, a larger mass collected would indicate a lower tube fouling. The results point out that tube fouling occurred for all cases tested, with the average particle mass recovery of approximately 80 to 85%. The results show that trials using argon had a relatively smaller tube fouling across all the injections and a narrower deviation among most injections compared to using nitrogen. Argon showed a 128% higher recovery in the first injection relative to nitrogen. However, the difference between the two gases diminished in the subsequent injections.

Fig. 3-3b shows the net specific charge values of amorphous silica observed after the runs. Overall, significant degree of charging was observed for all trials. However, trials using argon, in comparison, showed a 35% reduction in degree of charging in the first injection. Nevertheless, like tube fouling, the differences between the two gases were not as prominent in all the subsequent injections.

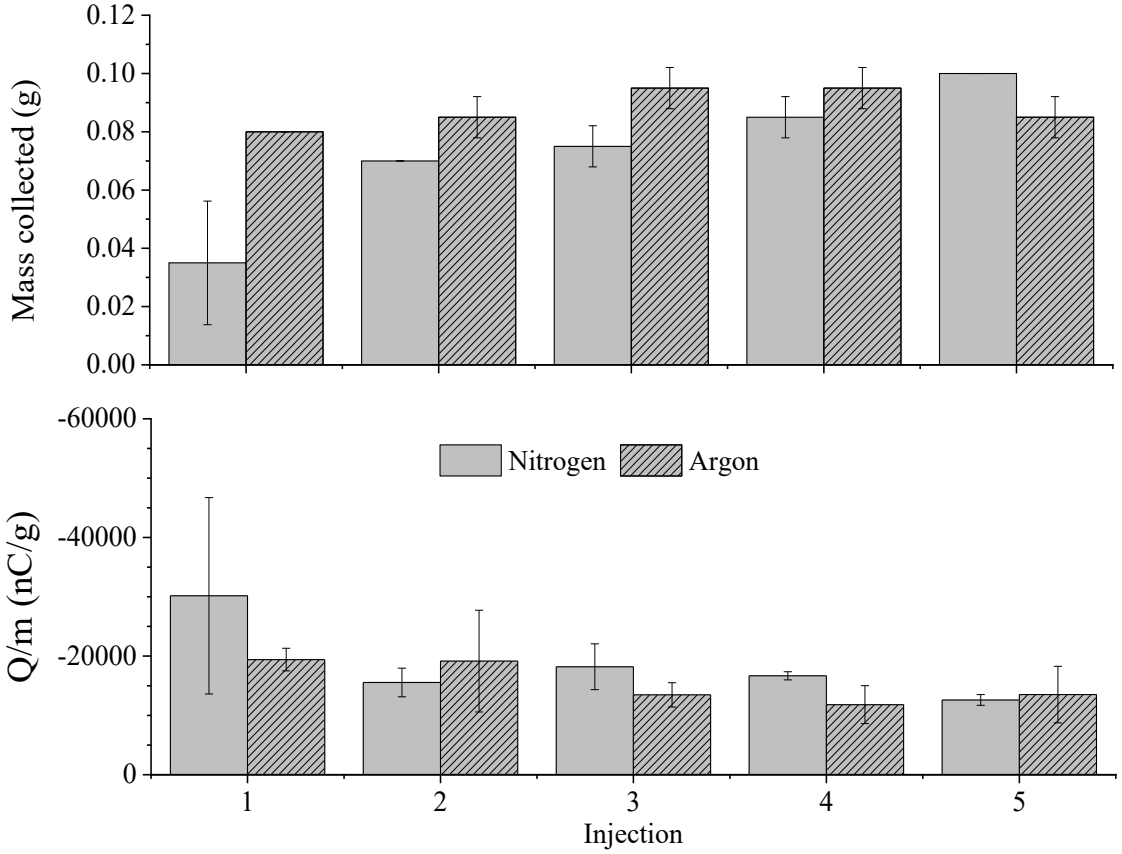

Fig. 3-3. Amount of mass collected after conveying, and the corresponding net specific charge observed in amorphous silica particles as a function of gas type and injection number.

Argon having a smaller dielectric strength was anticipated to result in less charging on the conveyed particles and as a result less fouling. Although the results observed for the first injection were in agreement with this, subsequent injections did not yield a significantly different result. To understand the reason behind this variation, we point the reader's attention to the fouled tube in injections 2-5. Since there are already silica particles fouled on the tube, there is a lingering probability that the conveying gas dislodges previously adhered particles, thereby improving the mass recovery in subsequent trials. Even though we see an increase in this parameter for all the subsequent runs, nitrogen shows the largest change. In addition to the mass of fouled particles, the possibility of repulsion should also be considered. Particles adhered to the tube wall repel other particles with the same polarity. This would reduce the area available for adherence and repel particles away from the wall. Furthermore, charge transfer between moving particle- and fouled particles would be lower than particle-bare wall collisions due to differences in work function. Finally, in relation to the commercial polyethylene reactors, even though we see argon performing better than nitrogen in reducing fouling of amorphous silica particles, the net specific charge of the particles conveyed using argon is still significantly large. The study by Gupte et al. [42] claimed significant reduction in

static under argon and helium conveying using similar particles, however, the study was conducted for 30 minutes using 11g of particles. A commercial process looking to mitigate electrostatic charging in pneumatically conveyed particles may or may not benefit using argon as the transporting gas. Thus, further investigation is required to expand on the results of this work, which was focused on the catalyst base only, and determine whether argon could satisfactorily improve the operation of catalyst conveying and subsequent fluidization in polyethylene processing.

Fig. 3-4 shows the results collated for silica conveyed at the same gas velocities. Even though the flow regime is still turbulent, the Stokes number is different. Silica recovery is consistent with the results obtained at 15 m/s. The recovery shows the same trend as the earlier trial wherein the first injection is noticeably smaller than subsequent injections. The mass recovery under argon was 2 times higher than the mass recovery under nitrogen. This is lower than the recovery in the earlier trial. However, argon is still observed to evoke better recovery in all the injections. The specific charge, however, is significantly lower than previous results. The difference between the specific charges in the first injection was close to 65%. This difference becomes more evident when compared against argon.

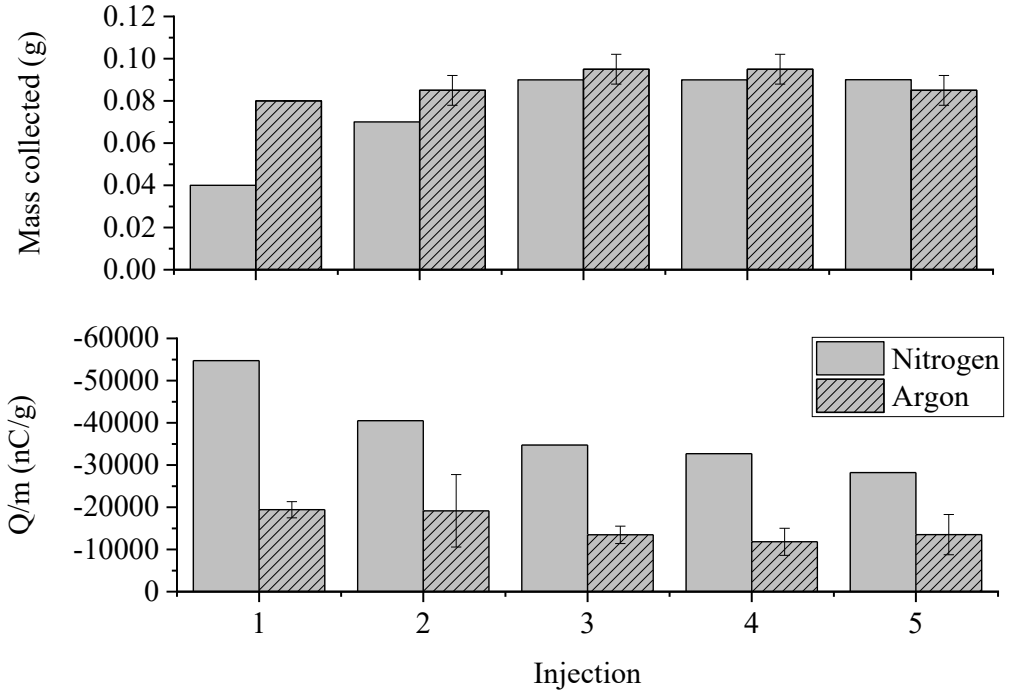

Fig. 3-4. Amount of particles mass collected after conveying and the corresponding net specific charge observed in silica at the same gas velocity.

The higher velocity increases the drag force on the particle which help in recovery but also increase the number of collisions between particles and the tube wall. Results from previous works [51] make a similar observation with respect to gas velocity and particle charging. Subsequent injections show a decreasing trend in specific charge values which might be due to the reduced charge transfer in a fouled tube. Thus, mass recovery and specific charge values can be expected to stabilize under continuous conveying where the tube fouling no longer changes.

3.4 Conclusions

The results published in this study attempts to establish a relation between the gas dielectric strength and charging behaviour observed in solids pneumatic conveying. It was anticipated that argon having a smaller dielectric strength than nitrogen would result in less charging on the conveyed particles and subsequently less fouling. Although the results observed for the first injections of amorphous silica, performed in a clean tube, were agreeable with this, subsequent injections did not yield a significantly positive result. This is of relevance as pneumatic conveying in commercial operations do not undertake purging after each injection, hence would display characteristics similar to injections numbered 2-5 in this study. Additionally, the influence of gas velocity was noticeable in the specific charge of the particles but not in the mass recovery. Higher gas velocities imply a higher drag force but also a higher degree of charging due to an increase in the number of collisions.

Acknowledgements

Financial support from Univation Technologies, LLC (USA) and The Natural Sciences and Engineering Research Council of Canada (NSERC) is acknowledged with gratitude.

References

[1] G. Hendrickson, Electrostatics and gas phase fluidized bed polymerization reactor wall sheeting, Chem. Eng. Sci. 61 (2006) 1041–1064. https://doi.org/10.1016/j.ces.2005.07.029.

[2] G.E. Klinzing, A review of pneumatic conveying status, advances and projections, Powder Technol. 333 (2018) 78–90. https://doi.org/10.1016/j.powtec.2018.04.012.

[3] M.B. John, E.P. John, Using inert gases for pneumatic conveymg, Powder Bulk Eng.

(1989) 17–19.

[4] G.E. Klinzing, F. Rizk, R. Marcus, L.S. Leung, Pneumatic Conveying of Solids: A theorical and practical approach, 2010.

[5] M. Nifuku, H. Katoh, A study on the static electrification of powders during pneumatic transportation and the ignition of dust cloud, Powder Technol. 135–136 (2003) 234–242. https://doi.org/10.1016/S0032-5910(03)00163-3.

[6] P. Mehrani, M. Murtomaa, D.J. Lacks, An overview of advances in understanding electrostatic charge buildup in gas-solid fluidized beds, J. Electrostat. 87 (2017) 64–78. https://doi.org/10.1016/j.elstat.2017.03.005.

[7] J. Cross, Electrostatics: Principles, Problems and Applications, 1987. https://doi.org/10.1088/0031-9112/38/11/030.

[8] S. Matsusaka, H. Maruyama, T. Matsuyama, M. Ghadiri, Triboelectric charging of powders: A review, Chem. Eng. Sci. 65 (2010) 5781–5807. https://doi.org/10.1016/j.ces.2010.07.005.

[9] J. Lowell, A.C. Rose-Innes, Contact electrification, Adv. Phys. 29 (1980) 947–1023. https://doi.org/10.1080/00018738000101466.

[10] J.H. Anderson, A comparison of experipmental data and model predictions for tribocharging of two-component electrophotographic developers, J. Imaging Sci. Technol. 38 (n.d.) 378–382. http://cat.inist.fr/?aModele=afficheN&cpsidt=3376350.

[11] F.R. Ruckdeschel, L.P. Hunter, Contact electrification between insulators: Phenomenological aspects, J. Appl. Phys. 46 (1975) 4416–4430. https://doi.org/10.1063/1.321469.

[12] L.H. Lee, Dual mechanism for metal-polymer contact electrification, J. Electrostat. 32 (1994) 1–29. https://doi.org/10.1016/0304-3886(94)90026-4.

[13] L.S. McCarty, G.M. Whitesides, Electrostatic charging due to separation of ions at interfaces: Contact electrification of ionic electrets, Angew. Chemie - Int. Ed. 47 (2008) 2188–2207. https://doi.org/10.1002/anie.200701812.

[14] P. Jiang, H. Bi, S. -C Liang, L. -S Fan, Hydrodynamic behavior of circulating fluidized bed with polymeric particles, AIChE J. 40 (1994) 193–206. https://doi.org/10.1002/aic.690400202.

[15] M.E. Abdel-kader, W.H. Gaber, F.A. Ebrahim, M.A. Abd Al-Halim, Characterization of the electrical breakdown for DC discharge in Ar-He gas mixture, Vacuum. 169 (2019) 108922. https://doi.org/10.1016/j.vacuum.2019.108922.

[16] K.P. Brand, Dielectric Strength, Boiling Point and Toxicity of Gases - Different: Aspects of the Same Basic Molecular Properties, IEEE Trans. Electr. Insul. EI-17 (1982) 451–456. https://doi.org/10.1109/TEI.1982.298489.

[17] A.E.D. Heylen, Maximization of argon-hydrocarbon Penning mixtures, J. Phys. D. Appl. Phys. 3 (1970) 789–796. https://doi.org/10.1088/0022-3727/3/5/321.

[18] H.R. Hiziroglu, M.S. Dincer, T.D. Nguyen, Breakdown voltages in SF6+argon mixtures under nonuniform electrostatic fields, Conf. Electr. Insul. Dielectr. Phenom. (CEIDP), Annu. Rep. 2 (1997) 579–582. https://doi.org/10.1109/ceidp.1997.641140.

[19] T. Miura, Observation of charge separation and gas discharge during sliding friction between metals and insulators, J. Phys. Conf. Ser. 646 (2015) 0–4. https://doi.org/10.1088/1742-6596/646/1/012057.

[20] T. Miura, I. Arakawa, Gas discharge caused by triboelectricity around a contact during friction between insulators, IEEE Trans. Dielectr. Electr. Insul. 14 (2007) 560–565. https://doi.org/10.1109/TDEI.2007.369513.

[21] T. Matsuyama, H. Yamamoto, Charge relaxation process dominates contact charging of a particle in atmospheric conditions, J. Phys. D. Appl. Phys. 28 (1995) 2418–2423. https://doi.org/10.1088/0022-3727/28/12/005.

[22] T. Matsuyama, H. Yamamoto, Charge-relaxation process dominates contact charging of a particle in atmospheric condition: II. the general model, J. Phys. D. Appl. Phys. 30 (1997) 2170–2175. https://doi.org/10.1088/0022-3727/30/15/008.

[23] J.R. Grace, H. Bi, Introduction to Circulating Fluidized Beds, Circ. Fluid. Beds. (1997) 1–20. https://doi.org/10.1007/978-94-009-0095-0_1.

[24] A. Peacock, Use and Fabrication of Polyethylene Products, Handb. Polyethyl. (2020) 469–518. https://doi.org/10.1201/9781482295467-20.

[25] T. Xie, K.B. McAuley, J.C.C. Hsu, D.W. Bacon, Gas Phase Ethylene Polymerization: Production Processes, Polymer Properties, and Reactor Modeling, 1994. https://doi.org/10.1021/ie00027a001.

[26] T.E. Nowlin, Business and Technology of the Global Polyethylene Industry, 2014. https://doi.org/10.1002/9781118946039.

[27] Data from www.sriconsulting.com/, (n.d.).

[28] A. Peacock, Commercial Development of Polyethylene, Handb. Polyethyl. (2020) 37–52. https://doi.org/10.1201/9781482295467-4.

[29] S.E. Horne Jr., J.P. Kiehl, J.J. Shipman, V.L. Folt, C.F. Gibbs, Ameripol SN — A C is-1 , 4-Poly isoprene : V, Ind. Eng. Chem. Res. 48 (1956) 784–791.

[30] T.E. Nowlin, Low pressure manufacture of polyethylene, Prog. Polym. Sci. 11 (1985) 29–55. https://doi.org/10.1016/0079-6700(85)90007-3.

[31] Y. Rao, P. Cai, K.J. Cann, F.D. Hussein, W.R. Mariott, P.A. Cao, Patent Issued for Supported Catalyst With Improved Flowability (USPTO 10,676,588), 2020.

[32] A. Sowinski, The Study of Reactor Wall Fouling in Gas-Solid Fluidized Beds Caused by Electrostatic Charge Generation, Dr. Thesis Diss. Univ. Ottawa. (2012).

[33] A. Sowinski, A. Mayne, P. Mehrani, Effect of fluidizing particle size on electrostatic charge generation and reactor wall fouling in gas-solid fluidized beds, Chem. Eng. Sci. 71 (2012) 552–563. https://doi.org/10.1016/j.ces.2011.11.031.

[34] A. Sowinski, L. Miller, P. Mehrani, Investigation of electrostatic charge distribution in gas-solid fluidized beds, Chem. Eng. Sci. 65 (2010) 2771–2781. https://doi.org/10.1016/j.ces.2010.01.008.

[35] D. Song, P. Mehrani, Comparison of electrostatic charge generation in gas-solid fluidized beds in turbulent versus pre-turbulent flow regime, Powder Technol. 319 (2017) 426–433. https://doi.org/10.1016/j.powtec.2017.07.013.

[36] D. Song, P. Mehrani, Effect of Fluidization Pressure on Electrostatic Charge Generation of Polyethylene Particles, Ind. Eng. Chem. Res. 56 (2017) 14716–14724. https://doi.org/10.1021/acs.iecr.7b04056.

[37] A. Giffin, P. Mehrani, Effect of gas relative humidity on reactor wall fouling generated due to bed electrification in gas-solid fluidized beds, Powder Technol. 235 (2013) 368–375. https://doi.org/10.1016/j.powtec.2012.10.037.

[38] M.I. Nimvari, A. Sowinski, P. Mehrani, Effect of temperature on triboelectrifcation of polyethylene particles in a pilot-scale pressurized gas-solid fluidized bed, Powder Technol. 405 (2022) 117524. https://doi.org/10.1016/j.powtec.2022.117524.

[39] M. Taghavivand, A. Sowinski, P. Mehrani, Triboelectric effects of continuity additives and a silica catalyst support on polyethylene fluidized bed wall fouling, Chem. Eng. Sci. 245 (2021) 116882. https://doi.org/10.1016/j.ces.2021.116882.

[40] B.D. Fulks, S.P. Sawin, C.D. Aikman, J.M. Jenkins III, Process for reducing sheeting during polymerization of alpha-olefins (USPTO 4,876,320-A), 1989.

[41] J. Hou, X. Liu, M.H. Rahman, H. Li, S. Sundaresan, J.R. Grace, X. Bi, Effect of gas properties and wall materials on particle charging in gas–solid fluidized beds, Can. J. Chem. Eng. (2022) 1–12. https://doi.org/10.1002/cjce.24568.

[42] M.K. Gupte, K. Tolley, A. Mutchler, S. Holland, Static reduction (USPTO 6,630,548 B1), 2003.

[43] K. Saleh, A. Traore Ndama, P. Guigon, Relevant parameters involved in tribocharging of powders during dilute phase pneumatic transport, Chem. Eng. Res. Des. 89 (2011) 2582–2597. https://doi.org/10.1016/j.cherd.2011.06.001.

[44] E.E. Smeltzer, M.L. Weaver, G.E. Klinzing, Individual electrostatic particle interaction in pneumatic transport, Powder Technol. 33 (1982) 31–42. https://doi.org/10.1016/0032-5910(82)85036-5.

[45] N. Schwindt, U. von Pidoll, D. Markus, U. Klausmeyer, M. V. Papalexandris, H. Grosshans, Measurement of electrostatic charging during pneumatic conveying of powders, J. Loss Prev. Process Ind. 49 (2017) 461–471.

https://doi.org/10.1016/j.jlp.2017.05.028.

[46] S. Matsusaka, H. Umemoto, M. Nishitani, H. Masuda, Electrostatic charge distribution of particles in gas-solids pipe flow, J. Electrostat. 55 (2002) 81–96. https://doi.org/10.1016/S0304-3886(01)00185-1.

[47] D. Song, P. Mehrani, Mechanism of particle build-up on gas-solid fluidization column wall due to electrostatic charge generation, Powder Technol. 316 (2017) 166–170. https://doi.org/10.1016/j.powtec.2017.01.031.

[48] M. Taghavivand, B. Elchamaa, A. Sowinski, P. Mehrani, Study of electrostatic charging of single particles during pneumatic conveying, Powder Technol. 355 (2019) 242–250. https://doi.org/10.1016/j.powtec.2019.07.046.

[49] M. Taghavivand, B.J. Cho, P. Mehrani, A. Sowinski, Electrostatic charging behaviour of a silica powder during pulse pneumatic conveying, Powder Technol. 366 (2020) 119–129. https://doi.org/10.1016/j.powtec.2020.02.031.

[50] M. Taghavivand, P. Mehrani, A. Sowinski, Triboelectric effects of a pneumatically injected silica catalyst support on polyethylene fluidized bed wall fouling, Powder Technol. 385 (2021) 287–298. https://doi.org/10.1016/j.powtec.2021.03.002.

[51] M.I. Nimvari, M. Taghavivand, K. Choi, A. Sowinski, P. Mehrani, Velocity measurement of pneumatically conveyed particles via a simple current signal technique and the influence of electrostatic charge, Powder Technol. 413 (2023) 118018. https://doi.org/10.1016/j.powtec.2022.118018.

[52] J. Guardiola, V. Rojo, G. Ramos, Influence of particle size, fluidization velocity and relative humidity on fluidized bed electrostatics, J. Electrostat. 37 (1996) 1–20. https://doi.org/10.1016/0304-3886(96)00002-2.

[53] F. Wang, J. Wang, Y. Yang, Distribution of electrostatic potential in a gas-solid fluidized bed and measurement of bed level, Ind. Eng. Chem. Res. 47 (2008) 9517–9526. https://doi.org/10.1021/ie800805t.

[54] W.O. Moughrabiah, J.R. Grace, X.T. Bi, Effects of pressure, temperature, and gas velocity on electrostatics in gas-solid fluidized beds, Ind. Eng. Chem. Res. 48 (2009)

320–325. https://doi.org/10.1021/ie800556y.

[55] A.C. Hoffmann, J.G. Yates, Experimental Observations of Fluidized Beds at Elevated Pressures, Chem. Eng. Commun. 41 (1986) 133–149. https://doi.org/10.1080/00986448608911716.

[56] X. Liu, S. Sundaresan, The effect of gas on tribocharging of particles in a vibrated bed, Powder Technol. 401 (2022) 117272. https://doi.org/10.1016/j.powtec.2022.117272.

[57] C.Y. Wen, Y.H. Yu, A generalized method for predicting the minimum fluidization velocity, AIChE J. 12 (1966) 610–612. https://doi.org/10.1002/aic.690120343.

[58] F. Chowdhury, A. Sowinski, M. Ray, A. Passalacqua, P. Mehrani, Charge generation and saturation on polymer particles due to single and repeated particle-metal contacts, J. Electrostat. 91 (2018) 9–15. https://doi.org/10.1016/j.elstat.2017.11.004.

[59] F. Chowdhury, B. Elchamaa, M. Ray, A. Sowinski, A. Passalacqua, P. Mehrani, Apparatus design for measuring electrostatic charge transfer due to particle-particle collisions, Powder Technol. 361 (2020) 860–866. https://doi.org/10.1016/j.powtec.2019.11.013.

[60] F. Chowdhury, M. Ray, A. Passalacqua, P. Mehrani, A. Sowinski, Electrostatic charging due to individual particle-particle collisions, Powder Technol. 381 (2021) 352–365. https://doi.org/10.1016/j.powtec.2020.12.012.

Chapter 4 Preliminary Bench-Scale Shake Tests Investigating the Influence of Dielectric Strength on Charge Saturation

4.1 Introduction

Commercial sectors that handle and process solids at times report operability issues caused by electrostatic charge generation. The impact of electrostatic charge generation could disrupt process productivity through particle agglomeration and adhesion on surfaces in contact, and even pose a serious risk of electrostatic discharge and subsequent explosions. Particle agglomeration might even change the particle characteristics, which impacts the operating parameters and cause delays and process shutdowns. Particle fouling might also plug conveying tubes, distributors, and other necessary equipment, causing a drop in productivity. Among the various processes that utilize solid handling, pneumatic conveying is thought to generate the largest amount of charges in solid handling systems [2]. Other operations that are affected by triboelectrification include gas-solid fluidization processes. Thus, it is pertinent to understand the impact of introducing highly charged particles into a well-established system. This study was carried out in relation to the polyethylene industry, wherein polymerization of ethylene monomers take place in a gas-phase catalytic fluidized bed reactor [26]. However, results obtained are applicable to other systems as well. In gas-phase polyethylene process using fluidized beds, collision between polymer particles and polymer-catalyst contribute to the generation of charge inside the reactor, which subsequently lead to the formation of fused mass of polymer and catalyst particles called sheets [1]. These sheets dislodge from the column wall and plug the distributor plate, which essentially shuts down the system. The possibility of other system parameters influencing the charging behaviour of polyethylene particles should be entertained from which gas type has received limited attention.

Matsuyama and Yamamoto in a study via experimentation and modeling reported that usage of argon reduced the magnitude of impact charging of solids [21,22]. Their study compared the impact charge gained by a single polymer particle in air and argon after it collides with a metal plate placed at an angle. A similar study by Miura et al., photographed micro-gap discharge occurring between the materials in contact. The study employed a pin-and-disk technique to generate triboelectric charges on either an insulating or conducting pin sliding on an insulator disk under various gases including argon, nitrogen, neon, krypton and air [19,20]. The authors concluded that gas discharge limits the charge gained by the pin, while also observing that inert

gases like argon with low dielectric strength better limit the charges compared to air and nitrogen. The dielectric strength of argon and nitrogen are reported to be 0.6 and 3.4 kV/mm at ambient conditions [16]. Recently, Liu and Sundaresan [56] studied the effect of argon and nitrogen on soda lime and polyethylene particles shaken in a small bench-scale vibratory bed. Different mass loadings were used to study the impact of breakdown voltage on the maximum charge gained by the particle. The study concluded that argon appeared to limit the charge on the particle to a lower absolute value.

In an earlier work, Cross demonstrated that the maximum charge possessable by a particle of a given surface area is dependant on the breakdown strength of the surrounding gas [7].

$$q_{max} = E\varepsilon_0 S = 2.64 \times 10^{-5}(\pi d_p)p \qquad \text{Equation 4-1}$$

Where E is the electric field strength generated by the charges, ε_0 is the permittivity of free space, S is the surface area that encloses all the charges and $p = 3\epsilon_r/(\epsilon_r + 2)$, ϵ_r is the dielectric constant of the polymer and d_p is the particle diameter. Evident from the equation above, as the maximum charge increases, the resulting electric field increases too. The rising electric field reaches the dielectric strength of the surrounding medium, which then serves to limit the maximum charge on the surface. Under normal conditions gases are electrically insulative and do not conduct electrons. However, under sufficiently high electric fields, gases may undergo ionization. Potential difference that generates strong electric fields can be formed by electrodes within a system or even by highly charged surfaces that develop a temporary potential between each other after a collision. The resulting free electrons get accelerated by the electric field leading to the generation of large number of charge carriers. This results in a conducive path being formed by the charge carries, increasing the conductivity of the gas and bridging the two electrodes or potential differences. This phenomenon is termed as *gas discharge*.

The limited studies reported in literature all make a similar conclusion in attributing the lower breakdown voltage of gases such as argon for the lower magnitude of charge observed in systems studied. Hence, it is evident that the gaseous environment around particle contact plays an important role in charge accumulation and charge dissipation. Considering the limited number of studies investigating the effect of gases with low dielectric strength on triboelectrification, particularly polymer particles, the objective of this study was to understand, at a small scale, the effect of different gases on the generation, accumulation,

saturation, and dissipation of charges on particles in relation to the gas-phase polyethylene process. This was achieved by shaking polyethylene particles inside metal containers. This is in continuation of an earlier work completed in our group by Chowdhury et al. [58–60] who studied the charge saturation of single particles made of various insulators colliding with each other and metallic plates under ambient air. This study aims to complete the objective by collecting data pertaining to the usage of nitrogen and argon in reducing electrostatic charge generation in polyethylene particles under movement. A comparison between the two gases is drawn to conclude on their usability in other solid-handling operations.

4.2 Materials and methods

Two different approaches were employed in this study. The first approach studied the contact charging behavior of a polyethylene particle colliding against a metallic surface. A single large polyethylene particle (Fig. 4-1a) was used, and a benchmark was first established under ambient conditions. The humidity recorded varied between 35% and 53% for the ambient trials. Trials under nitrogen and argon were subsequently performed in a glove box under controlled temperature (23 - 25°C) and relative humidity (1 - 5% RH). On account of the large particle size, shaking was performed manually in an up-and-down motion. The particle was obtained by sieving a commercially produced linear low-density polyethylene (LLDPE) resin and selecting the largest particle. The average diameter of the particle was found to be 5 mm. The particle was washed, dried, and neutralized using a fan type ionizer (SMC IZF10 R) before commencing the trials. The same particle was used in all the trials and neutralization was only carried out after the completion of a trial.

The second approach related the charging behaviour of multiple polyethylene particles against a metallic surface. 2 grams of polyethylene particle of two different sizes (Fig. 4-1b) were used in this approach. Particles in the second approach were selected based on their mean diameter in accordance with previous polyethylene fluidization study carried out in Chapter 2. It was found that particles with a mean diameter between 0.5 mm to 0.6 mm would foul the column walls and 1.2 mm was close to the average mean diameter of the main batch of polyethylene resin used. The particles were sieved from the same LLDPE resin used in the first approach. The trials were performed under argon and nitrogen conditions only. The temperature and the relative humidity inside the glove box were set to the same standards as before. Different set of particles were used in each trial and for each data point. Simply put, for example, 6 different sets of particles of 0.55 mm, corresponding to the 6 shake durations, were used in completing

one trial under argon. All sets of particles were ionized in ambient condition before being introduced into the glove box. It was found that the ionizer did not function in argon environment, hence this step was necessary.

(a) (b)

Fig. 4-1. 5 mm polyethylene particle used in the first approach (a); 1.2 mm polyethylene particle used in the second approach (b).

A cubical metal container with a lid was used in both the approaches (Fig. 4-2). The material of the container is similar to that of our earlier work by Chowdhury et al., [58]. As stated earlier, in the first approach, the container was shaken manually, whereas in the second approach, the container was fixed to an orbital shaker (OHAUS ISLD04HDG) shaken at a predetermined RPM (Fig. 4-3). The operating parameters and the particle characteristics are summarized in Table 4-1.

Table 4-1. Particle characteristics and shake test operating parameters

Properties	**Single particle study**	**Multiple particle study**
Particle type	LLDPE	LLDPE
Average Particle size (mm)	5	0.5 and 1.2
Particle mass (g)	NA	2
Shaking criteria	15 to 300 shakes	1100 RPM
Duration of trial (mins)	NA	2 to 30
Temperature (°C)	23-25°C	23 - 25
Relative humidity (%)	1 - 5	1 - 5
Container dimension (mm)	55 x 55 x 55	55 x 55 x 55

Fig. 4-2. Metallic container and the lid used in the study

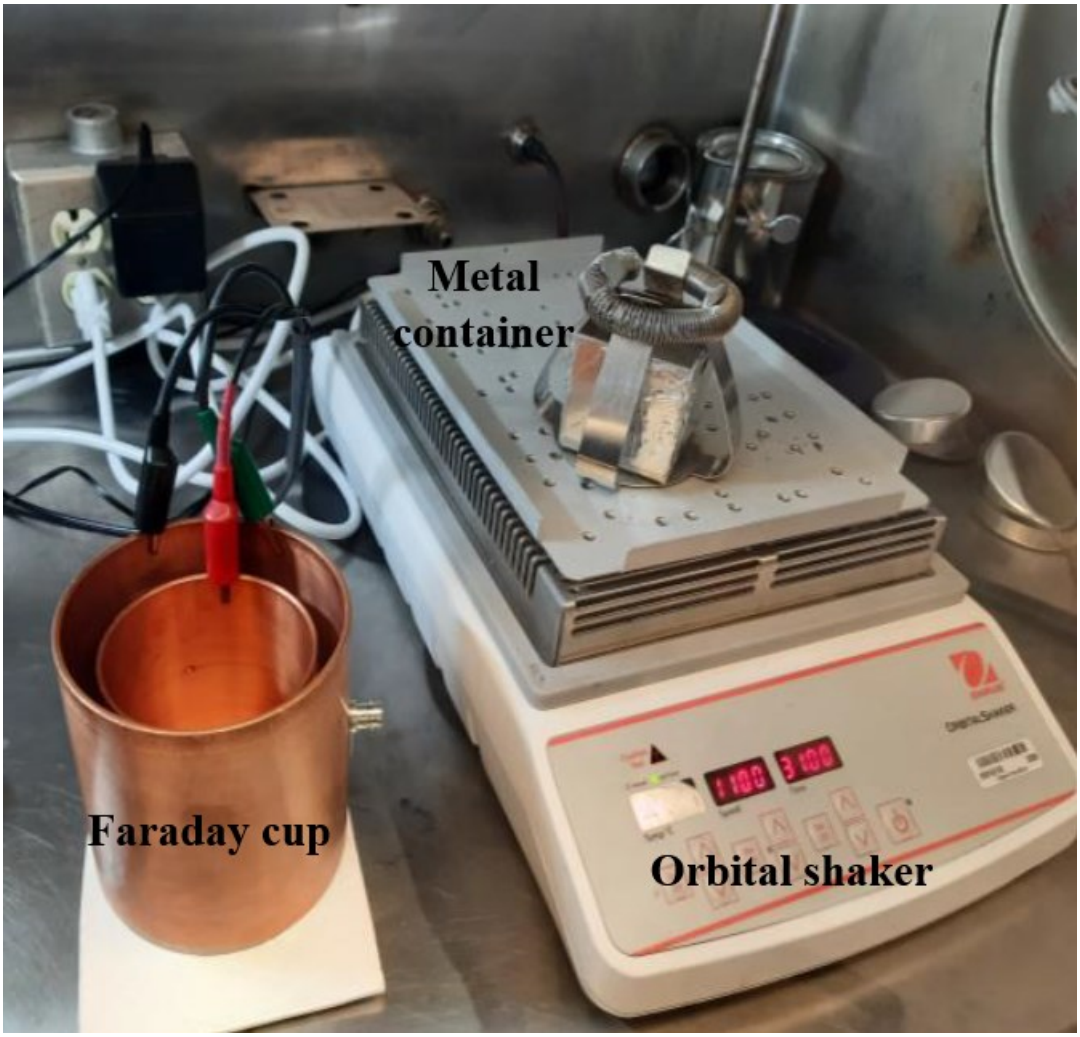

Fig. 4-3. Orbital shaker apparatus with the Faraday cup setup and metallic container used in the study

The charge measurement before and after shaking was performed using a Faraday cage (see Fig. 4-3) connected to an electrometer (Keithley 6514). The single particle shake tests were first conducted under ambient air to establish a benchmark. Subsequently, all other trials were performed inside a glove box under controlled humidity and temperature, filled with either nitrogen or argon. The number of shakes were predetermined, and relevant charge values were recorded for individual shake data points. In the second approach, shaking duration was fixed instead of number of shakes.

4.3 Results and discussions

4.3.1 First approach- Large single particle trials

Fig. 4-4 shows the results for the single particle trial under argon and nitrogen atmosphere compared with ambient air condition. The charges were averaged out over two trials yielding comparable results. The charges on the particle appear to plateau at approximately 200 shakes with ambient air but drop further at 250 shakes. Nitrogen shows a similar trend, saturating at around the 200 shakes mark, while argon reaches a saturation much earlier and exhibits a smaller saturation value. Additionally, the charges under argon seem to reverse the trend and saturate at a newer, smaller value at approximate 200 shakes.

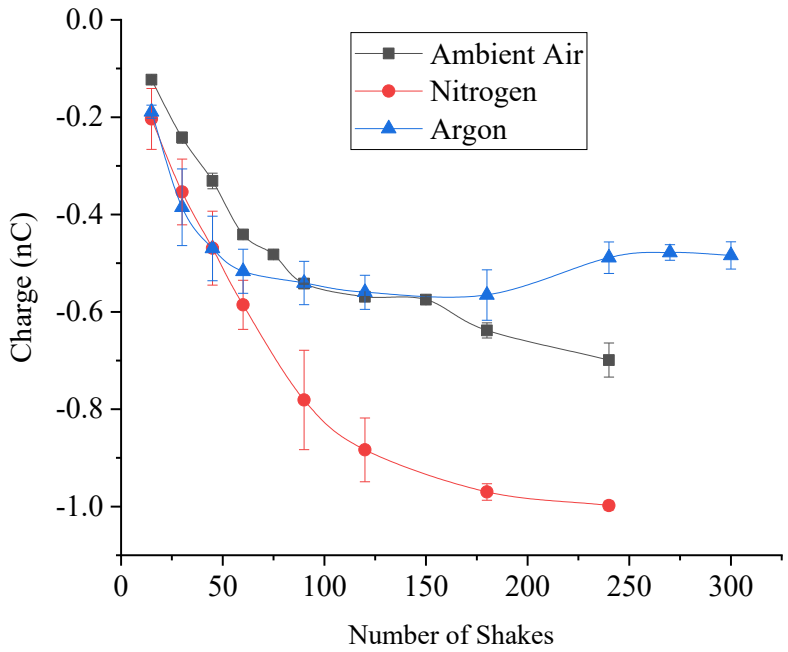

Fig. 4-4. Charge generated on the single 5 mm polyethylene particle when shaken in ambient air (RH~38%), argon (RH~3%), and nitrogen (RH~3%).

4.3.2 Second approach- Multi particle shake trials

Fig. 4-5 shows the result collated for the 0.55 mm and 1.2 mm particles under argon and nitrogen. Smaller particles (0.55 mm) were charged positively in contact with the aluminum cup walls, while larger particles (1.2 mm) were found to charge negatively. Earlier results for the single large particle (5 mm) also showed a negative polarity under both gases. Results clearly indicate that particles shaken under argon gained a smaller net specific charge and as well reached charge saturation at much earlier time in comparison with nitrogen trials.

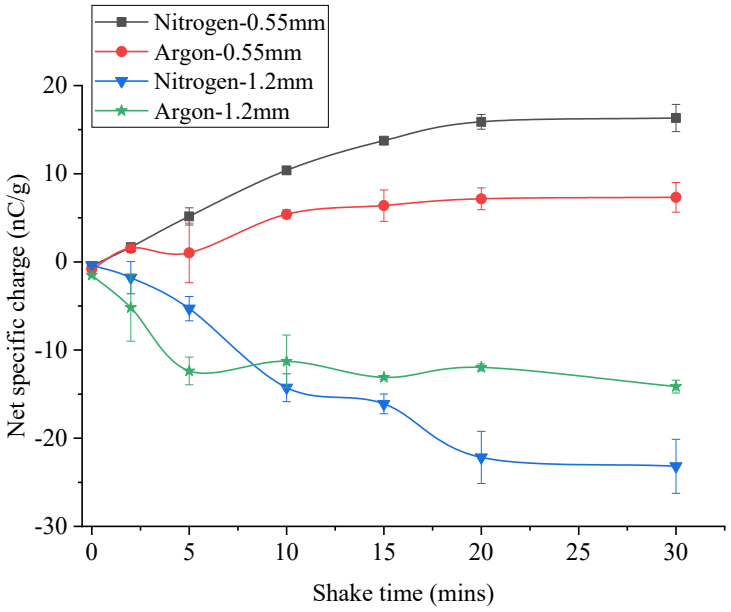

Fig. 4-5. Net specific charge generated on 0.55 mm and 1.2 mm polyethylene particles when shaken in argon and nitrogen environment.

4.4 Conclusions

The results published in this study attempts to establish a relation between dielectric strength and charging behaviour observed in solids under continuous collisions. Polarity of the charge gained by polyethylene particles seem to be dependant on the size of the particles. However, regardless of the size, argon seems to better regulate charge generation through triboelectrification relative to nitrogen. Furthermore, single particle trials in ambient air (RH ~ 38%) were comparable with argon but lacked the upward trend observed in argon. Relative humidity thus seems to help dissipate charges and reduce the overall charge held by the particle. The impact of relative humidity on multiple smaller particles is, however, unknown.

Acknowledgements

Financial support from Univation Technologies, LLC (USA) and The Natural Sciences and Engineering Research Council of Canada (NSERC) is acknowledged with gratitude.

References

[1] G. Hendrickson, Electrostatics and gas phase fluidized bed polymerization reactor wall sheeting, Chem. Eng. Sci. 61 (2006) 1041–1064. https://doi.org/10.1016/j.ces.2005.07.029.

[2] G.E. Klinzing, A review of pneumatic conveying status, advances and projections, Powder Technol. 333 (2018) 78–90. https://doi.org/10.1016/j.powtec.2018.04.012.

[3] M.B. John, E.P. John, Using inert gases for pneumatic conveymg, Powder Bulk Eng. (1989) 17–19.

[4] G.E. Klinzing, F. Rizk, R. Marcus, L.S. Leung, Pneumatic Conveying of Solids: A theorical and practical approach, 2010.

[5] M. Nifuku, H. Katoh, A study on the static electrification of powders during pneumatic transportation and the ignition of dust cloud, Powder Technol. 135–136 (2003) 234–242. https://doi.org/10.1016/S0032-5910(03)00163-3.

[6] P. Mehrani, M. Murtomaa, D.J. Lacks, An overview of advances in understanding electrostatic charge buildup in gas-solid fluidized beds, J. Electrostat. 87 (2017) 64–78. https://doi.org/10.1016/j.elstat.2017.03.005.

[7] J. Cross, Electrostatics: Principles, Problems and Applications, 1987. https://doi.org/10.1088/0031-9112/38/11/030.

[8] S. Matsusaka, H. Maruyama, T. Matsuyama, M. Ghadiri, Triboelectric charging of powders: A review, Chem. Eng. Sci. 65 (2010) 5781–5807. https://doi.org/10.1016/j.ces.2010.07.005.

[9] J. Lowell, A.C. Rose-Innes, Contact electrification, Adv. Phys. 29 (1980) 947–1023. https://doi.org/10.1080/00018738000101466.

[10] J.H. Anderson, A comparison of experipmental data and model predictions for tribocharging of two-component electrophotographic developers, J. Imaging Sci.

Technol. 38 (n.d.) 378–382. http://cat.inist.fr/?aModele=afficheN&cpsidt=3376350.

[11] F.R. Ruckdeschel, L.P. Hunter, Contact electrification between insulators: Phenomenological aspects, J. Appl. Phys. 46 (1975) 4416–4430. https://doi.org/10.1063/1.321469.

[12] L.H. Lee, Dual mechanism for metal-polymer contact electrification, J. Electrostat. 32 (1994) 1–29. https://doi.org/10.1016/0304-3886(94)90026-4.

[13] L.S. McCarty, G.M. Whitesides, Electrostatic charging due to separation of ions at interfaces: Contact electrification of ionic electrets, Angew. Chemie - Int. Ed. 47 (2008) 2188–2207. https://doi.org/10.1002/anie.200701812.

[14] P. Jiang, H. Bi, S. -C Liang, L. -S Fan, Hydrodynamic behavior of circulating fluidized bed with polymeric particles, AIChE J. 40 (1994) 193–206. https://doi.org/10.1002/aic.690400202.

[15] M.E. Abdel-kader, W.H. Gaber, F.A. Ebrahim, M.A. Abd Al-Halim, Characterization of the electrical breakdown for DC discharge in Ar-He gas mixture, Vacuum. 169 (2019) 108922. https://doi.org/10.1016/j.vacuum.2019.108922.

[16] K.P. Brand, Dielectric Strength, Boiling Point and Toxicity of Gases - Different: Aspects of the Same Basic Molecular Properties, IEEE Trans. Electr. Insul. EI-17 (1982) 451–456. https://doi.org/10.1109/TEI.1982.298489.

[17] A.E.D. Heylen, Maximization of argon-hydrocarbon Penning mixtures, J. Phys. D. Appl. Phys. 3 (1970) 789–796. https://doi.org/10.1088/0022-3727/3/5/321.

[18] H.R. Hiziroglu, M.S. Dincer, T.D. Nguyen, Breakdown voltages in SF6+argon mixtures under nonuniform electrostatic fields, Conf. Electr. Insul. Dielectr. Phenom. (CEIDP), Annu. Rep. 2 (1997) 579–582. https://doi.org/10.1109/ceidp.1997.641140.

[19] T. Miura, Observation of charge separation and gas discharge during sliding friction between metals and insulators, J. Phys. Conf. Ser. 646 (2015) 0–4. https://doi.org/10.1088/1742-6596/646/1/012057.

[20] T. Miura, I. Arakawa, Gas discharge caused by triboelectricity around a contact during

friction between insulators, IEEE Trans. Dielectr. Electr. Insul. 14 (2007) 560–565. https://doi.org/10.1109/TDEI.2007.369513.

[21] T. Matsuyama, H. Yamamoto, Charge relaxation process dominates contact charging of a particle in atmospheric conditions, J. Phys. D. Appl. Phys. 28 (1995) 2418–2423. https://doi.org/10.1088/0022-3727/28/12/005.

[22] T. Matsuyama, H. Yamamoto, Charge-relaxation process dominates contact charging of a particle in atmospheric condition: II. the general model, J. Phys. D. Appl. Phys. 30 (1997) 2170–2175. https://doi.org/10.1088/0022-3727/30/15/008.

[23] J.R. Grace, H. Bi, Introduction to Circulating Fluidized Beds, Circ. Fluid. Beds. (1997) 1–20. https://doi.org/10.1007/978-94-009-0095-0_1.

[24] A. Peacock, Use and Fabrication of Polyethylene Products, Handb. Polyethyl. (2020) 469–518. https://doi.org/10.1201/9781482295467-20.

[25] T. Xie, K.B. McAuley, J.C.C. Hsu, D.W. Bacon, Gas Phase Ethylene Polymerization: Production Processes, Polymer Properties, and Reactor Modeling, 1994. https://doi.org/10.1021/ie00027a001.

[26] T.E. Nowlin, Business and Technology of the Global Polyethylene Industry, 2014. https://doi.org/10.1002/9781118946039.

[27] Data from www.sriconsulting.com/, (n.d.).

[28] A. Peacock, Commercial Development of Polyethylene, Handb. Polyethyl. (2020) 37–52. https://doi.org/10.1201/9781482295467-4.

[29] S.E. Horne Jr., J.P. Kiehl, J.J. Shipman, V.L. Folt, C.F. Gibbs, Ameripol SN — A C is-1 , 4-Poly isoprene : V, Ind. Eng. Chem. Res. 48 (1956) 784–791.

[30] T.E. Nowlin, Low pressure manufacture of polyethylene, Prog. Polym. Sci. 11 (1985) 29–55. https://doi.org/10.1016/0079-6700(85)90007-3.

[31] Y. Rao, P. Cai, K.J. Cann, F.D. Hussein, W.R. Mariott, P.A. Cao, Patent Issued for Supported Catalyst With Improved Flowability (USPTO 10,676,588), 2020.

[32] A. Sowinski, The Study of Reactor Wall Fouling in Gas-Solid Fluidized Beds Caused by Electrostatic Charge Generation, Dr. Thesis Diss. Univ. Ottawa. (2012).

[33] A. Sowinski, A. Mayne, P. Mehrani, Effect of fluidizing particle size on electrostatic charge generation and reactor wall fouling in gas-solid fluidized beds, Chem. Eng. Sci. 71 (2012) 552–563. https://doi.org/10.1016/j.ces.2011.11.031.

[34] A. Sowinski, L. Miller, P. Mehrani, Investigation of electrostatic charge distribution in gas-solid fluidized beds, Chem. Eng. Sci. 65 (2010) 2771–2781. https://doi.org/10.1016/j.ces.2010.01.008.

[35] D. Song, P. Mehrani, Comparison of electrostatic charge generation in gas-solid fluidized beds in turbulent versus pre-turbulent flow regime, Powder Technol. 319 (2017) 426–433. https://doi.org/10.1016/j.powtec.2017.07.013.

[36] D. Song, P. Mehrani, Effect of Fluidization Pressure on Electrostatic Charge Generation of Polyethylene Particles, Ind. Eng. Chem. Res. 56 (2017) 14716–14724. https://doi.org/10.1021/acs.iecr.7b04056.

[37] A. Giffin, P. Mehrani, Effect of gas relative humidity on reactor wall fouling generated due to bed electrification in gas-solid fluidized beds, Powder Technol. 235 (2013) 368–375. https://doi.org/10.1016/j.powtec.2012.10.037.

[38] M.I. Nimvari, A. Sowinski, P. Mehrani, Effect of temperature on triboelectrifcation of polyethylene particles in a pilot-scale pressurized gas-solid fluidized bed, Powder Technol. 405 (2022) 117524. https://doi.org/10.1016/j.powtec.2022.117524.

[39] M. Taghavivand, A. Sowinski, P. Mehrani, Triboelectric effects of continuity additives and a silica catalyst support on polyethylene fluidized bed wall fouling, Chem. Eng. Sci. 245 (2021) 116882. https://doi.org/10.1016/j.ces.2021.116882.

[40] B.D. Fulks, S.P. Sawin, C.D. Aikman, J.M. Jenkins III, Process for reducing sheeting during polymerization of alpha-olefins (USPTO 4,876,320-A), 1989.

[41] J. Hou, X. Liu, M.H. Rahman, H. Li, S. Sundaresan, J.R. Grace, X. Bi, Effect of gas properties and wall materials on particle charging in gas–solid fluidized beds, Can. J. Chem. Eng. (2022) 1–12. https://doi.org/10.1002/cjce.24568.

[42] M.K. Gupte, K. Tolley, A. Mutchler, S. Holland, Static reduction (USPTO 6,630,548 B1), 2003.

[43] K. Saleh, A. Traore Ndama, P. Guigon, Relevant parameters involved in tribocharging of powders during dilute phase pneumatic transport, Chem. Eng. Res. Des. 89 (2011) 2582–2597. https://doi.org/10.1016/j.cherd.2011.06.001.

[44] E.E. Smeltzer, M.L. Weaver, G.E. Klinzing, Individual electrostatic particle interaction in pneumatic transport, Powder Technol. 33 (1982) 31–42. https://doi.org/10.1016/0032-5910(82)85036-5.

[45] N. Schwindt, U. von Pidoll, D. Markus, U. Klausmeyer, M. V. Papalexandris, H. Grosshans, Measurement of electrostatic charging during pneumatic conveying of powders, J. Loss Prev. Process Ind. 49 (2017) 461–471. https://doi.org/10.1016/j.jlp.2017.05.028.

[46] S. Matsusaka, H. Umemoto, M. Nishitani, H. Masuda, Electrostatic charge distribution of particles in gas-solids pipe flow, J. Electrostat. 55 (2002) 81–96. https://doi.org/10.1016/S0304-3886(01)00185-1.

[47] D. Song, P. Mehrani, Mechanism of particle build-up on gas-solid fluidization column wall due to electrostatic charge generation, Powder Technol. 316 (2017) 166–170. https://doi.org/10.1016/j.powtec.2017.01.031.

[48] M. Taghavivand, B. Elchamaa, A. Sowinski, P. Mehrani, Study of electrostatic charging of single particles during pneumatic conveying, Powder Technol. 355 (2019) 242–250. https://doi.org/10.1016/j.powtec.2019.07.046.

[49] M. Taghavivand, B.J. Cho, P. Mehrani, A. Sowinski, Electrostatic charging behaviour of a silica powder during pulse pneumatic conveying, Powder Technol. 366 (2020) 119–129. https://doi.org/10.1016/j.powtec.2020.02.031.

[50] M. Taghavivand, P. Mehrani, A. Sowinski, Triboelectric effects of a pneumatically injected silica catalyst support on polyethylene fluidized bed wall fouling, Powder Technol. 385 (2021) 287–298. https://doi.org/10.1016/j.powtec.2021.03.002.

[51] M.I. Nimvari, M. Taghavivand, K. Choi, A. Sowinski, P. Mehrani, Velocity

measurement of pneumatically conveyed particles via a simple current signal technique and the influence of electrostatic charge, Powder Technol. 413 (2023) 118018. https://doi.org/10.1016/j.powtec.2022.118018.

[52] J. Guardiola, V. Rojo, G. Ramos, Influence of particle size, fluidization velocity and relative humidity on fluidized bed electrostatics, J. Electrostat. 37 (1996) 1–20. https://doi.org/10.1016/0304-3886(96)00002-2.

[53] F. Wang, J. Wang, Y. Yang, Distribution of electrostatic potential in a gas-solid fluidized bed and measurement of bed level, Ind. Eng. Chem. Res. 47 (2008) 9517–9526. https://doi.org/10.1021/ie800805t.

[54] W.O. Moughrabiah, J.R. Grace, X.T. Bi, Effects of pressure, temperature, and gas velocity on electrostatics in gas-solid fluidized beds, Ind. Eng. Chem. Res. 48 (2009) 320–325. https://doi.org/10.1021/ie800556y.

[55] A.C. Hoffmann, J.G. Yates, Experimental Observations of Fluidized Beds at Elevated Pressures, Chem. Eng. Commun. 41 (1986) 133–149. https://doi.org/10.1080/00986448608911716.

[56] X. Liu, S. Sundaresan, The effect of gas on tribocharging of particles in a vibrated bed, Powder Technol. 401 (2022) 117272. https://doi.org/10.1016/j.powtec.2022.117272.

[57] C.Y. Wen, Y.H. Yu, A generalized method for predicting the minimum fluidization velocity, AIChE J. 12 (1966) 610–612. https://doi.org/10.1002/aic.690120343.

[58] F. Chowdhury, A. Sowinski, M. Ray, A. Passalacqua, P. Mehrani, Charge generation and saturation on polymer particles due to single and repeated particle-metal contacts, J. Electrostat. 91 (2018) 9–15. https://doi.org/10.1016/j.elstat.2017.11.004.

[59] F. Chowdhury, B. Elchamaa, M. Ray, A. Sowinski, A. Passalacqua, P. Mehrani, Apparatus design for measuring electrostatic charge transfer due to particle-particle collisions, Powder Technol. 361 (2020) 860–866. https://doi.org/10.1016/j.powtec.2019.11.013.

[60] F. Chowdhury, M. Ray, A. Passalacqua, P. Mehrani, A. Sowinski, Electrostatic charging due to individual particle-particle collisions, Powder Technol. 381 (2021)

352–365. https://doi.org/10.1016/j.powtec.2020.12.012.

Chapter 5 Conclusion and Future work

Industrial processes involving solids and particulates handling and processing may report generation of electrostatic charge due to collisions among the solid particles and nearby surfaces. Although electrostatic charge generation is a common cause of concern in a variety of industrial processes, this thesis focused on gas-phase fluidization and pneumatic conveying. Polyethylene (PE) manufacturing features a reaction stage carried out in large catalytic fluidized bed reactors which see significant particle collisions. Furthermore, catalyst particles used in the process are introduced through a dry feeding method utilizing pneumatic conveying. Within the fluidised bed reactor, there is significant contact among PE particles, PE particles and the reactor wall, and PE particles and catalyst particles. These contacts constitute triboelectric charging of the polymer particles, which leads to adherence of highly charged particles onto the reactor wall, forming sheets and in turn, causing operational issues. In addition to the triboelectrification of the particles inside the reactor, catalyst particles are anticipated to charge in transit even before entering the system. Due to the small size of the particles, high gas velocity, and the non-linear pathway of the conveying pipe, triboelectrification of the particles in the conveying line is expected. Charged particles may agglomerate, block the conveying tube, increase power demand, and even interfere with the rate of reaction and reactor productivity. Therefore, understanding the causes of triboelectrification and devising an approach to possibly reduce and avoid particle fouling were the objectives of this thesis. The results obtained in this research, however, are also applicable to other gas-phase processes and systems where particle charging is observed due to contact electrification.

Overall, the thesis emphasis was directed on mitigating PE particle fouling in fluidization columns and catalyst particle fouling in conveying tubes. In particular, the influence of different gases on the electrostatic charging and subsequent fouling of polyethylene and catalyst particles were studied. The gases used in this study, namely nitrogen and argon, displayed a large difference in their dielectric strengths, which was envisaged to be influential in limiting the maximum charge gained by the particles.

5.1 Conclusions

The influence of argon on net charge (Q), net specific charge (Q/m) and the degree of fouling was prominent in fluidization experiments. Although pneumatic conveying and shake tests did

not yield a similarly significant result, they still showed a favourable outcome with argon relative to nitrogen.

The gas-phase fluidization study was performed using a 0.1 m in diameter stainless-steel fluidization column at ambient pressures and temperatures. Faraday cages were used to measure the charges on the particles across three different regions (region 1, region 2, and fines) which were examined individually using a unique approach. The approach ensured almost every particle associated with the different regions were part of the charge and mass measurement. Thus, reliance on sampling was avoided. Fluidization column wall fouling was significantly reduced by 90% when fluidization was carried out with pure argon in comparison to pure nitrogen. In order to minimize argon usage while simultaneously optimizing charge and fouling reduction, binary mixture of argon and nitrogen were used. It was found that at the lowest argon volume tested (10 vol % argon), fouling reduced by 50%. Meanwhile, equal volumes of nitrogen and argon showed a reduction of 80% in wall fouling. This signified a key finding that presence of minimal amount of argon could still be beneficial in significant reduction of wall fouling.

In all trials, the majority of the reduction in fouling was observed in region 1 where particle-particle and particle-wall contacts were the greatest. This region was believed to house the largest electric field within the column, thus generated the highest probability of gas discharge. Considering the employability of the findings in commercial reactors, successive fluidization was also studied. Argon was introduced for short durations (8% and 15% of the total gas volume) at the end of a completed nitrogen trial. The results were favourable as they showed that small intervals of pure argon fluidization generated similar charging and fouling results as pure argon.

Although argon generated significantly lower column wall fouling and charging in the fluidized bed, the same magnitude of reduction was not observed in pulse pneumatic conveying of dehydrated amorphous silica (i.e., typical catalyst base). This could be attributed to the low residence time of the particles inside the conveying tube which implies a short interval of interaction between the particles and gas molecules. Additionally, charging, and fouling values seemed to vary between the two gases for the first injection. Subsequent injections exhibited comparable values, assumed to be caused by particle adhesion from previous injections and subsequent repulsion of like-charged particles.

Bench-scale shake tests helped validate the findings at a much smaller scale wherein argon performed better in minimizing the saturation charges on single large PE particles and multiple smaller PE particles. Furthermore, we observed a change in polarity among smaller and larger particles.

In short, argon is observed to aid minimize triboelectrification of polyethylene particles in gas solid operations including fluidized beds, and solids pneumatic conveying. Binary mixtures of argon and nitrogen exhibit similar characteristics in reducing fluidizing particles' charge and their adhesion to the column wall. Thus, the inert nature of argon makes it suitable in commercial processes wherein triboelectrification is considered a nuisance.

5.2 Future works

Although a proof of concept was established through this thesis, further experiments will help validate the findings concerning the effectiveness of gases including argon in reducing triboelectrification and its adverse consequences. In this regard, the following recommendations are proposed to further our understanding on the influence of different gases on electrostatic charging:

1. The study investigated the influence of binary gas mixtures on electrostatic charging, with 10% argon being the lowest concentration used. Reducing the concentration of argon even lower might offer insight into the non-linear relationship between charging and argon concentrations.
2. Considering the hypothesis of gas discharge limiting the maximum charge on a particle, sulfur hexafluoride can be used as a fluidizing gas to verify the influence of dielectric strength since SF_6 exhibits a very high dielectric strength.
3. The study was conducted at ambient temperature and pressures. The dependence of dielectric strength on pressure shows an inverse relationship, but with temperature shows a direct relationship. Thus, fluidization trials at high pressure and temperature might yield significant results. Additionally, these conditions mimic industrial polyethylene reactor conditions.
4. Simulate the electric fields within the fluidization column and pneumatic conveying line to identify regions where gas molecules have the highest probability to get ionized, thereby dissipating the charge on surrounding particles. This would find practical application in injecting argon in localized areas of high electric fields.

5. Pneumatic conveying of active catalyst in polyethylene industries is carried out using nitrogen. Studying the impact of argon on conveying of such active and deactivated catalyst would hold practical applications.

Appendix- A Experimental Apparatus

Fig. A-1 Fluidization column used in this study showing the stainless-steel column and the two Faraday cages.